ISBN 978-82-998920-3-2 - The 2014 Joint National PhD Conference Medical Imaging and MedViz Conference (printed version)

ISBN 978-82-998920-4-9 - The 2014 Joint National PhD Conference Medical Imaging andMedViz Conference (PDF version)

The 2014 Joint National PhD Conference in Medical Imaging and MedViz Conference

Grand Terminus Hotel, Bergen, Norway

17-18 June 2014

MedIm and MedViz Conference 2014

Bergen, Hotel Grand Terminus 17th of June

Foreword

Dear conference delegate,

We cordially welcome you to Bergen to the 2nd joint Conference between MedIm and MedViz. This is the 6th National PhD Conference in medical imaging by MedIm and the 8th MedViz conference in medical imaging and visualization.

Medical imaging and visualization contribute significantly to diagnosis and treatment of many patients. The doctor bases many clinical decisions on information displayed in medical images. Often, interventions and image-directed therapy are performed in close proximity to image acquisition and diagnostic procedures.

The aim of this conference is to present state-of-the-art research in medical imaging and visualization. Furthermore, we want to provide a forum for users and developers to discuss common challenges and exchange scientific ideas. We aim to create a common meeting place where research line students, PhD students and postdocs can meet with basic scientist, clinicians and engineers to enable translational communication and research.

The conference runs for two days with both a scientific and a social program. The scientific program is divided in five oral presentation sessions and one speed poster session. The oral presentation sessions have the following themes: Image and signal processing, Visualization and Modelling, Preclinical imaging, Biomedical and molecular imaging and Clinical imaging. The speed poster session allows a greater proportion of the attendees to personally present their work in one minute to the entire audience, immediately followed by a poster discussion. The social program includes a sail trip with dinner onboard the majestic sailing ship *"Statsraad Lehmkuhl"*, a 3-mastered bark, built in 1914 one hundred years ago.

We are particularly grateful to the international faculty for coming to Bergen to share their expertise with us. Furthermore, without the help and efforts from our local organizing committee and national speakers, this conference would not be possible.

We are also happy to inform you that the best poster, the best oral presentation and the best picture from the students will be awarded a prize.

Thank you all for coming to Bergen and we wish you a pleasant stay.

Sincerely yours,

Odd Helge Gilja	Olav Haraldseth	Ragnar Nortvedt
MedViz Scientific Director	MedIm Scientific Director	MedViz Program Manager

International Faculty
Christoph Dietrich, Caritas Krankenhaus Bad Mergentheim, Germany
Bradley Erickson, Mayo Clinic, Rochester, USA
Bernhard Preim, University of Magdeburg, Germany
Steven Sourbron, Leeds Institute of Genetics, Health and Therapeutics, England
João Manuel R.S. Tavares, University of Porto, Portugal

Local Organizing Committee
Elin Myhrvold Riple
Hanne Lehn
Kim Nylund
Veronika Šoltészová
Ragnar Nortvedt
Cecilie Brekke Rygh
Erik Ingebrigtsen
Stefan Bruckner
Alexandra Vik

Norwegian Research School in Medical Imaging
Olav Haraldseth
Knut Matre
Alexandra Vik
Ivar Sjaastad
Svanhild Schønberg
Tor Ivar Hansen
Rune Sundset
Arvid Lundervold
Erik Ingebrigtsen
Atle Bjørnerud
Lisa J. Kjønigsen
Catharina de Lange Davies
Karen Sørensen
Hallvard Olsvik

MedViz
Odd Helge Gilja
Elin Myhrvold Riple
Dag Magne Ulvang
Arvid Lundervold
Njål Brekke
Christopher Giertsen
Ragnar Nortvedt
Ingfrid S. Haldorsen
Helwig Hauser
Alexander Malyshev
Jarle Rørvik
Alf Henrik Andreassen

Abstract Committee
Alexander Malyshev
Cecilie Brekke Rygh
Knut Matre
Veronika Šoltészová
Emmet McCormack
Ragnar Nortvedt

Funding agency:
The Research Council of Norway

Program for the 2014 Joint National PhD Conference in Medical Imaging and MedViz Conference

Conference Venue: Grand Terminus Hotel, Bergen, Norway

Tuesday June 17

0730 - 0900 Registration and coffee. Poster assembly in the poster area
0900 - 0915 **Welcome**: Rector Dag Rune Olsen, UiB
Prof. Arvid Lundervold, UiB, Bergen & Prof. Odd Helge Gilja, UiB/HUS, Bergen

Session I: Image and signal processing
Chairs: Xue-Cheng Tai & Dag Magne Ulvang
0915 – 0945 **Invited speaker:** Bradley Erickson, Mayo Clinic, Rochester, USA: *Using Big Data and Machine Learning to Find Relationships between MRI and Genomics in Brain Tumors*
0945 - 1030 **Oral presentations by PhD candidates:**
Jacek Blumenfeld, Lodz/UiB, Bergen: *Skull segmentation in 3-D CT head images – use of atlases for improvement of accuracy.*
Erik Hanson, UiB, Bergen: *Poroelastic regularization of image registration*
Solomon Tesfamicael, NTNU, Trondheim: *Clustered Compressive Sensing in Medical Imaging using Bayesian framework.*
Tomasz Wozniak, Lodz/UiB, Bergen: *Biomedical images segmentation based on Chan-Vese level-set approach*
1030 - 1100 **Invited speaker:** João Manuel R. S. Tavares, University of Porto, Portugal: *Biomedical Image Analysis based on Computational Registration Methods*
1100 – 1115 Coffee & tea

Session II: Visualization & Modelling
Chairs: Helwig Hauser & Knut Matre
1115 – 1145 **Invited speaker:** Bernhard Preim, University of Magdeburg, Germany: *Visual Analytics of Image-Centric Cohort Studies in Epidemiology*
1145 – 1230 **Oral presentations by PhD candidates:**
Jørn Bersvendsen, UiO, Oslo: *Statistical shape model of the right ventricle for segmentation in 4D echocardiography*
Lars Hofsøy Breivik, UiO, Oslo: *Multiscale Nonlocal Means method for Ultrasound despeckling*
Naiad Hossain Khan, NTNU, Trondheim: *Automatic measurement of biparietal diameter with a portable ultrasound device*
Torstein Yddal, UiB, Bergen: *Ultrasound transducers with an optical window*
1230 – 1300 **Invited speaker:** Steven Sourbron, Leeds Institute of Genetics, Health and Therapeutics, England: *Tracer-kinetic modelling in renal MRI*
1300 – 1400 Lunch

Session III: Posters
Chairs: Cecilie Brekke Rygh & Hanne Lehn
1400 – 1445 **Speed poster presentations** (1 minute each, 30 sec to change speaker)
1445 – 1530 **Poster discussion**, coffee & tea

Session IV: Preclinical imaging
Chairs: Arvid Lundervold & Ragnar Nortvedt
1530 - 1600 **Invited speaker:** Emmet Mc Cormack, UiB, Bergen: *Preclinical Imaging of Cancer*
1600 - 1645 Oral presentations by PhD candidates
Jane Cebulla, NTNU, Trondheim: *Evaluation of the novel SPIO GEH121333 for monitoring changes in tumor vascularity and vascular permeability after antiangiogenic treatment using MRI*
Morteza Esmaeili, NTNU, Trondheim: *Post-exercise impacts on energy metabolism of heart failure rats*

Sveinung Fjær, UiB, Bergen: *Magnetization transfer ratio (MTR) increased unexpectedly in EAE induced mice.*
Alexandr Kristian, UiO, Oslo: *Use of dynamic 2-[18F]-fluoroethyl-choline PET for evaluation of choline metabolism in breast carcinoma xenografts*

1645 - 1715 **Invited speaker:** Rune Sundset, UiT– The Arctic University of Norway: *Preclinical PET imaging in Tromsø – research facilities and course opportunities*

1800 - 2200 Sailing with Statsraad Lehmkuhl and Conference Dinner on board

Wednesday June 18

Session V: Biomedical and molecular imaging
Chairs: Bjørn Tore Gjertsen & Stefan Bruckner

0900 – 0930 **Invited speaker:** Atle Bjørnerud, UiO, Oslo: *Magnetic Resonance based perfusion imaging of the brain*

0930 – 1030 **Oral presentations by PhD candidates:**
Kai Beckwith, NTNU, Trondheim: *SU-8 nanopillars: A flexible system for investigating cell response and function on nanostructured surfaces*
Ravinea Manotheepan, UiO, Oslo: *Exercise training reduces CaMKII-dependent phosphorylation of the cardiac ryanodine receptor and arrhythmogenic SR Ca2+ leak in mice with mutant cardiac ryanodine receptor 2*
Maria Omsland, UiB, Bergen: *Cell-to-cell communication in acute myeloid leukemia by tunnelling nanotubes*
Marianne Ruud, UiO, Oslo: *Stretch-induced modulation of cardiomyocyte Ca2+ homeostasis, signaling, and structure*
Endre Stigen, UiB, Bergen: *Optimization of NTR reporter genes for preclinical and GDEPT imaging*

1030 – 1100 **Invited speaker:** Catharina de Lange Davies, NTNU; Trondheim: *US-mediated delivery of nanoparticles to tumor tissue*

1100 - 1115 Coffee & tea

Session VI: Clinical imaging
Chairs: Odd Helge Gilja & Jarle Rørvik

1115 - 1145 **Invited speaker:** Christoph Dietrich, Caritas Krankenhaus Bad Mergentheim, Germany: *CEUS quantification in clinical practice*

1145 - 1230 **Oral presentations by PhD candidates:**
Trond Engjom, UiB, Bergen: *Contrast enhanced ultrasound of the pancreas show impaired perfusion in pancreas insufficient cystic fibrosis patients*
Judit Haasz, UiB, Bergen: *Longitudinal changes in visual working memory performance and frontoparietal intrinsic connectivity network synchronization after non-cortical stroke*
Kam Sripada, NTNU, Trondheim: *Multimodal MRI analysis of brain structure and connectivity in young adults born preterm with very low birth weight: Visual-motor function in early adulthood*
Jose R. Teruel, NTNU, Trondheim: *High Order Diffusion Tensor Imaging for Breast Cancer Differentiation*

1230 - 1300 **Invited speaker:** Ingfrid Haldorsen, HUH/UiB: *Functional imaging for individualized cancer treatment*

1300 - 1400 Lunch

Session VII: **Posters**

1400 – 1445 Poster discussion, coffee & tea

1445 – 1530 **Panel for discussion: Your experience with cross-disciplinary research**
Bernhard Preim, Odd Helge Gilja and two PhD candidates / post docs

1530 – 1550 **Awards for the best picture, PhD poster and PhD oral presentation**

1550 – 1600 Conclusive remarks by Ragnar Nortvedt, MedViz

SPEED POSTER PRESENTERS

1	Marie Austdal	NTNU
2	Habib Baghirov	NTNU
3	Violeta Lozano Botellero	NTNU
4	Mohammadmehdi Bozorgi	NTNU
5	Ulrik Carling	UiO/OUS
6	Ioanna Chronaiou	HiST
7	Eli Eikefjord	UiB/HUS
8	Benedicte Falkenberg-Jensen	OUS
9	Andreas Finnøy	NTNU
10	Dilla Handini	OUS
11	Tonje Haukaas	NTNU
12	Antonio Pelegrina Jiménez	Gjøvik University College
13	Terje Kolstad	OUS
14	Kjetil Børve Lund	UiB
15	Hani Nozari Mirarkolaei	UiO
16	Aliona Nacu	UiB
17	Rahul Kumar	OUS
18	Rajesh Kumar	NTNU
19	Elise Sandsmark	NTNU
20	Sahba Shafiee	UiB
21	Hanne Sorger	NTNU
22	Anne Line Stensjøen	NTNU
23	Turid Torheim	NMBU
24	Siren Tønnesen	OUS/UiO
25	Sigmund Ytre-Hauge	HUS

Abstracts for session
Image and signal processing

Abstracts are organized in the order of presentations

Participant category: Invited speaker

Using Big Data and Machine Learning to Find Relationships between MRI and Genomics in Brain Tumors

Bradley J. Erickson [(1)]

bje@mayo.edu

1. Mayo Clinic, Rochester, USA

1. Big Data Principles

Healthcare and hospitals have made tremendous strides over the past 2 decades in converting from paper and film to bits. Governments have a strong interest in promoting this trend because it allows more effective and efficient sharing of information about patients, which should decrease costs while improving outcomes. This has resulted in exponential growth of medical data. While there are appropriate cause for concern when so much information about people becomes accessible, it also provides a tremendous opportunity for answering long-standing questions in new ways, and asking entirely new questions.

When the IT industry hears 'big data' they typically think of google or facebook where millions to billions of signals are used to identify the activities and interests of individuals in order to improve the probability of providing/selling some product or service. In medical care, the focus is typically different—the focus is usually on finding signals that reflect propensity or presence of a disease, or effects or some therapy. That is particularly true in the context of taking care of a patients, versus healthcare system optimization.

Google made a splash in 2009 when they identified outbreaks and then began to predict flu outbreaks with great precision (Ginsberg, Nature, 2009). They claimed: 'Because the relative frequency of certain queries is highly correlated with the percentage of physician visits in which a patient presents with influenza-like symptoms, we can accurately estimate the current level of weekly influenza activity in each region of the United States, with a reporting lag of about one day. This approach may make it possible to use search queries to detect influenza epidemics in areas with a large population of web search users.' Google Flu Trends was quick, accurate, and theory-free. They didn't need to develop a clever hypothesis—the data did the driving. They started with 50 million search terms and simply looked for those that matched areas of early or impending outbreaks. The Edward Snowden leaks have shown the certain governments are also very interested in what pervasive data might reveal.

A. Understand the data

There have been tremendous advances in the ability to collect, manage, and mine large data sets, but the possibilities for abuse are as great as the proper use. And the 'abuse' may not always be intentional. Because the scale of data can be very large, large teams of people are often involved in the analysis. That means that the people doing the analysis are usually at least 1 step removed from the data source, making misinterpretation a likely event. It is critical that those doing analysis understanding the source and potential biases present in a signal when they are using it. Four years after Google Flu Trends published its results, the system predicted a major outbreak in one part of the US. But the outbreak was substantially smaller than predicted. Some might claim victory on this, but it is important to recognize that because there is no attempt to understand the nature of the relationship between the inputs and the output, expectations of quantitative and reliable predictions are overblown. I think that just as mining is both exciting and exhausting because of the unpredictability, Data Mining is also fraught with unpredictable results.

B. Understand the biases

Traditional research projects had had samples that often were fairly large portions of the total data set. Big Data by definition is very large, meaning that samples will be small relative to

the entire data set. Viktor Mayer-Schonberger (Oxford Internet Institute) says Big Data means N=All. Statisticians ppoint out that two types of error deserve attention: Sample Error and Smaple Bias. Sample error is an error caused by having too few data points to correctlly characterize the whole. Big Data should not have this problem—the whole concept is that you have a very large data set, and that you use it all. Sample Bias is more subtle and I think is a larger risk for big data. Because the data is collected in an automated fashion, there is at least 1 extra level of disconnection from data in to data out. That makes it more challenging to identify subtle biases in the data. Twitter and Facebook are among the largest 'Big Data' processors in the world. But they have important biases in their data: It only includes people with computers or smartphones, and among those, only those that are using social media. Big data also tends to have high dimensionality, which can also introduce subtle biases.

C. Multiple Comparisons Problem

With big data, there are MANY variables that can be tested for their ability to predict some outcome. Take the example study of «Does Asprin Work?» This is a broad question that needs much more detail. Work for what? Let's focus on headache. There are many types of headache, so we will need to record which type of headache each person gets. Will also want to record demographics—age, gender, race, etc. Pretty soon the 'Big Data' sets we have have been dissected into rather small samples, and the familiar problems of spurious associations can appear. The problem with Big Data is more insidious because the collection of data can hide correlations between elements that might otherwise appear independent.

Science of the past 1-2 decades has focused heavily on the 'hypothesis' and many flatly state that if there is no hypothesis, there is no science. Big Data can do hypothesis testing, when searches are made to specific questions. However, it can also be used for Hypothesis-Free studies, or 'Hypothesis-generation' by searching for major factors or strong associations between a variable of interest and other data points. Of course, one must be careful when doing such hypothesis-generation to use an independent hypthesis-testing data set, or you will likely find the same association.

2. MRI signals

MRI is a wonderful imaging technology because it provide a rich array of information about the tissue of interest. While there is some understanding of the properties being measured (e.g. T1 or T2 times), the resulting signal intensities that are observed are much more complex to understand. For instance, primary brain tumors are usually quite apparent on T2-weighted images. That can be because the tumors have leaky blood-brain barriers(BBB), so that plasma leaks into the interstitial space, resulting in more free water, and an overall increase in the T2 relaxation time. But increased T2 signal can also be observed in tumors where there is no BBB disruption, but there is some material (probably water) that is increased within the cells. More complex effects are seen when the tumor hemorhages because the hemoglobin molecule has various magnetic properties as it is metabolized. Proteins are notoriously complex to characterize because they can have short or long T1 and T2 depending on the amount of water and the specific protein/complexes present. Given these caveats, there is a tendency for cellular areas of tumors to have intermediate to lower T2 vlaues and intermediate to higher values on T1. Areas of BBB dissruption will show enhancement when paramagnetic agents like gadolinium are injected in the blood. Areas with more fluid will be brighter on T2 and darker on T1, but that can be seen in both necrotic/dead tumor and in the edema surrounding the more tumourous appearing parts of the tumor.

Textures appear to have important information as well. Part of the training of radiologists includes looking at many cases so that the appearance of various radiological entities can be efficiently and accurately diagnosed. Terms like 'ground glass appearance' and 'salt and pepper appearance' are commonly used phrases that reflect a distinct textural appearance that is not currently quantitative or measureable. Recent reports (Megyesi et al. 2004) have reported that oligodendrogliomas with 1p19q deletions have a distinctive appearance compared to non-deleted tumors. The differences include T2 texture and also edge sharpness.

The challenges of dealing with visual appearances as diagnostic criteria have led to the creation of the Quantitative Imaging and Biomarker Alliance (QIBA), which is designed to establish the validit of various techniques for diagnosing and measuring disease. While the main focus is for measuring cancer, it is also including non-cancer diseases like emphysema. While some of the activities of QIBA include a better understanding of how best to measure disease using convenitonal imaging methods, much of the QIBA activity is focused on establishing the methods and measures for newer functional or molecular methods. Among them are diffusion and perfusion imaging for brain tumors. Current activities focus on the devleopment of phantoms that allow characterization of measurements possible on commercial imaging devices. Early results show that even a seemingly well-accepted and understood measure like Apparent Diffusion Coefficient can show some variability across vendors and software levels. A particular challenge with these newer modalities is that the standards for storing information about how the images are acquired are not standardized in DICOM, or that imaging devices in the field may not be updated to use recently adopted standards—such a problem was recently discovered for 1 vendor's MRI scanners.
Perfusion imaging is a more complex measurement to make, and the images are much more challenging to process. We have described that for ROIs based on contrast-enhancing tumor, the calculation of rCBV by 3 FDA-cleared software packages results in different clinical conclusions in about 1/3 of cases. CBV is not the only parameter that can be extracted from perfusion images, with things like leakage rates (Ktrans and K2), relative height of the baselines before and after contrast might also be useful in assessing tumor status.
Spectroscopy is a very rich imaging method that provides an array of information about each voxel location. Early spectroscopic imaging could only work on relatively large voxels, but steady improvements are occuring making spectroscopic data more and more valuable in the assessment of tumors.

3. Genomics and Other Metrics Relevant to Brain Tumors

The Genomics Revolution was extremely popular in both the lay press and in the scientific literature. The story is compelling, and in several instances, there have been dramatic cures to cancer and other diseases thanks to a much better understanding of the human genome. In the case of brain tumors, specific genetic, epigenetic, and chromosomal markers have been shown to significnatly impact prognosis, and to predict therapy effectiveness. Two clear exmaples are this are 1p19q deletion in oligodendrogliomas, and MGMT methylation in glioblastomas (GBM) and probably other astrocytomas.

4. Where are we?

'Big Data' usually refers to databases with millions to billions of data elements collected from a variety of sources and collated into a database. Most reports on evaluation of brain tumor MRIs to predict outcomes or assess therapies are between 50 and 120 patients. That is not really 'big data' and therefore, big data methods are probably not appropriate. We have implemented a database with more than 400 GBMs and 300 Oligodendrogliomas with varying levels of associated clinical and genomic data. The imaging studies for these patients were collected from a clinical database, and are subject to the issues of other big data proejcts—the data is not collected in a uniform fashion (e.g. 1.5T and 3T, various imaging techniques) with varying imaging frequency (2 months is common for GBM, 6 months is common for OG). While it is appealing to contemplate apply truly naive imaging methods to this database, it is clearly too small to permit that. At this point, we feel obligated to presage some hypothesis of specific measures to test versus some outcome variable.
We feel we are taking one small step toward 'big data' by combining multiple measures with less restrictive hypotheses. We select measures that either have been proven or postulated to be of value in brain tumor imaging. After computing some number of features (10's-100's), we use feature reduction methods to identify those that seem most impactful and not correlated with others. We then apply traditional machine learning methods from different

families (e.g. Bayes, SVM, Trees) to identify features that are important for predicting the outcome. It is our belief that those features found to be important by a majority of ML methods are likely truly predictive, and end up in our final feature set.
The lecture will focus more on the actual findings we and others have developed as a result of 'Big Data' / Hypothesis-Free science. Some of the interesting findings and pitfalls will be discussed.

Participant category: PhD Candiate/Research Program Student

Skull segmentation in 3-D CT head images – use of atlases for improvement of accuracy

Jacek Blumenfeld [(1)], Marek Kociński [(1)], Andrzej Materka [(1)], Arvid Lundervold [(2,3)]

jacek.blumenfeld@dokt.p.lodz.pl

1. Institute of Electronics, Lodz University of Technology, Poland
2. Neuroinformatics and Image Analysis Laboratory, Department of Biomedicine, University of Bergen, Bergen, Norway
3. Department of Radiology, Haukeland University Hospital, Bergen, Norway

Introduction In computed assisted surgery, CT images can be used to visualize three-dimensional (3-D) regions of interest (ROIs), such as individual bones or skull as a whole. A difficult task – image segmentation – is performed before. Segmented bone regions should accurately reflect the actual skull structure. The results of the segmentation are affected by CT image quality. This depends on the X-ray dose radiation, which is minimized in practice – leading to increased image noise, slice thickness and poor resolution. Reduced image quality causes segmentation errors. In the worst case, the picture may not contain certain bone structures (Fig. 1d). A number of bone tissue segmentation methods have been reported in literature. However, the segmented data differ significantly from actual structures due to limitations of the imaging techniques. Currently, segmented images are manually edited to fill in the missing parts. The aim of this work it to develop a method for automatic segmentation and post-edition of data, able to detect the missing fragments of bone tissues and their complement. Work is attempted to verify whether using atlases of bone structures can help correct visualization results. Methods and possible Implication 3-D cross-sectional CT images of the head were used for initial segmentation of skull, as a reference for further work. Adaptive tresholding was used for bone segmentation. The results of tresholding were corrected using the mathematical-morphology operations. A sample of segmentation result is shown in Fig. 1. The marching cubes algorithm with additional smoothing was used for visualization. The data obtained from the segmentation are over-segmented. The voxel values corresponding to the thick structures like nasal bones are close to the values of the soft tissues, hence the algorithm does not label them as bone. Next step of work is to create atlas of all neurocranium and viscerocranium bones. For this purpose high-resolution 3-D CT images of head are being collected. Besides voxels information, the atlas data should contain dependences between the structures (vicinity, interconnections) and descriptors of bone structure. Those will be used in addition to the segmentation results to detect possible image errors. The main challenge is to make the algorithm distinguish errors caused by image imperfection from the actual properties of the subject's tissue.

See image on next page.

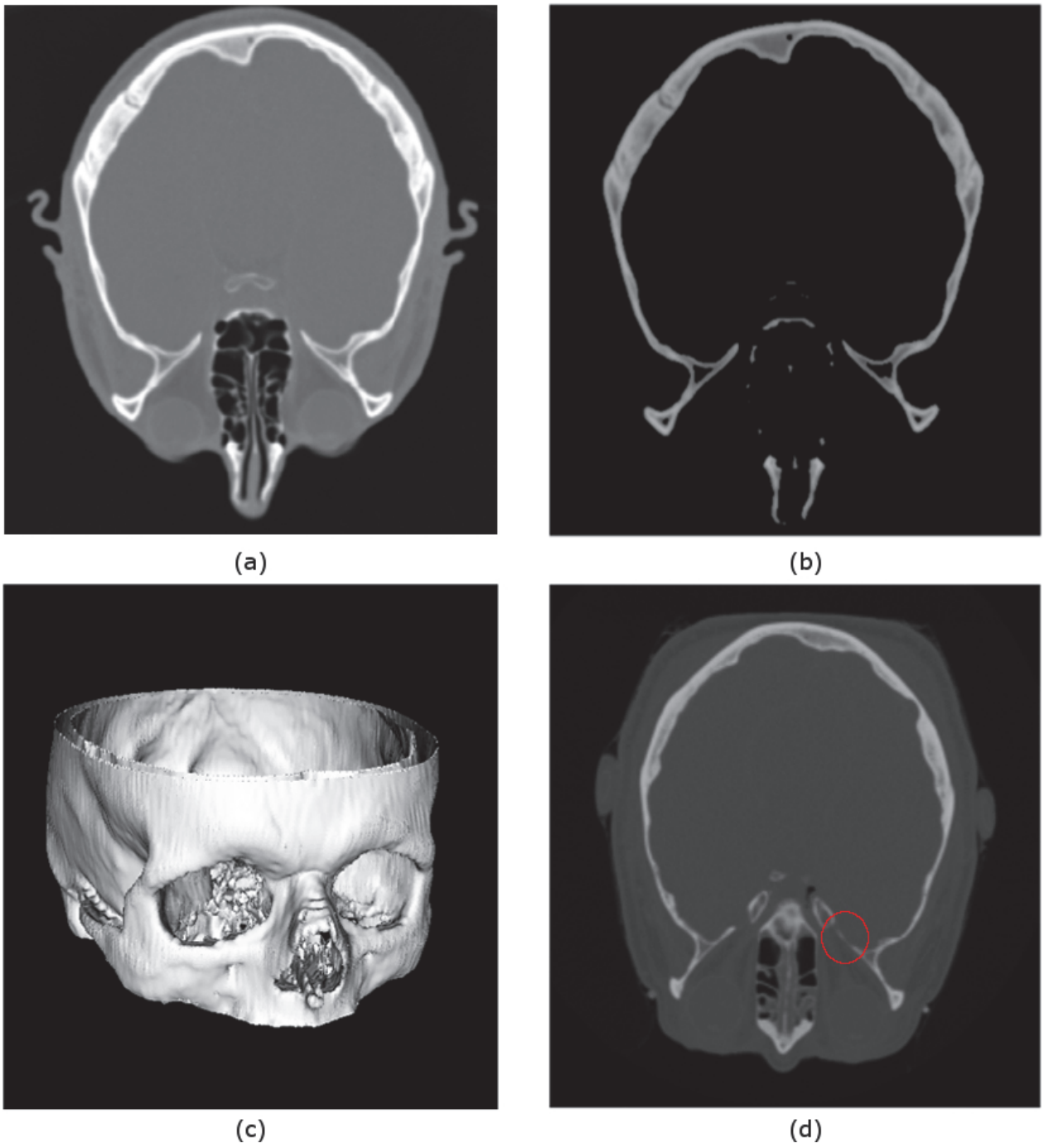

Head CT image (voxels size: 0.47mm x 0.47mm x 1mm) before segmentation (a), after segmentation (b), visualization of the skull based on segmented data (c). Slice of lower resolution CT image (voxels size: 1mm x 1mm x 1mm)

Participant category: PhD Candiate/Research Program Student

Poroelastic regularization of image registration

Erik Hanson [1,2], Erlend Hodneland [2], Antonella Z. Munthe-Kaas [1], Arvid Lundervold [2,3], Jan Nordbotten [1]

erik.hanson@math.uib.no

1. Department of Mathematics, University of Bergen
2. Department of Biomedicine, University of Bergen
3. Department of Clinical Medicine, University of Bergen,

Introduction: Image registration is an important processing step in several medical imaging applications, in particular analysis of image sequences corrupted with patient or organ movement. The mathematical nature of the problem is in general ill-posed, thus a suitable regularization term is highly required. The role of the regularization term is to reduce the number of possible outcomes to a set of physically admissible deformations. Classically, linear elasticity is applied as a regularization term, modeling the tissue as a linearly deformable object. However, this model does not account for the porous properties of human tissue. In the proposed project we model the deformation of human kidney as a porous material. This approach is expected to improve the model for deformation of human tissue compared to linear elasticity. Methods: Starting out with the model for linear elasticity we add Darcy's law for flow and the continuity equation for fluid mass balance. This results pointwise in four poroelastic equations for the combined deformation and pressure field. We use normalized gradients as a data term in the registration. This will act as a force term in the poroelastic system. The resulting nonlinear system of equations is solved in two steps, first approximating the linear system for a fixed force, and then updating the force based on the current deformation approximations. The two steps are combined in an alternating scheme converging to a desirable solution. Results: Applied to a data set of ten DCE-MRI time series of human kidneys, we successfully model the combined deformation and pressure field during patient motion. Our results demonstrate that the poroelastic deformation model gives lower temporal variation of the measured signal compared to linear elasticity, which is an indicator for improved registration. Discussion: The proposed approach is novel and represents a physically more realistic model for deformation of human tissue. Our numerical experiments indicate that the poroelastic effect is not negligible for the deformation and pressure gradients experienced in human kidney during patient motion in the MRI scanner. The proposed model is expected to improve the overall registration accuracy and thereby improve the post-processing steps like estimation of physiological parameters such as perfusion.

Participant category: PhD Candiate/Research Program Student

Clustered Compressive Sensing in Medical Imaging using Bayesian framework

Solomon Tesfamicael [(1)], Faraz Barzideh [(1)]

tesfamic@iet.ntnu.no

1. IET, NTNU

This paper provides clustered compressive sensing (CCS) based image processing using Bayesian framework applied to medical images. Some images, for example like magnetic resonanse images (MRI) are usually very weak due to the presense of noise and due to the weak nature of the signal itself. Compressed sensing (CS) paradigm can be applied inorder to boost such signals. We applied CS paradigm via Bayesian framework. Using different sparse prior informations and in addition incorprating the special structure that can be found in sparse signal improves image processing. This is shown in the results of this paper. Then first, we applied our analysis on Shepp-logan phantom and then to MRi data. The results show that applying the clustered compressive sensing give better results than the non clustered version.

See image on next page.

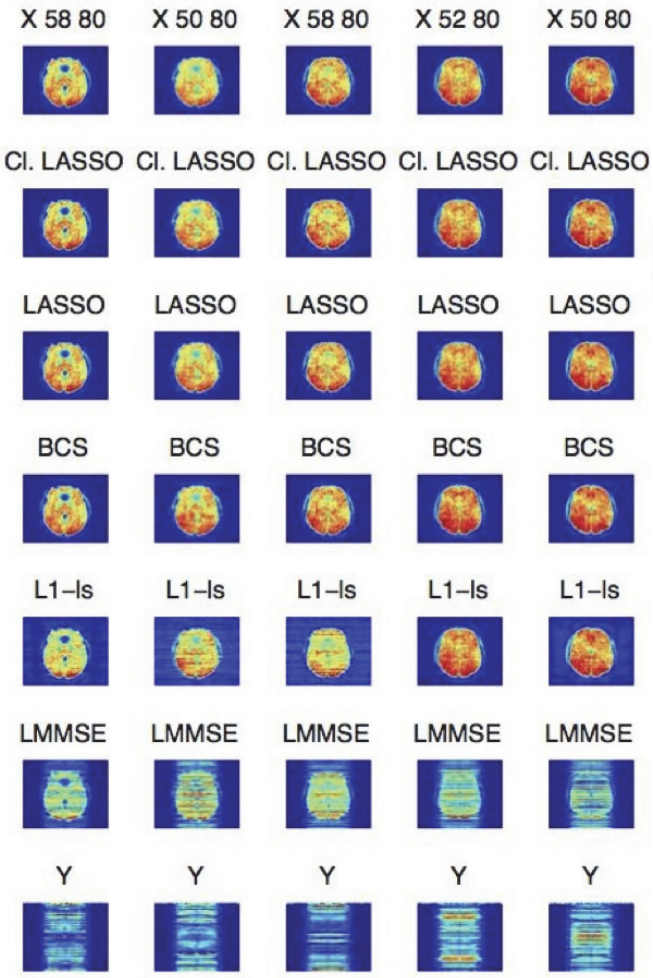
X 58 80
X 50 80
X 58 80
X 52 80
X 50 80
Cl. LASSO
Cl. LASSO
Cl. LASSO
Cl. LASSO
Cl. LASSO
LASSO
LASSO
LASSO
LASSO
LASSO
BCS
BCS
BCS
BCS
BCS
L1–ls
L1–ls
L1–ls
L1–ls
L1–ls
LMMSE
LMMSE
LMMSE
LMMSE
LMMSE
Y
Y
Y
Y
Y

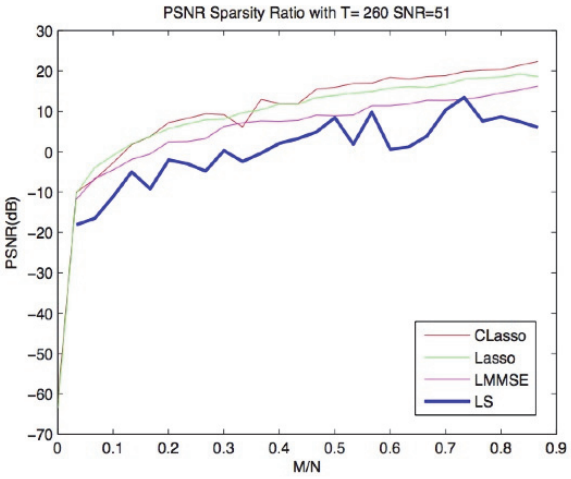
PSNR Sparsity Ratio with T= 260 SNR=51
PSNR(dB)
M/N
CLasso
Lasso
LMMSE
LS

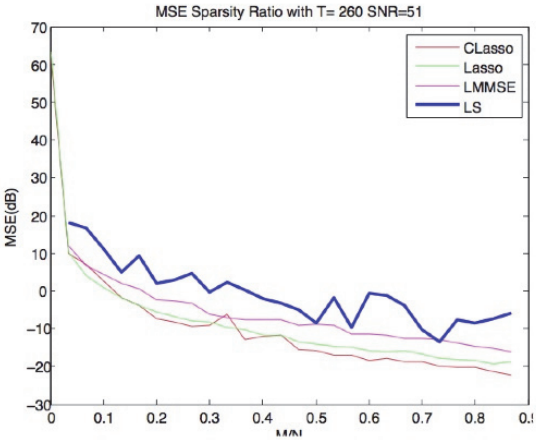
MSE Sparsity Ratio with T= 260 SNR=51
MSE(dB)
CLasso
Lasso
LMMSE
LS

Participant category: PhD Candiate/Research Program Student

Biomedical images segmentation based on Chan-Vese level-set approach

Tomasz Wozniak [(1)]

tomasz.wozniak11@gmail.com

1. Institute of Electronics, Lodz University of Technology, Poland

1. Introduction: Image segmentation is usually a crucial step in the whole analysis process. It is especially important in the case of medical images since segmentation efficiency defines quality of medical diagnosis support system. This work describes level-set method based on Chan-Vese mathematical model [1] and presents the examples of segmentation results. This technique is versatile and widely used for analysis of different types of biomedical images. Since LS technique is rather time consuming, the algorithm was implemented on the GPU using CUDA technology. 2. Methods: The main idea in level-set active contour model is to iteratively evolve a curve that is controlled by some parameters estimated from the image. The motion of the curve is obtained by solving the curve evolution partial differential equations (PDE) [1], adapted in this study to three-dimensional data space. Finally, the curve ends its evolution by fitting to objects' boundaries within the given image. Analysis of MR image with resulution of 704x704 with 96 slices using Intel Core i7-4700MQ processor took 3 hours. In the final implementation CUDA technology for nVidia GeForce GTX 760M was applied reducing segmentation time about 20 times. 3. Results: Fig. 1 presents segmentation results of two biomedical images obtained by different medical imaging modalities techniques. Left contrast MR T2 image (MIP) shows segmentation results of small blood vessels in hands. The research was conducted at the Institute of Electronic, Technical University of Lodz and Department of Diagnostic Imaging, Medical University of Lodz. Right multi-photon excitation microscopy image (MIP) presents segmented neural cell; it was provided by Biomedicine Department, University of Bergen. 4. Discussion: It is possible to build fast and effective algorithm that allows analyzing different types of biomedical images. However, further development is required. The final version of the software tool should facilitate image pre-processing (noise reduction, thresholding etc.) that improves segmentation results significantly. In addition, the application should also include a 3D visualization tool, which would be helpful in assessing quality of performed segmentation. Acknowledgements: The project has been funded by National Science Centre, Poland (decision No. DEC-2013/08/M/ST7/00943). References: 1. Chan, T. F., Vese, L. A.: Active Contours Without Edges. IEEE Transaction on Image Processing, 10(2), 2001, pp. 266-277

See image on next page.

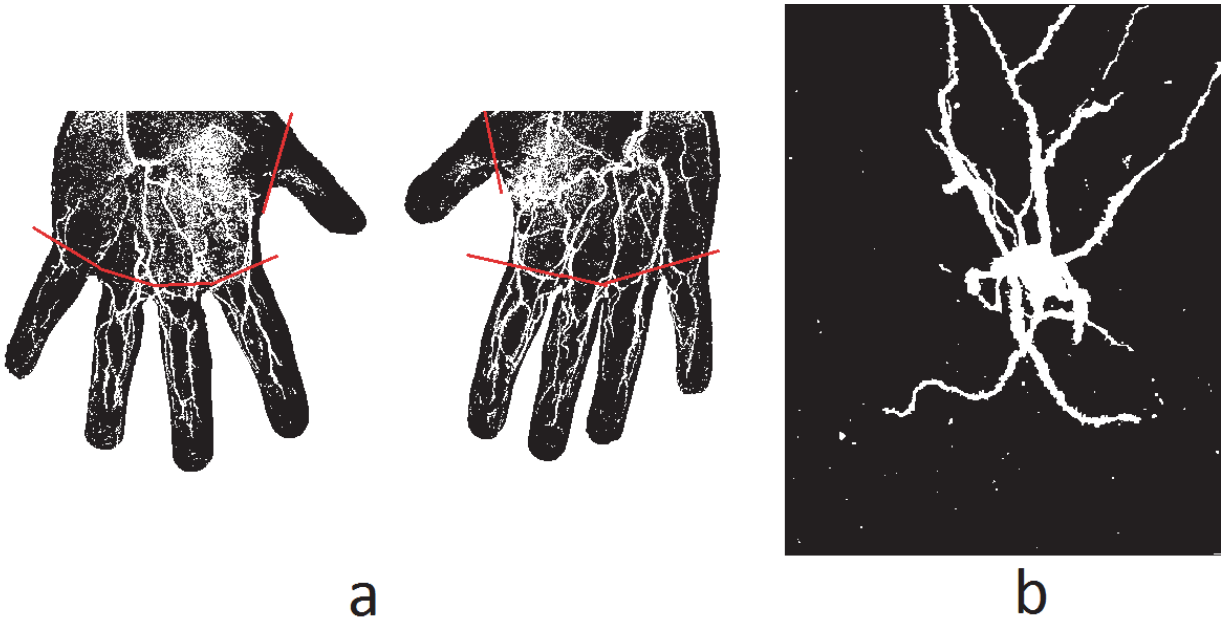

MIP of segmentation result of small blood vessels in fingers (a) and MIP of semgentation neural cell (b)

Participant category: Invited speaker

Biomedical Image Analysis based on Computational Registration Methods

João Manuel R. S. Tavares [1]

tavares@fe.up.pt, www.fe.up.pt/~tavares

1. Instituto de Engenharia Mecânica e Gestão Industrial, Departamento de Engenharia Mecânica, Faculdade de Engenharia, Universidade do Porto, Portugal

Keywords: Image Matching, Image Alignment, Image Fusion, Spatio-Temporal Registration

Abstract

Image registration, which has become a paramount research topic, is the process of transforming an image so that the associated entities are properly adjusted to the homologous entities in a second image (Figure 1). Such transformations have not only been applied to static bi-dimensional (2D) and tridimensional (3D) images, but also to 2D and 3D image sequences. For example, in Medical Imaging, computational methods of image registration have been assuming an essential role in supporting enhanced image-based diagnosis by addressing: the automatic identification of regions of interest in images (i.e. image segmentation), the fusion of information acquired by different imaging systems (i.e. image fusion), the more effective follow-up of organs and pathologies, and the definition of the best plans in computer-assisted surgery or in radiotherapy treatments, among other roles [1]. Hence, the computational registration of medical images is an extremely useful tool for clinicians and researchers since, after the accurate registration of the data involved, tasks such as shape reconstruction, comparison of a given clinical case with previous cases are facilitated and can be performed with less subjectivity. Moreover, the identification of regions of interest and information fusion can be handled automatically.

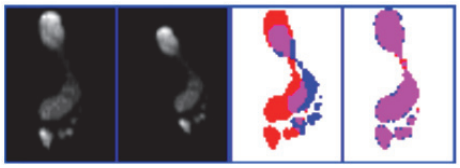

Figure 1 – Registration of two plantar pressure images: original images, and the two plantar pressure regions overlapped (in pseudo-colors) before and after the registration process [1, 12].

Other topics of image analysis are usually associated to image registration, including: image matching, i.e., the searching for correspondences between related images [2-6], similarity measurements, optimization, and image interpolation, especially due to the application of the registration transformations in the image discrete domain [1], Figure 2.

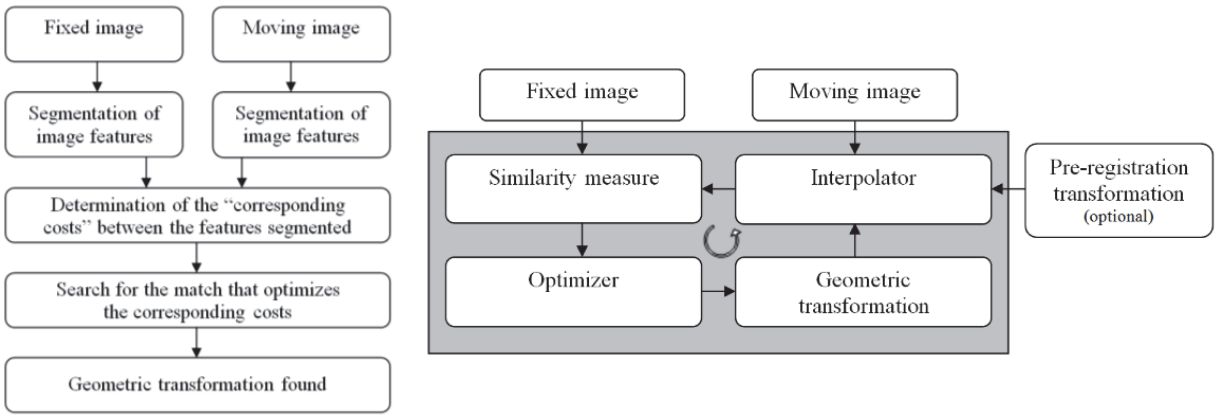

Figure 2 – Topics usually considered in image registration methodologies based on the matching of features (on the left) and based on the optimization of a similarity measure (on the right) [1].

During this presentation, the topic of medical image registration is going to be introduced; computational methodologies for matching and registering static images and image sequences that we have developed are going to be described; and application of cases involving static images, image sequences and images acquired by different medical imaging modalities are going to be presented and discussed [2-15]. The experimental examples that will be presented and discussed include the registration and analysis of plantar pressure in static images and in image sequences [4-13], the computer aided diagnosis of Parkinson´s disease based on I-123-FP-CIT SPECT brain images [14], and the enhanced 3D reconstruction of organs, in this case the bladder, in medical images acquired from different angles [15], Figure 3.

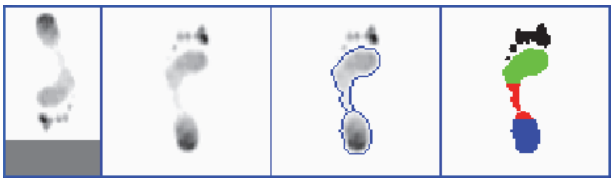

a)

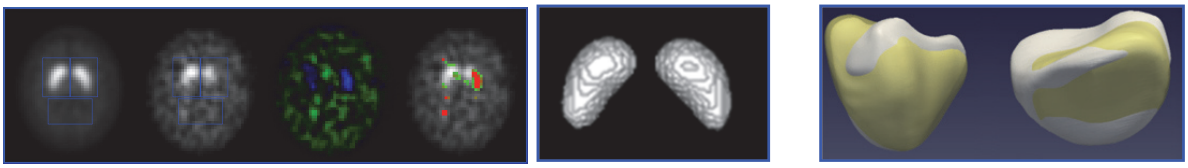

b) c)

Figure 3 – Examples of biomedical image analysis based on computational methods of image registration: a) original plantar pressure image, image after size, position and orientation normalization, segmentation of the main plantar region and identification of the important plantar regions based on a template image for the left foot [9]; b) identification of the ROIs in SPECT brain images and statistical comparisons relatively to population representative templates and 3D reconstruction of the ganglia basal [14], c) 3D reconstruction of the bladder from magnetic resonance images of the axial and sagittal planes [15].

Acknowledgments

The works that will be presented here have been partially developed in the scope of the project "A novel framework for Supervised Mobile Assessment and Risk Triage of Skin lesions via Non-invasive Screening", with reference PTDC/BBB-BMD/3088/2012, financially supported by Fundação para a Ciência e a Tecnologia (FCT) in Portugal.

References

[1] F.P.M. Oliveira, J.M.R.S. Tavares. Medical Image Registration: a Review. Computer Methods in Biomechanics and Biomedical Engineering 17(2):73-93, 2014
[2] F.P.M. Oliveira, J.M.R.S. Tavares. Matching Contours in Images through the use of Curvature, Distance to Centroid and Global Optimization with Order-Preserving Constraint. Computer Modeling in Engineering & Sciences, 43(1):91-110 2009.
[3] F.P.M. Oliveira, J.M.R.S. Tavares. Algorithm of dynamic programming for optimization of the global matching between two contours defined by ordered points. Computer Modeling in Engineering & Sciences 31(1):1-11, 2008.
[4] J.M.R.S. Tavares, J. Barbosa, A.J. Padilha, Matching Image Objects in Dynamic Pedobarography. RecPad 2000 - 11th Portuguese Conference on Pattern Recognition, Porto, Portugal, 11-12 May 2000.
[5] J.M.R.S. Tavares, L.F. Bastos. Improvement of modal matching image objects in dynamic pedobarography using optimization techniques, Progress in Computer Vision and Image Analysis, 73, World Scientific, pp. 339-368, 2010.
[6] L.F. Bastos, J.M.R.S. Tavares. Matching of Objects Nodal Points Improvement using Optimization. Inverse Problems in Science and Engineering 14(5):529-541, 2006.
[7] F.P.M. Oliveira, J.M.R.S. Tavares. Enhanced Spatio-Temporal Alignment of Plantar Pressure Image Sequences using B-splines. Medical & Biological Engineering & Computing 51(3):267-276, 2013.
[8] F.P.M. Oliveira, J.M.R.S. Tavares. Registration of Plantar Pressure Images. The International Journal for Numerical Methods in Biomedical Engineering 28(6-7):589-603, 2012.
[9] F.P.M. Oliveira, A. Sousa, R. Santos, J.M.R.S. Tavares. Towards an Efficient and Robust Foot Classification from Pedobarographic Images. Computer Methods in Biomechanics and Biomedical Engineering 15(11):1181-1188, 2012.
[10] F.P.M. Oliveira, A. Sousa, R. Santos, J.M.R.S. Tavares. Spatio-temporal Alignment of Pedobarographic Image Sequences. Medical & Biological Engineering & Computing 49(7):843-850, 2011.
[11] F.P.M. Oliveira, J.M.R.S. Tavares. Novel Framework for Registration of Pedobarographic Image Data, Medical & Biological Engineering & Computing 49(3):313-323, 2011.
[12] F.P.M. Oliveira, T.C. Pataky, J.M.R.S. Tavares. Registration of pedobarographic image data in the frequency domain. Computer Methods in Biomechanics and Biomedical Engineering 13(6):731-740, 2010.
[13] F.P.M. Oliveira, T.C. Pataky, J.M.R.S. Tavares. Rapid pedobarographic image registration based on contour curvature and optimization. Journal of Biomechanics 42(15):2620-2623, 2009.
[14] F.P.M. Oliveira, D.B. Faria, D.C. Costa, J.M.R.S. Tavares. A robust computational solution for automated quantification of a specific binding ratio based on [123I]FP-CIT SPECT images. The Quarterly Journal of Nuclear Medicine and Molecular Imaging 58(1):74-84, 2014.
[15] Z. Ma, R.N. Jorge, T. Mascarenhas, J.M.R.S. Tavares. A Level Set Based Algorithm to Reconstruct the Urinary Bladder from Multiple Views. Medical Engineering & Physics 35(12):1819-1824, 2013.

Abstracts for session
Visualization and modelling

Abstracts are organized in the order of presentations

Interactive Visual Analysis of Cohort Study Data

Paul Klemm, Bernhard Preim*
Department of Simulation and Graphics, University of Magdeburg, Germany

ABSTRACT

Epidemiological population studies impose information about a set of subjects (a *cohort*) to characterize disease-specific risk factors. Cohort studies comprise heterogenous variables (*features*) describing the medical condition as well as demographic and lifestyle factors. The data are analyzed using a priori defined hypotheses to find statistically significant correlations between features (*associations*). Modern cohort studies incorporate medical image data. The statistically driven epidemiological workflow only allows to determine *associations* between image-derived metrics, such as distances extracted from landmarks of the segmentation model.

In this talk, we present methods for analyzing image-centric cohort study data with focus on assessing influences on organ shape. To account for epidemiological key requirements such as reproducibility and statistical resilience of results, the epidemiological workflow is analyzed and divided into different steps. Based on this analysis, an Interactive Visual Analysis (*IVA*) approach is proposed that enables epidemiologists to examine both image-based as well as non-image data, e.g., sociodemographic features and attributes derived from the image data. This approach enables hypotheses validation and generation by incorporating human pattern recognition as well as data mining methods. Using all reliable information from the image segmentation linked to non-image features aims to unveil *associations* by applying an iterative analysis approach.

Index Terms: J.3 [Life and Medical Sciences]: Health—

1 EPIDEMIOLOGICAL BACKGROUND AND ADDRESSED PROBLEMS

Epidemiology characterizes the influence of causes to disease and health conditions of defined populations. Cohort studies are population-based studies involving usually large numbers of randomly selected individuals and comprising numerous attributes, ranging from self-reported interview data to results from various medical examinations, e.g., blood and urine samples (*features*). Since recently, medical imaging has been used as an additional instrument to assess risk factors and potential prognostic information. The statistically driven epidemiological workflow only allows to determine *associations* between image-derived metrics, such as distances extracted from landmarks of the segmentation model.

Epidemiological data is analyzed for statistical resilience of features associated with an epidemiological outcome of a disease. For example, when clinical observations suggest a correlation between breast fat content and breast cancer in women, these two features are extracted from the data and correlated. *Confounders* are features, which bias an epidemiological outcome next to analyzed features. Age for example strongly correlates with most types of cancer and therefore a result needs to be age-adjusted.

*e-mail: bernhard.preim@ovgu.de

To meet requirements for reproducibility and comprehensibility it is essential to understand the epidemiological workflow. Visual analysis of cohort study data aims to extend the standard epidemiological workflow for the following aspects:

- Enable epidemiologists to examine both image-based as well as non-image data, e.g., sociodemographic features and attributes derived from the image data.
- Provide methods that assess local variations of shape of a anatomical structure under different medical related or lifestyle influences.
- Visual validation of presumptions and hypothesis about heterogenous features influencing various diseases using appropriate visualizations.
- Use of data mining tools such as clustering or the principal component analysis provides possibilities to group subjects regarding shape or other features.

To design methods suitable for application in the epidemiological context it is essential to understand how epidemiologists work. This workflow is briefly described in the following section.

1.1 Epidemiological Workflow

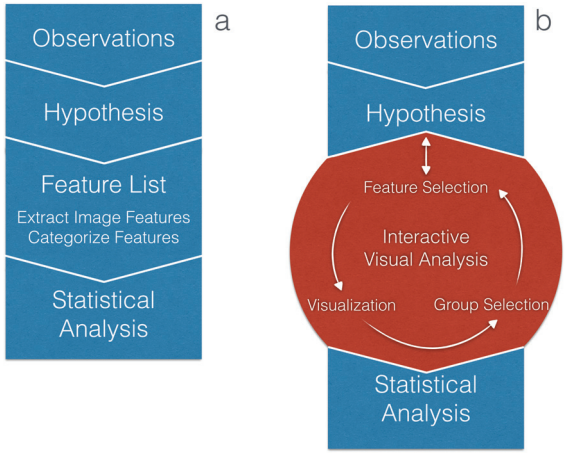

Figure 1: Interactive Visual Analysis (*IVA*) tools complement parts of the epidemiological workflow instead of replacing them. The appropriate combination of statistical and interactive-driven analysis shows promising potential to unveil the information in the data. (a) shows the standard epidemiological workflow, (b) the *IVA* supported one.

Figure 1 presents the epidemiological workflow inspired by Thew and colleagues [4]:

1. A hypothesis is derived from observations made by clinicians in their daily routine.
2. A set of features depicting conditions affected by the hypothesis is compiled accordingly.

3. Confounding features are identified and taken into account (for example using stratification).

4. Statistical methods, such as regression analysis, assess the association of selected features with the investigated disease.

Reproducibility of results is an epidemiological key requirement. It is difficult to achieve, since many physicians are involved when thousands of test persons are examined and interviewed. If the data acquisition process changes, an information bias is introduced to the data, hampering inference in and between acquisition cycles.

In longitudinal cohort studies, grouping subjects using epidemiological features is essential in order to allow per-group risk determination. Grouping depends on the underlying hypothesis. Age for example is divided into groups (e.g. in 20 year steps) when investigating its influence on a condition. These groups strongly depend on the condition of interest. Thus, there is no standard method for categorization.

To determine whether a subject is prone to be affected by a certain disease, *relative risks* are expressed through the evaluation of p-values, which indicate statistical significance. Graphic data representation is largely used to present results rather than gaining insight.

1.2 Epidemiological Data

Epidemiological data are highly heterogenous and incomplete. Information about medical history and examinations, genetic conditions, geographical data, questionnaire results and image data yield a complex data space for each subject. For ethical, legal or medical reasons some features cannot be gathered for each subject. The most obvious example are women-specific questions about menstrual status or number of born children. Follow-up examinations or questions about conditions like medications taken after a diagnosed disease also yield features only available for a small amount of subjects.

Indicators for medical conditions as well as questions about a subject's lifestyle are also often *dichotomous*–they have two manifestations (*Yes* or *No*). Dichotomous data can also be derived by aggregating features to yield only two manifestations (e.g. subjects younger or older than 50 years). Medical examinations mostly comprise categorical (e.g. levels of back pain) and continuous values (e.g. age or body size).

Image analysis. Decisions have to be made on how image data are *compared* and *quantified*. Segmentation masks representing the voxels of an anatomical structure would be ideal, since many different key figures, e.g., volume, largest diameter or aspect ratio, can be derived from them. Since reliable and efficient segmentation techniques for these data are not available in general, epidemiologists are forced to measure the data by hand, which is a very tedious work with respect to the number of necessary landmarks and the number of subjects. Information derived by landmarks, such as top and bottom point of a vertebra, are by far not as expressive and versatile as segmentation masks describing its whole shape. They are also prone to a high inter-observer variability and are hard to reproduce. This gains even more importance when analyzing multiple time steps. Morphometric information from landmarks comprises thickness, diameter or length of a structure as well as grey value distribution in an area (used for determining the type of tissue) [3].

2 Methods

This talk presents the current results of a project funded by the German Research Council within their "Scaleable Visual Analytics" priority programme. The project "Visual Analysis in Public Health" is divided into two sets of work packages, one set related to image analysis (automatic object detection and segmentation) and the other to visualization and less to data analysis. In particular, we focus on the following aspects:

- Building an Interactive Visual Analysis (IVA) system which is based on analysis of the epidemiological workflow to allow rapid hypothesis validation- and generation.
- Combine shape variability visualization techniques with information visualizations of non-image data.
- Provide similarity measures and visualizations that involve associations between features out of the focus of the epidemiologists to allow for hypothesis generation [1].
- Use data mining to derive shape-based groups of subjects using clustering techniques [2].

The proposed methods are introduced as part of an Interactive Visual Analysis approach presented in the following section. For all activities, we employed a lumbar spine data set from the Study of Health in Pomerania [5]. It consists of 6.753 subjects from two cohorts with 77 parameter compiled by domain experts. The image data was segmented using a tetrahedron-based finite element model [2].

2.1 Interactive Visual Analysis for Cohort Study Data

The proposed *IVA* workflow consists of three major steps: Feature selection, visualization and brushing. A hypothesis-driven analysis usually starts with the selection of features. A feature selection from a shape-based clustering creates shape groups. *Hypothesis generation* with focus on image data starts with a shape-based clustering. The feature is mapped using an automatically chosen visualization appropriate for its data type. The visualization techniques have to combine both image-and non-image data in order to set domain and range data in relation to each other. In our system, the visualization can either be brushed or new features can be added to the analysis. Brushing methods are subdivided using the previously described *IVA* patterns. Brushed regions are treated like features as they divide the subject space just like categorical features. Selecting features also triggers a *multivariate analysis* using contingency values to highlight features associated with selected features. A sample workflow using interaction and visualization techniques can be seen in Figure 2.

2.2 Visualization and Analysis of Lumbar Spine Canal Variability

Hypothesis generation is triggered by suggesting interesting feature correlations based on organ shape [2]. This allows for assessment of shape groups, which can not be accomplished with standard epidemiological methods. Clustering using Agglomerative Hierarchical Clustering is carried out to form groups that exhibit low intra-group and high inter-group shape variability. The clusters are visualized by means of representatives to reduce visual clutter and simplify a comparison between subgroups of the cohort. Figure 3 shows a clustering results for subjects with lumbar back pain which leads to interesting results regarding major shape classes as well as potentially pathological outliers.

3 Future Work and Ongoing Research

This work may be extended in several ways involving research in InfoVis, SciVis, Visual Analytics and data mining with strong focus on statistics.

3.1 Multi-parameter Regression Visualization

Regression analysis estimates the relationship between variables. Linear relationships between parameter are often visualized by plotting both of them in a scatterplot and draw a regression line into it. This technique is only appropriate for relating two continuous parameters at once. A technique combining regression analysis of multiple heterogenous parameters could provide a quick visual

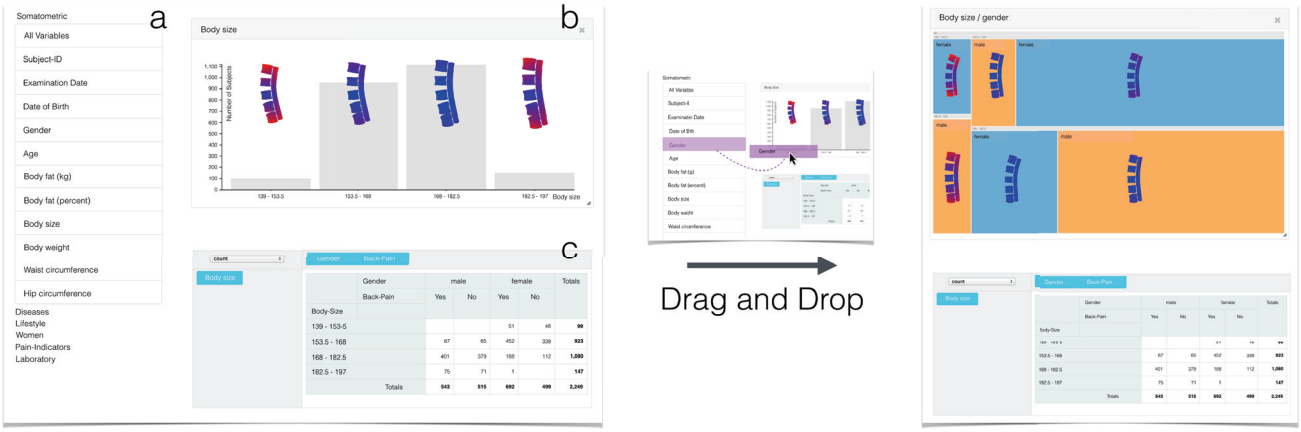

Figure 2: (Left) Screenshot from the *IVA* system, which is divided as follows: (a) The sidebar containing all features as well as the groups defined in the analysis process; (b) the canvas area where features can be added via drag and drop and the visualization can be chosen automatically according to the data type; (c) the interactive pivot table showing the exact numbers for each displayed feature combination. The data displayed is used to analyze the lumbar spine. Features can be added freely on the canvas via drag and drop. Dropping the *age* parameter on the already plotted *body size* container creates a mosaic plot combining both features (right).

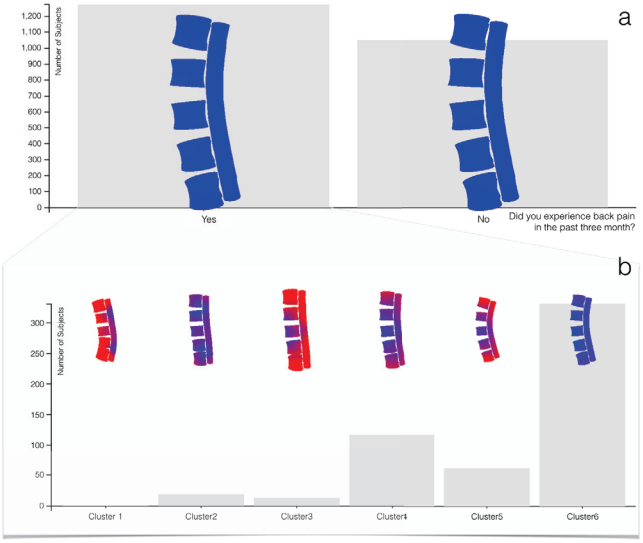

Figure 3: (a) Dichotomous questionnaire answer to "*Did you experience back pain in the past three months?*". Mean shapes between the groups show no difference. (b) Shape-based clustering for all subjects who suffered from back pain yields 6 groups. Note that the difference in subject count is due to the missing shape information for some subjects.

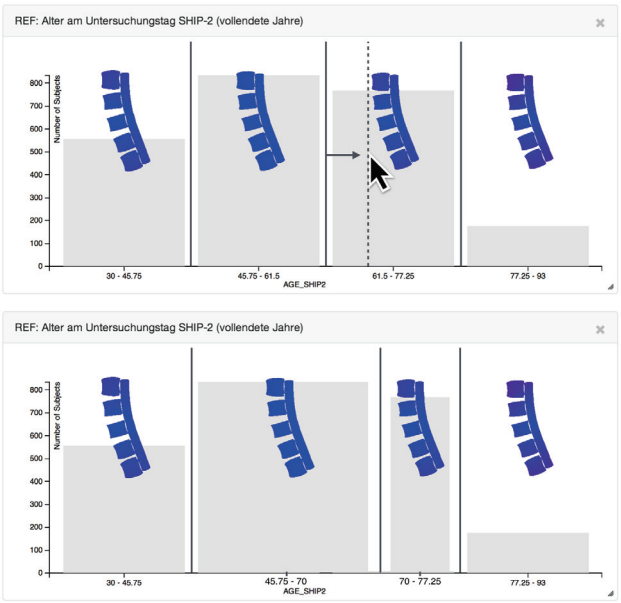

Figure 4: Adaptive discretization via brush handles on a bar chart representation of age overlaid by mean shape of the lumbar spine.

feedback about parameter correlations. Since there are many different distribution functions known to epidemiologists, the regression analysis also has to consider different regression functions.

3.2 Integrate Feature Discretization with Information- and Shape Visualization

In epidemiology, continuous features such as age, body size or blood fat values are usually discretized for statistical analysis. For age this could be groups of subjects older or younger than 50 years. How the data is discretized is related to the currently investigated hypothesis. If an Interactive Visual Analysis systems aims to support fast hypothesis validation, an intuitive way of variable discretization has to be provided.

The presented methods in Figure 2 need to be extended by including dynamic brushes to information visualization which allow for fast adaption of the discretization. This approach takes full advantage of the concept of combining information visualization of non-image data and mean-shape representation of the selected groups. A conceptual example for bar charts can be seen in Figure 4. Applying this technique to more complex visualization techniques such as mosaic plots is not as easy to accomplish. A possible solution is a set of appropriate visualizations ordered as a visualization matrix as small multiples. Enough space to render mean shape representations limits the minimum size of the plots.

3.3 Principal Component Analysis Guided Subject Separation

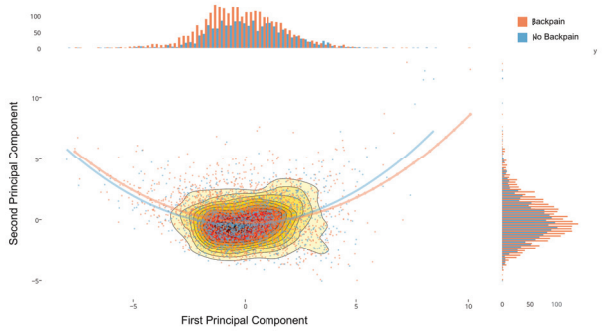

Figure 5: Scatterplot of the first two principal components derived from a PCA of all metric variables associated with the lumbar spine dataset (17 non-image variables, 9 image-derived describing the lumbar spine shape). Subjects reporting back pain are mapped to orange color, those who do not blue. The difference between the subject groups remains very little.

The principal component analysis (PCA) can be used to obtain feature spaces with high variance. It also assesses the influence of each included feature in this feature space. Figure 5 shows a scatterplot of the first two principal components of the lumbar spine data set. Dichotomous variables indicating pathologies can be used to group subjects and to check whether they can be distinguished in the resulting feature space and which principal components can be used best for this distinction. The results shown are preliminary and subject of active research.

3.4 User Guidance using Similarity Measures

Visualizing the covariance matrix is a first step to guide the attention of epidemiologists to feature associations, they did not expect, triggering a new cycle of the Interactive Visual Analysis loop. New ways are desirable which enable a more intuitive way to incorporate associations directly into the information visualizations. Currently this requires to use huge covariance matrices, which occupy a large portion of screen space.

Comparison between categorical (or discretized metric) features is essential in the epidemiological application domain. A feasible approach to this problem are parallel sets, which are a parallel coordinates inspired visualization. Category frequency is mapped rather than the data points. Selecting an attribute will map each category to a distinct color so that they can be traced through all visualized dimensions. Highlighting a category may be accomplished by drawing the selected category in a higher saturation leading to a pop-out effect. It is also useful to display a histogram for the selected category annotated with statistical information. Zooming into a category will only display the particular box on an axis and make more room for connections to other axes.

Since parallel sets quickly become cluttered with increasing number of dimensions and manifestations, the number of comparable features in one plot is limited. I want to improve the existing visualization technique to better support categorical feature comparison.

Acknowledgements

SHIP is part of the Community Medicine Research net of the University of Greifswald, Germany, which is funded by the Federal Ministry of Education and Research (grant no. 03ZIK012), the Ministry of Cultural Affairs as well as the Social Ministry of the Federal State of Mecklenburg-West Pomerania. Whole-body MR imaging was supported by a joint grant from Siemens Healthcare, Erlangen, Germany and the Federal State of Mecklenburg-Vorpommern. The University of Greifswald is a member of the "Centre of Knowledge Interchange" program of the Siemens AG. This work was supported by the DFG Priority Program 1335: Scalable Visual Analytics.

References

[1] P. Klemm, L. Frauenstein, D. Perlich, K. Hegenscheid, H. Völzke, and B. Preim. Clustering Socio-demographic and Medical Attribute Data in Cohort Studies. In *Bildverarbeitung für die Medizin (BVM)*, pages 180–185, 2014.

[2] P. Klemm, K. Lawonn, M. Rak, B. Preim, K. D. Tönnies, K. Hegenscheid, H. Völzke, and S. Oeltze. Visualization and analysis of lumbar spine canal variability in cohort study data. In *Proc. of Vision, Modeling and Visualization*, pages 121–128, 2013.

[3] B. Preim, P. Klemm, H. Hauser, K. Hegenscheid, S. Oeltze, K. Toennies, and H. Völzke. *Visualization in Medicine and Life Sciences III*, chapter Visual Analytics of Image-Centric Cohort Studies in Epidemiology. Springer, 2014.

[4] S. Thew, A. Sutcliffe, R. Procter, O. de Bruijn, J. McNaught, C. C. Venters, and I. Buchan. Requirements Engineering for e-Science: Experiences in Epidemiology. *Software, IEEE*, 26(1):80–87, 2009.

[5] H. Völzke, D. Alte, C. Schmidt, et al. Cohort Profile: The Study of Health in Pomerania. *International Journal of Epidemiology*, 40(2):294–307, Mar. 2011.

Participant category: PhD Candiate/Research Program Student

Statistical shape model of the right ventricle for segmentation in 4D echocardiography

Jørn Bersvendsen [1, 2, 3], Stig Urheim [4], Fredrik Orderud [1], Eigil Samset [1,2,3]

jornb87@gmail.com

1. GE Vingmed Ultrasound
2. University of Oslo
3. Center for Cardiological Innovation
4. Oslo University Hospital

Introduction: Research on segmentation methods of the right ventricle has for a long time been neglected in favor of the left ventricle. However, as the right heart's role in cardiovascular diseases is being more widely recognized, interest in right ventricle segmentation is growing. Modeling of the right ventricle is inherently more challenging than the left ventricle, because of increased anatomical complexity and larger inter-patient variations. For echocardiography in particular, weak myocardial borders and a challenging acquisition makes the problem even harder. We aim to develop a geometrical model of the right ventricle that will support a robust and computationally efficient automatic segmentation method for 4D echocardiographic images. Methods: We propose to use a Doo-Sabin subdivision surface as the underlying geometrical representation of the right ventricle. This enables an anatomically accurate model with a compact parameterization, and inherently enforces regularization and C1 continuity. The surface is parameterized by 35 control vertices; 9 on the septum, 12 on the free wall, 5 at the tricuspid annulus, 8 at the outflow tract, and one at the apex. We derive the statistical modes of variation from manual segmentations of 12 short axis cine-MRI recordings each with 20 phases, including healthy subjects and patients with heart disease from an open access database [1]. For each patient and each phase, the endocardial borders in all slices were traced manually. The Doo-Sabin surface was then fitted by minimizing the sum of Euclidean distances between surface points and endocardial border using gradient descent optimization. Results: The dice similarity coefficient between the fitted subdivision representation and manual segmentation were 0.90 ± 0.030. Using the first 24 modes of variation, constituting at least 95 % of the total variance, the leave-one-out reconstruction point-point distances were 3.1 ± 1.4 mm. Conclusions: The proposed Doo-Sabin surface was well suited to represent the right ventricle, and using only 24 modes of variation resulted in acceptable reconstruction accuracy. References: [1] Radau P, Lu Y, Connelly K, Paul G, Dick AJ, Wright GA, "Evaluation Framework for Algorithms Segmenting Short Axis Cardiac MRI" The MIDAS Journal - Cardiac MR Left Ventricle Segmentation Challenge.

See image on next page.

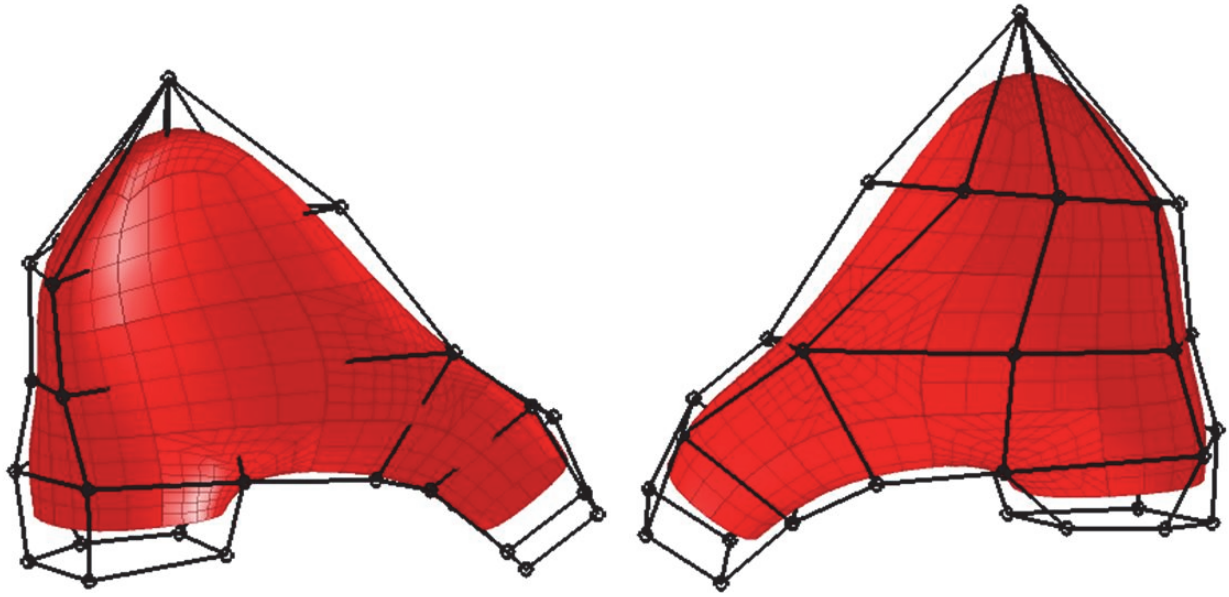

Subdivision surface viewed from septum and free wall sides respectively. The black lines are the control mesh parameterizing the surface. The red surface is the corresponding limit surface.

Participant category: PhD Candiate/Research Program Student

Multiscale Nonlocal Means method for Ultrasound despeckling

Lars Hofsøy Breivik [(1)], Sten Roar Snare [(1)], Hani Nozari Mirarkolaei [(1)], Erik Normann Steen [(2)], Anne H Schistad Solberg [(1)]

lhbreivik@gmail.com

1. University of Oslo Department of Informatics
2. GE Vingmed Ultrasound

Speckle noise is inherent in ultrasound (US) images and the main source of image degradation, causing reduced contrast and separability of anatomical structures. In this paper we propose a real-time multiscale despeckling filter based on the recently proposed nonlocal means (NLM) filter. We identify two major limitations of the classical NLM filter for ultrasound despeckling: Computational complexity and inability to distinguish speckle structure from signal. To simultaneously solve these two problems we propose an ultrasound tailored multiscale NLM filter. The classical NLM filter restores image pixels by a weighted averaging scheme where weights are determined by pixel neighborhood similarities in large search windows. Our proposed despeckling method applies a cascade of NLM filters from fine to coarse scale. With each new scale, the applied NLM filter is increasingly selective (structure preserving), and the size of its search window is increased. The number of samples examined per scale is constant, such that only sampling stride increases. The filter has been tested using an optimized OpenCL GPU implementation. It is applied to the US image prior to scan conversion to allow a more uniform filter response and better adaption to the point spread function of the imaging system. Our filter achieves consistent real-time frame rates above 60 frames per second on a mid-range GPU on real ultrasound images. Our results, as seen in the figure, show that areas of fully formed speckle (FFS) are effectively smoothed while structured anatomical details are preserved. FFS regions are increasingly smoothed through the scales, reducing the bias introduced by local spatial correlation in the speckle. In structured areas, the increasing selectivity of the filtering at higher scales limits the smoothing across edges and even small structured features. When compared to 5 other recent despeckling filters, including diffusion and NLM based approaches, our method performed comparably or favorably according to the Structural Similarity Index (SSIM), the Ultrasound Despeckling Assessment Index (USDAI) and the Peak Signal-to-Noise Ratio (PSNR) on Field 2 simulated images.

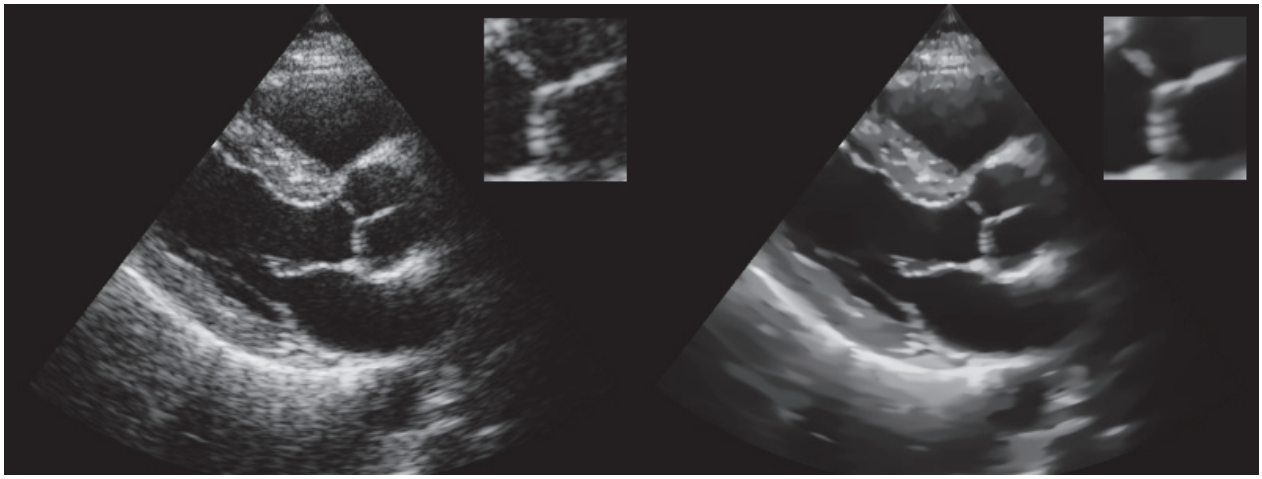

Participant category: PhD Candiate/Research Program Student

Automatic measurement of biparietal diameter with a portable ultrasound device

Naiad Hossain Khan [(1)], Eva Tegnander [(2,3)], Johan Morten Dreier [(2)], Sturla Eik-Nes [(2,3)], Hans Torp [(1)], Gabriel Kiss [(1)]

naiad.khan@ntnu.no

1. ISB, MI Lab and Department of Circulation and Medical Imaging, NTNU, Trondheim, Norway
2. National Center for Fetal Medicine (NCFM), St. Olavs Hospital, Trondheim, Norway
3. Department of Laboratory Medicine, Children's and Women's Health (LBK), NTNU, Trondheim, Norway

Knowledge of the exact gestational age and expected day of delivery is essential for providing optimal medical surveillance. Fetal biparietal diameter (BPD) computed by ultrasound has been shown to correlate well with gestational age (before week 22) or it can be used for detecting growth abnormalities, later in the pregnancy. We have been developing a portable ultrasound scanner (the Umoja scanner) that can be used by midwives in LMIC countries with limited ultrasound and technological expertise. The aim of this work was to develop a technique for automatized computation of BPD which can run on tablet devices. An ultrasound image containing a contour of a fetal head is recorded with the prototype scanner. The image is preprocessed: converted to grayscale, gain adjusted, smoothed, dilated/eroded and finally binary thresholded. The potential contour candidates and their Cartesian coordinates are identified by applying the Canny edge detector. Region candidates for the measurement are found by connected component analysis on the edge detection result. A line connecting the two most distant edges across the skull is computed. The original grayscale values along this line are used to identify the top and the bottom edge points which are used for measuring the BPD value. All image processing is performed using OpenCV (Open source Computer Vision), which is optimized for tablet devices. 27 ultrasound images suitable for BPD measurement were acquired by an experienced midwife and 9 student midwives with limited or no prior ultrasound experience, on 8 different fetuses from 18 to 34 weeks. Both manual (experienced midwife) and automatic BPD measurements were computed. The correlation plot and the error versus reference plot are shown in the figure, the mean error ± 1.96*STD was 0.72±3.62 [mm], while the correlation coefficient was R=0.9932. The automatic measurement failed in 4 cases. The overall computation time on a Nexus 10 tablet was 3.47 seconds, therefore our tool is suited for a portable device with limited computation power. The agreement of the proposed algorithm with the reference measurements is comparable to the interobserver agreement for BPD (2.9mm from literature study). Testing of the method on an extended dataset, including fetuses at different gestational ages is ongoing.

See image on next page.

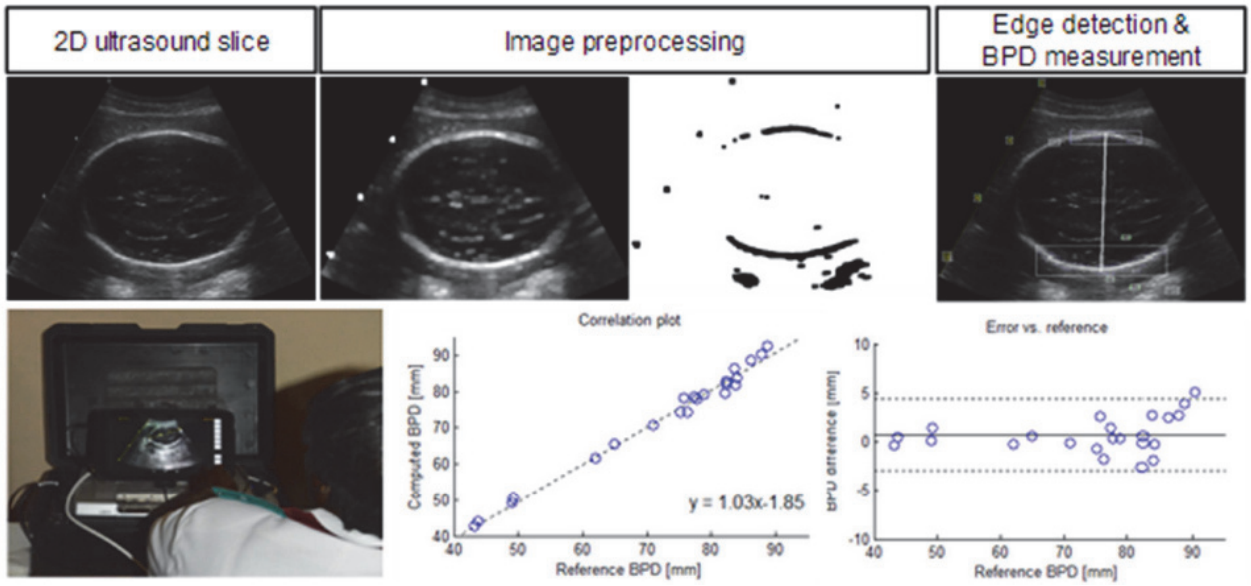
2D ultrasound slice
Image preprocessing
Edge detection & BPD measurement
Correlation plot
Computed BPD [mm]
Reference BPD [mm]
y = 1.03x-1.85
Error vs. reference
BPD difference [mm]
Reference BPD [mm]

Participant category: PhD Candiate/Research Program Student

Ultrasound transducers with an optical window

Torstein Yddal [1,2,4], Spiros Kotopoulis [2,1], Odd Helge Gilja [2,3], Michiel Postema [1,4]

Torstein@yddal.net

1. Department of Physics and Technology, University of Bergen, Allégaten 55, 5007 Bergen, Norway
2. Department of Physics and Technology, University of Bergen, Allégaten 55, 5007 Bergen, Norway
3. Department of Clinical Medicine, University of Bergen, Jonas Lies vei 65, 5021 Bergen, Norway
4. The Michelsen Centre for Industrial Measurement Science and Instrumentation, 5892 Bergen, Norway

Ultrasound is one of the most cost-effective deep tissue clinical imaging modalities. Near all ultrasound transducers are fabricated from piezoelectric materials that require metal surface electrodes, making the transducers opaque. With the increasing need for multi-modal and compact imaging and therapeutic tools new transducers fabrication techniques need to be evaluated. In our work we evaluate several designs that allow a large optical window in combination with ultrasonic propagation collinear to the imaging path. Three types of transducers were made based on a stacked design, in two different sizes. The optical windows were 20-mm and 10-mm with outer diameters of 50-mm and 38-mm respectively. The devices were characterised for acoustic bandwidth and sensitivity using a pulse receive technique. The acoustic power was measured using a custom made radiation force balance. The beam profile was measured using a three-dimensional scanning chamber with a mobile needle-hydrophone. The transient response waveform of a burst wave was captured using the needle hydrophone, and an FFT was performed to get the power spectrum to determine the linearity of the ultrasound generation of the transducer. The frequency response showed that these transducers had a large FWHM bandwidth of 56%. The field scans showed that the acoustic propagation pattern was very similar to traditional ultrasound transducers, yet the different constructions affected the focal distance and sidelobes. In addition surface scans, indicated that in all transducers glass window acted like an oscillating diaphragm generating ultrasound. The acoustic power measurements indicated that these devices could exceed acoustic powers of 16 W. Traditional ultrasonic imaging only requires several milliwatts whereas therapeutic application only require several watts. These transducers indicate their potential for multimodal imaging and therapy for example combining endoscopy with ultrasound surgery, or simultaneous ultrasound and bioluminescence imaging.

Participant category: Invited speaker

Tracer-kinetic modelling in renal MRI

Steven Sourbron [1]

S.Sourbron@leeds.ac.uk

1. University of Leeds, UK

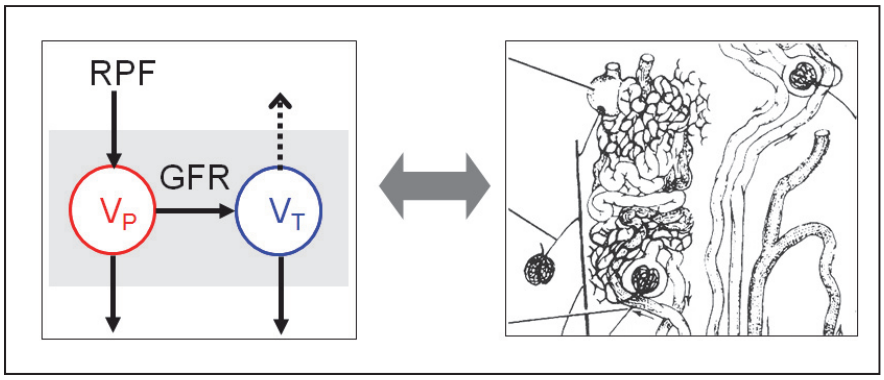

The past 10-15 years have seen a rapid expansion in the number of functional renal MRI methods [1], including diffusion-weighted imaging (DWI), Diffusion-Tensor Imaging (DTI), Intra-voxel Incoherent Motion (IVIM), Blood Oxygenation-Level Dependent MRI (BOLD), Sodium imaging, Elastography, Arterial Spin Labelling (ASL), and MR Renography (MRR). Apart from DWI, the latter is the most mature of these methods and closest to being translated into clinical routine.

The basic approach in MRR is identical to other Dynamic contrast-enhanced MRI (DCE-MRI), DCE-CT and dynamic nuclear medicine methods [2], and involves the rapid injection of an MR contrast agent followed by fast dynamic imaging (1-2s per acquisition). The MR signals are converted into tracer concentrations and the temporal structure of these data is analysed to produce values for important functional parameters such as Single-Kidney Glomerular Filtration Rate (SK-GFR), Renal Blood Flow (RBF), Filtration fraction, Tubular Mean Transit Time, etc.

A key ingredient in this approach is the tracer-kinetic model, which provides the link between the functional parameters and the temporal concentration patterns. These models are effectively extreme simplications of the complex internal structure of the kidney – which only include as free parameters those structural features which are effectively measurable. A key problem within the field of MRR at the moment is that different modelling traditions arose in the various groups that developed the field [3,4]. Due to differences in terminology and notations it is often difficult to see how these models relate to each other and under which conditions they are to be applied.

The purpose of this talk is provide an intuitive physical classification of the various tracer-kinetic models that have been proposed for MRR, along with examples of application, a comparison of the pros and cons of each model, and some guidelines as to which model should be applied under which conditions.

References

1. JL. Zhang, G. Morell, H. Rusinek, EE. Sigmund, H. Chandarana, LO. Lerman, PV. Prasad, D. Niles, N. Artz, S. Fain, P-H. Vivier, AK. Cheung, VS. Lee. New magnetic resonance imaging methods in nephrology. Kidney Int 2014; 85: 768-778.

2. S Sourbron, DL Buckley. Tracer kinetic modelling in MRI: estimating perfusion and capillary permeability. Phys Med Biol 2012; 57: R1-33.
3. L Bokacheva, H Rusinek, JL Zhang, Q Chen, VS Lee. Estimates of glomerular filtration rate from MR renography and tracer kinetic models. J Magn Reson Imaging. 2009 Feb;29(2):371-82.
4. S Sourbron. Compartment modelling for magnetic resonance renography. Z. Med Phys. 2010; 20: 101-14.

Abstracts for session
Preclinical imaging

Abstracts are organized in the order of presentations

Participant category: Invited speaker

Preclinical Imaging of Cancer

Emmet McCormack [1, 2]

emmet.mc.cormack@med.uib.no

1. Department of Clinical Science, University of Bergen
2. Institute of Medicine, Hematology section, Haukeland University Hospital

Now more than ever before we are dependant on the use of imaging technologies such as X-ray, CT, MRI and ultrasound to allow us visualise within the human body, permitting diagnosis and treatment of illness and disease. However, a newer modality, optical imaging is fast emerging as one of the most promising modalities to visualise, treat and understand how diseases such as cancer interact with its environment. Similar to how we see with our own eyes, fast pulses of laser light illuminate tissue and highly sensitive detectors, which can multiply the initial signal of light detected, can permit the differentiation of diseased and normal tissues on the basis of light absorption. Furthermore, in animal models of cancer, the cancer cells themselves can be labelled with red fluorescent or luminescent markers to distinguish them from normal animal tissue. This procedure has permitted the development of human disease models in animals, and is now being used as a standard technique in preclinical screening of anticancer drugs. The exciting potential of this modality is not only the fact that it permits more accurate screening of new drugs in cancer models but that the normal environments supporting the cancers can be interrogated through the use of novel "fluorescence lifetime" technology. Using this technology, which permits visualisation of multiple targets, researchers can now examine the cancer microenvironment like never before in live intact animals. In the future it is hoped that this form of imaging should aid the development of more specific targeted drug therapies. In addition, use of this technology may aid in not only the development of new probes for accurate optical imaging of human disease but also complement existing imaging modalities such as MR, Ultrasound and PET-CT, providing multi-modality translational imaging of human disease.

Participant category: PhD Candiate/Research Program Student

Evaluation of the novel SPIO GEH121333 for monitoring changes in tumor vascularity and vascular permeability after antiangiogenic treatment using MRI

Jana Cebulla [1,2], Else Marie Huuse [2,3], Dan E Meyer [4], Karina Langseth [5], Siver Andreas Moestue [1,2], Tone Frost Bathen [1,2]

jana.cebulla@ntnu.no

1. MR Cancer Group
2. Department of Circulation and Medical Imaging, Norwegian University of Science and Technology, Trondheim
3. MI lab
4. Biomedical Imaging & Physiology Laboratory, GE Global Research Center, Niskayuna, NY, United States
5. GE Healthcare AS, Oslo

Novel preclinical superparamagnetic iron oxide particles (SPIO) GEH121333 (GE Global Research, Niskayuna, NY, USA, supplied through GE Healthcare AS, Oslo, Norway) were used to monitor vascular response to anti-angiogenic treatment in ovarian xenografts. GEH121333 particles have a relatively large diameter and a high r1/r2 rate, which makes them suitable for both R1 (1/T1) and R2 contrast. Changes in R2 and R2* relaxation rates can be used to calculate a theoretically derived marker for blood vessel density $Q=\Delta R2/(\Delta R2^*)^{(2/3)}$. Tissue T1 values after clearance of iron particles from the blood give information about tumor vessel permeability. Xenografts of the human ovarian cancer cell line TOV-21G were grown on the hind leg of athymic mice (n=7). MRI was performed on a 7T Bruker Biospec. Images of 4 tumor slices were acquired using a Multi Echo Spin Echo sequence for R2 and a Multi echo gradient echo for R2* measurements. Five mice were imaged on day 0 and 1 both before and 15 min after i.v. injection of GEH121333 particles (10mg Fe/kg). Pre contrast R2 and R2* maps were subtracted from the post-contrast maps to obtain ΔR2 and ΔR2* maps. Q values were calculated for each voxel. On day 0 right after the post contrast imaging three mice were treated i.p.with 5mg/kg Bevacizumab while two control mice received saline. For the other two mice T1 maps were obtained using a RARE sequence before and 0.5, 24, 48, 72 and 96h after a single injection of GEH121333. Median T1 values were calculated for each tumor. Bevacizumab is known to normalize the tumor vasculature within 24h of administration by decreasing vessel density and permeability. Fig. A shows that Q increased in the control tumors from day 0 to day 1, but decreased or did not change in the treated tumors, which may be caused by the treatment. T1 was higher in treated tumors 24h after injection of GEH121333 compared to controls (Fig. B), which suggests less leakage of particles in the treated tumors. The tumor T1 values recovered to 90% of baseline after 72h (Fig. B). This indicates that longitudinal studies should be performed with > 72h between injections to allow washout of particles. The results from this pilot study suggest that the novel contrast agent GEH121333 can be used to evaluate changes both in T1, R2 and R2*, attributable to underlying changes in permeability and blood vessel density, respectively.

See image on next page.

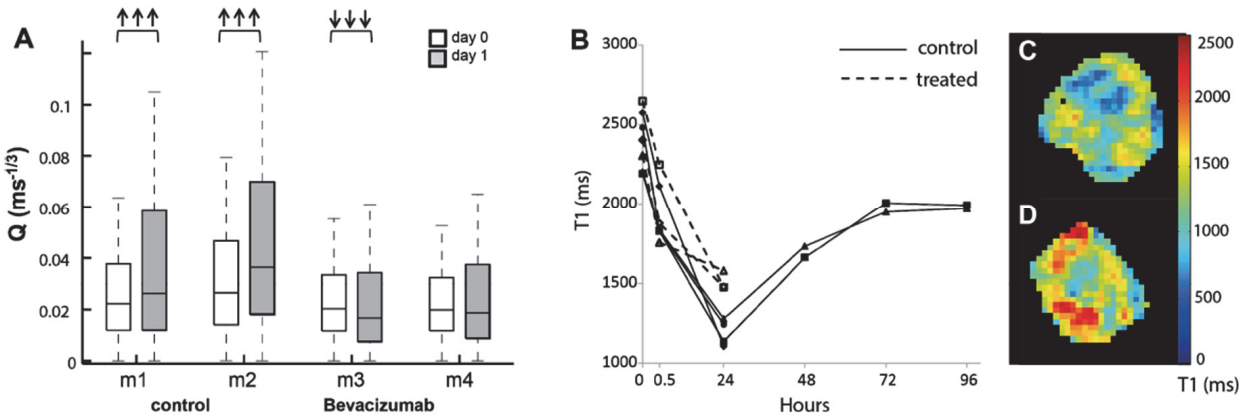

Fig. A) Box plots of Q for individual tumors for day 0 and day 1. ↑↑↑/↓↓↓ $p<0.001$(incease/decrease from day 0 to day 1) two-tailed Mann- Whitney U test. B) Median T1 values for each tumor. C,D) post contrast T1 maps for control (C) and treated

Participant category: PhD Candiate/Research Program Student

Post-exercise impacts on energy metabolism of heart failure rats

Morteza Esmaeili [(1)], Tomas Stølen [(1)], Martin Wohlwend [(1)], Morten A. Høydal [(1)], Øivind Rognmo [(1)], Tone F. Bathen [(1)], Øyvind Ellingsen [(1, 2)]

m.esmaeili@ntnu.no

1. Department of Circulation and Medical Imaging, Norwegian University of Science and Technology (NTNU), Trondheim, Norway
2. Department of Cardiology, St Olavs Hospital, Trondheim, Norway

PURPOSE: Exercise improves the cardiac performance of patients with myocardial infarction (MI), however, the relative beneficial and/or detrimental effect of moderate versus high intensity training is uncertain. Phosphorus (31P) magnetic resonance spectroscopy (MRS) allows detection of high energy phosphate in the heart muscles; adenosine triphosphate (ATP) and phosphocreatine (PCr). Reduced myocardial PCr/ATP ratio in heart failure patients correlates with the New York Heart Association (NYHA) classes1. The purpose of this study was to investigate myocardial phosphate energy reservoir in the left ventricle from rats with MI after exposure to moderate intensity (Mod) and high intensity (High) aerobic interval training regimens. METHODS: Animal models: MI was induced by ligation of the descending artery in rats2. Exercise training is described in detail elewhere2. Tissue extraction: The rats were anesthetized and the hearts were removed and placed in icecold saline for dissection. To avoid fibrotic and ischemic parts, tissue from the septum towards the apex was cut out from every heart and immediately frozen. Time from removal of the heart to snap freeze was approximately 1min and did not differ between groups. MR experiments: Snap-frozen myocardial tissue samples were extracted3 and High resolution 31P MR spectra (Bruker Avance III 600MHz/54mm US-Plus) were obtained with proton decoupling, a 30˚ flip angle, 8192 scans, TR=3.62s, and a spectral width of 14577Hz. MR spectra were analyzed using jMRUI software4. Metabolites were quantified by normalizing the area under the peak to the total area under the metabolites; inorganic (Pi), ATP, and PCr. RESULTS: Both modes of exercise training increased ATP concentration in sham and MI groups (Fig.1). PCr levels in MI group were depleted significantly compared with sham control ($P < 0.05$), although a trend toward increased PCr storage was observed in the post-exercise MI group. CONCLUSION: ATP production increased with training but seems not to be consumed to produce PCr, evidenced by the lower PCr levels in MI rats. The results demonstrate the potential of 31P MRS for investigating the efficacy of different exercise regimens in cardiac performance. REFERENCES: 1.Neubauer S et al. Circulation. 1997 2.Kemi OJ et al. Cardiovasc Res. 2005 3.Gribbestad IS et al. NMR Biomed. 1994 4.Naressi A et al. MAGMA 2001.

See image on next page.

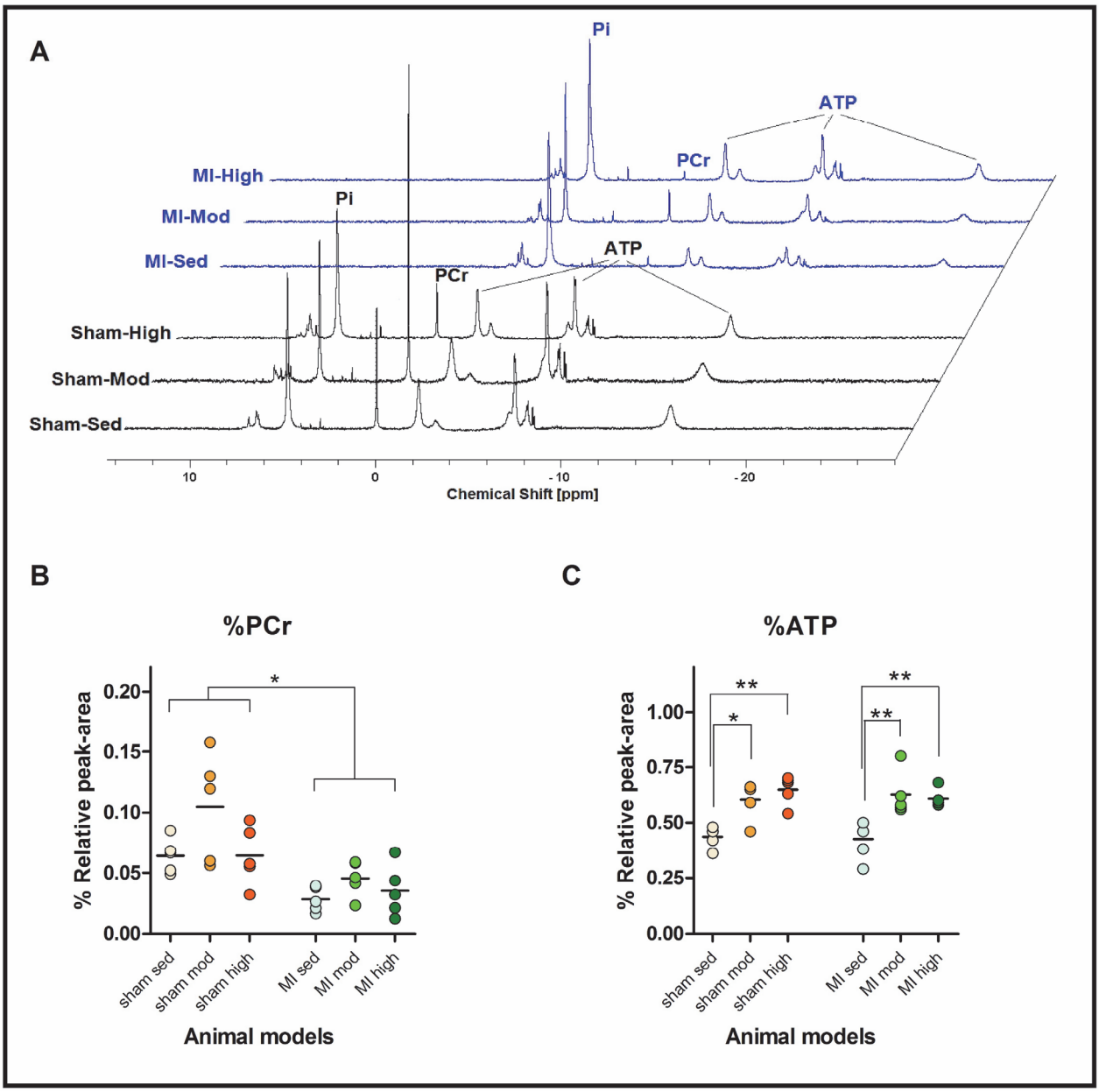

Figure 1: (A) 31P MR spectra of heart muscle extracts of MI and healthy rats; sedate, moderate- and high-intensive trained. (B) MI caused significant decrease in PCr. Dots indicate the normalized PCr measured from individual MR spectra. (C) ATP production

Participant category: PhD Candiate/Research Program Student

Magnetization transfer ratio (MTR) increased unexpectedly in EAE induced mice.

Sveinung Fjær [1,2], Stig Wergeland [1,2], Lars Bø [1,2]

sveinung@fjaer.com

1. KG Jebsen Centre for MS-Research, Department of Clinical Medicine, University of Bergen, Bergen, Norway
2. The Norwegian Multiple Sclerosis Competence Centre, Department of Neurology, Haukeland University Hospital, Bergen, Norway

Magnetization transfer ratio (MTR) is a magnetic resonance imaging (MRI) technique proposed to detect changes in the myelin content of the central nervous system (CNS). An increase in MTR value should indicate an increase in myelin content, while a decrease in MTR should correspond to a decrease in myelin content. This is of special interest in multiple sclerosis (MS), a disease of the CNS characterized by inflammation and demyelination. Experimental autoimmune encephalomyelitis (EAE) is an animal model which causes inflammation and demyelination in the CNS, making it a good model for MS. In this study 18 mice were induced with EAE, while 6 mice was kept as controls. MR imaging was done at baseline, 18 days after EAE induction and 32 days after EAE induction. Histology samples was taken after 18 and 32 days. Weight and disease score was measured throughout the study. We expected to see a decrease in MTR in EAE mice compared to the controls, due to the demyelination caused by the EAE induction. Contrary to our expectations, the EAE mice had an significant increase in MTR value. The MTR values did not correlate to disease progression, weight, myelin content or T-cells. Preliminary results suggest that an increase iron content due to inflammation may cause the MTR increase.

Participant category: PhD Candiate/Research Program Student

Use of dynamic 2-[18F]-fluoroethyl-choline PET for evaluation of choline metabolism in breast carcinoma xenografts

Alexandr Kristian [1,3], Patrick Riss [4,8], Hong Qu [5], Olav Engebråten [1,2], Gunhild Mari Mælandsmo [1,7], Eirik Malinen [6]

alexandr.kristian@gmail.com

1. Department of Tumor Biology, Oslo University Hospital, Oslo, Norway
2. Department of Oncology, Oslo University Hospital, Oslo, Norway
3. Institute of Clinical Medicine, University of Oslo, Oslo, Norway
4. Department of Chemistry, University of Oslo, Oslo, Norway
5. Instittute for Basic Medical Sciences, University of Oslo, Oslo, Norway
6. Department of Physics, University of Oslo, Oslo, Norway
7. Department of Pharmacy, University of Tromsø, Tromsø, Norway
8. Norsk Medisinsk Syklotronsenter AS, Rikshospitalet, Oslo, Norway

Introduction: Breast carcinomas (BC) can have abnormal choline (Cho) metabolism that vary for different subtypes of BC. Several modalities like ex vivo and in vivo magnetic resonance spectroscopy (MRS) and positron emission tomography (PET) may be useful to study Cho metabolism in vivo. So far, mainly single frame 2-[18F]-fluoroethyl-choline ([18F]FECh) PET imaging with different acquisition timing has been used to evaluate Cho metabolism. The purpose of this study was to investigate uptake of [18F]FECh in three different breast cancer xenografts (BCXs) models using dynamic multi-frame PET (dPET) and pharmacokinetic modeling. Materials and Methods: Nine athymic nude mice bearing bilateral MAS98.12 (basal-like), HBCx34 or MAS98.06 (both luminal B) BCXs were subjected to a 90 minute dPET scan following a bolus injection of 10MBq of [18F]FECh. A well-established two-tissue compartment model was fitted to the uptake curves voxel-by-voxel, providing estimates of transfer rates between the vascular, non-metabolized and metabolized compartments. The rate constants k1, k2, k3, MRCho and the intravascular fraction vb were estimated. Additionally, analyses of terminal blood samples and tumor cell suspension incubated with [18F]FECh was performed. Results: [18F]FECh uptake in all BCXs was similar to surrounding normal tissue, thus creating no image contrast. The average liver uptake was 10 times higher than the tumor uptake (panel a of the figure). The uptake in MAS98.12 was higher than in the other two BCXs during the whole course of the acquisition, and was significantly higher than in HBCx34 at 10 to 30 minutes after injection (panel b of the figure). No significant differences were found for k1, MRCho or the intravascular fraction vb. Both k2 and k3 were significantly lower for the MAS98.12 xenograft (panel c of the figure). [18F]FECh uptake in MAS98.12 cell suspension was 4.2 times lower ($p=0.035$) than in MAS98.06 cell suspension, in line with in vivo results and earlier gene expression and MRS analysis. In terminal blood sample, 68% of [18F]FECh was found in the blood cell fraction, 6% was bounded to plasma proteins and 26% was free. No [18F]FECh metabolites were identified in the free plasma fraction Conclusions: dPET demonstrated that different subtypes of breast cancer have different uptake of [18F]FECh. Rate constants, unlike SUV, were in line with earlier finding by MRS and gene expression analysis, as well as in vitro uptake in cell suspensions.

See image on next page.

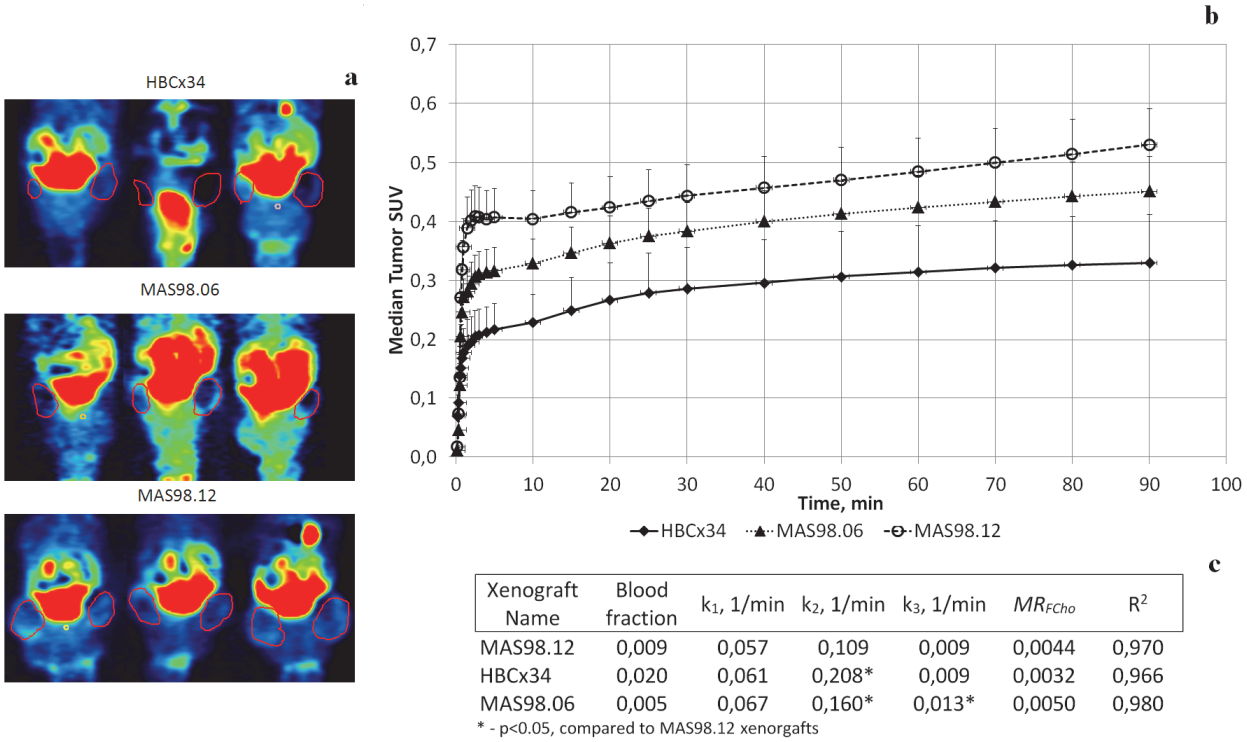

c

Xenograft Name	Blood fraction	k_1, 1/min	k_2, 1/min	k_3, 1/min	MR_{FCho}	R^2
MAS98.12	0,009	0,057	0,109	0,009	0,0044	0,970
HBCx34	0,020	0,061	0,208*	0,009	0,0032	0,966
MAS98.06	0,005	0,067	0,160*	0,013*	0,0050	0,980

* - p<0.05, compared to MAS98.12 xenorgafts

(a) Coronal PET images for three BCXs. Red line indicates location of bilateral xenografts. (b) Median SUV curves for HBCx34, MAS98.06 and MAS98.12 xenografts. Standard deviation for positive direction only is showed. (c) Pharmacokinetic modeling data fro

Participant category: Invited speaker

Preclinical PET imaging in Tromsø – research facilities and course opportunities

Samuel Kuttner [1,2], Siri Knudsen [3], Rune Sundset (presenting author) [2,4]

rune.sundset@unn.no

1. Department of Radiology and Nuclear Medicine, University Hospital of North Norway
2. Medical Imaging Research Group, Department of Clinical Medicine, Faculty of Health Science, University of Tromsø
3. Unit of Comparative Medicine, Section for Research Service, Faculty of Health Science, University of Tromsø
4. Northern Norway Regional Health Authority Trust, Bodø, Norway

Molecular imaging has an increasing significance in basic and applied preclinical research. Positron emission tomography (PET) and single photon emission tomography (SPECT) are today the two most important techniques to visualize metabolic, physiological and functional information on a molecular level. Fusing such studies with computed tomography (CT) enables anatomical localization in the image. The Northern Norway Regional Health Authority Trust together with University Hospital of North Norway and The University of Tromsø have recently invested in a Triumph® II PET/SPECT/CT (Trifoil Imaging Inc., Northridge, CA, US), which combines the three imaging modalities in a single unit, and allows scanning of small rodents, guinea pigs and rabbits. The spatial resolution is about 1 mm for PET, 0.5-1.6 mm for SPECT (collimator dependent), and 0.1 mm for CT. The system has advanced software for image fusion and analysis of both static and dynamic image data. We will present the process of installation of this system at the animal facility at the University of Tromsø and the upcoming national annual PhD course in preclinical PET.

Abstracts for session
Biomedical and molecular imaging

Abstracts are organized in the order of presentations

Participant category: Invited speaker

Magnetic Resonance based perfusion imaging of the brain

Atle Bjørnerud [1, 2]

atle.bjornerud@fys.uio.no

1. The Intervention Centre, Oslo University Hospital
2. Department of Physics, University of Oslo

Magnetic Resonance Imaging (MRI) is a powerful tool for non-invasive measurement of brain perfusion and related hemodynamic parameters. Several different MR-based techniques are currently available for use both in research and clinical routine. This presentation will introduce the most important techniques and give an overview of some important clinical applications as well as some more exploratory methods which may provide new insights into central disease mechanisms in oncology and neurodegenerative disease in the years to come.

Participant category: PhD Candiate/Research Program Student

SU-8 nanopillars: A flexible system for investigating cell response and function on nanostructured surfaces

Kai Beckwith [(1)], Pawel Sikorski [(1)]

kai.beckwith@ntnu.no

1. Dept. of Physics, NTNU

Surface nanostructures have emerged as a novel cell interface, enabling precise control over cell-substrate interactions. "Tall and thin" (high aspect-ratio) nanostructures are of particular interest in several applications, ranging from cell motility control to efficient substrate-mediated gene transfection. However, there is some controversy about the detailed interactions between the cultured cells and the nanostructures, in part due to lack of controllable systems which are simple to fabricate and study. In this work polymer nanostructures such as nanopillars and nanolines were precisely produced by electron beam lithography directly on glass coverslips. AGS and HeLa cells cultured on the samples were studied with (live cell) high resolution confocal microscopy, total internal reflection (TIRF) microscopy and scanning electron microscopy to obtain detailed information on cell-nanopillar interactions. The cells adhered to and spread on the nanopillar arrays without any influence on cell viability, as shown by live-cell imaging of calcein-AM labelled cells (Figure 1A). Depending on the inter-pillar spacing, the cells were observed as either 'floating' on the pillars, or 'adhered', where they engulfed the pillars and spread on the substrate. TIRF imaging showed that on closely spaced pillars, primarily the edges of the cell maintained contact with the glass subtrate, while the central parts of the cell only maintained contact with the top of the pillars (Figure 1B). Actin filaments highly co-localized with pillars at engulfment sites, indicating active mechanosensing of the pillars by the cells (Figure 1C). By simply altering the shape of nanostructures from pillars to lines assymetric cell shapes could be induced. The presented system offers a simple and rapid way to prototype different high-aspect ratio designs for novel cell interfaces. The polymer-based nanostructures have the advantage of a low temperature, single-step fabrication process. Additionally, the surface chemistry is highly tunable. As the features were patterned directly on glass cover slips, integration with optical microscopy was facile, allowing high resolution imaging of cell-nanopillar interactions in both live and fixed cells. The nanopillars have promise as a simple functional system for e.g. cell guidance or molecular delivery via the nanopillars.

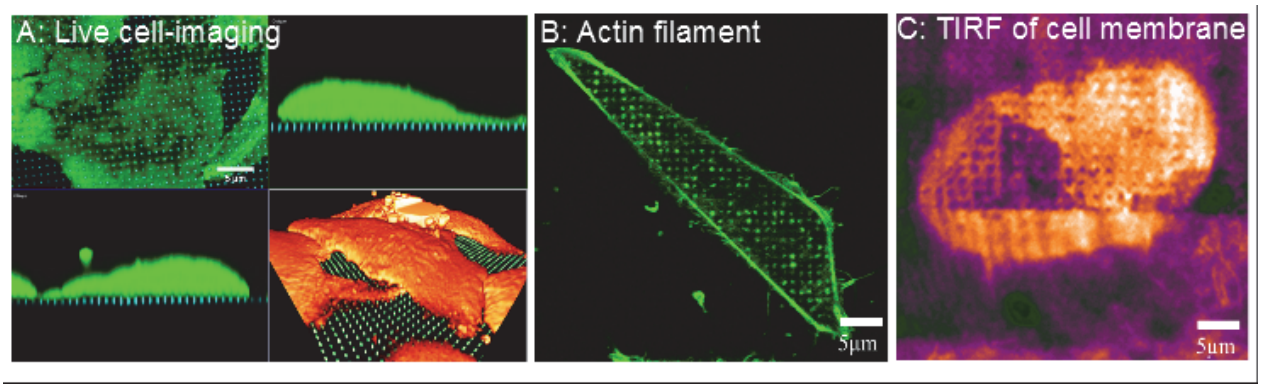

A: Live-cell imaging shows spreading of HeLa cells (green) on the nanopillars (blue). B: The signal from the cell's actin filament is increased at the position of the nanopillars. C: A cell at the boundary of a nanopillar area demonstrating differential s

Participant category: PhD Candiate/Research Program Student

Exercise training reduces CaMKII-dependent phosphorylation of the cardiac ryanodine receptor and arrhythmogenic SR Ca2+ leak in mice with mutant cardiac ryanodine receptor 2

Ravinea Manotheepan [1,2], Tore Kristian Danielsen [1,2], Mani Sadredini [1,2], Steven Lehnart [3], Ivar Sjaastad [1,2], Mathis Korseberg Stokke [1,2,3]

ravinea.manotheepan@medisin.uio.no

1. Institute for Experimental Medical Research (IEMR), Oslo University Hospital and University of Oslo, Oslo, Norway
2. KG Jebsen Cardiac Research Center and Center for Heart Failure Research, University of Oslo, Oslo, Norway
3. Heart Research Center Göttingen, Dept. of Cardiology & Pulmonology, Göttingen, Germany
4. Clinic for Internal Medicine, Lovisenberg Diakonale Hospital, Oslo, Norway

Catecholaminergic Polymorphic Ventricular Tachycardia caused by RyR2 mutations predisposes to stress-induced arrhythmias due to disrupted Ca2+ handling in ventricular cardiomyocytes. We tested the effect of exercise training (ET) on Ca2+ handling in mice with a human RyR2 mutation (RyR-R2474S). C57BI6 mice were employed to test the efficacy of a two-week ET protocol, comprising 5 eight-minute intervals at 80-90% of the running speed at maximal oxygen uptake (VO2max, ml/kg/min), and two-minute active rest periods at 60%. Then RyR2-R2474S mice were subjected to the same protocol. ET mice (C57BI6-ET) increased VO2max by 7±1% compared to baseline (152±2 vs. 142±2, P<0.05), no change was found in sedentary mice (C57BI6-SED) (139±2 vs. 140±3). Autophosphorylated CaMKII was reduced in C57BI6-ET compared to C57BI6-SED (52±9 vs. 100±8%, P<0.05), as was CaMKII-dependent Ser2814-phosphorylated RyR2 (37±12 vs. 100±15%, P<0.05). Thr17-phosphorylated phospholamban was unaltered (69±18 vs. 100±5%). Contrary, C57BI6-ET exhibited increased PKA-dependent Ser16-phosphorylated phospholamban (140±11 vs. 100±9%, P<0.05) but no change in Ser2808-phosphorylated RyR2. ET RyR2-R2474S mice (RyR2-RS-ET) increased VO2max by 10±2% compared to baseline (142±3 vs. 130±2, P<0.05), while VO2max in RyR2-RS-SED decreased by 3±2% (128±2 vs. 132±2, P<0.05). RyR2-RS-ET compared to RyR2-RS SED showed decreased levels of Ser2814-phosphorylated RyR2 (38±3 vs. 100±13%, P<0.05), but no alterations in Thr17-phosphorylated phospholamban. Contrary, RyR-RS-ET mice exhibited increased levels of Ser2808-phosphorylated RyR2 (150±14 vs. 100±16%, P<0.05) and Ser16-phosphorylated phospholamban (167±25 vs. 100±14%, P<0.05). Whole-cell Ca2+ imaging in cardiomyocytes showed decreased SR Ca2+ leak normalized to SR Ca2+ content in RyR2-RS-ET vs. SED bothe in abscence (F/F0: 11±2 vs. 25±5, P<0.05) and presence of isoprenaline (ISO) (F/F0: 29±4 vs. 15±3, P<0.05). The decreased leak was associated with a decrease in frequency of Ca2+ waves after 4Hz stimulation in RyR2-RS-ET vs. SED (0.35±0.13 vs. 1.03±0.22, P<0.05), as well as in ISO-stimulated cells after both 1Hz (0.36±0.09 vs. 1.65±0.21, P<0.05) and 4Hz stimulation (1.33±0.24 vs. 3.02±0.24, P<0.005). Two weeks of high-intensity exercise training in C57BI6-WT and RyR2-RS increased VO2max, decreased CaMKII-dependent phosphorylation of RyR2, reduced SR Ca2+ leak and Ca2+ wave frequency. These effects of ET may decrease the propensity for arrhythmias in CPVT.

Participant category: PhD Candiate/Research Program Student

CELL-TO-CELL COMMUNICATION IN ACUTE MYELOID LEUKEMIA BY TUNNELING NANOTUBES

Maria Omsland [(1)], Øystein Bruserud [(1,2)], Bjørn Tore Gjertsen [(1,2)], Vibeke Andresen [(1)]

maria.omsland@k2.uib.no

1. Department of Clinical Science, University of Bergen, Bergen, Norway
2. Department of Internal Medicine, Hematology Section, Haukeland University Hospital, Bergen, Norway

Introduction: Acute myeloid leukemia (AML) is a heterogeneous and aggressive blood cancer originating in the bone marrow. An improved understanding of cellular communication in AML could provide new information with respect to disease-linked mechanisms, progression, treatment and resistance. The tunneling nanotube (TNT) is a novel type of cell-to-cell communicator, 50-200 nm in diameter, F-actin containing structure connecting two or more cells. TNTs have been observed in a variety of cells. It has been shown to transport different components for instance mitochondria, cell membrane components, multi-resistance genes and pathogens. The exact molecular mechanisms behind TNT formation are still unclear, but the TNFαIP2 protein, is one of the suggested molecules needed for TNT formation. We aim to quantify TNTs in AML cell lines and AML patient cells, investigate the role of this structure following conventional therapy and further map the molecular mechanisms responsible for TNT formation in AML. Methods: The following cell lines were studied: OCI-AML3, NB4, HL-60, MV4-11 and MOLM-13. Primary cells: PBMCs from nine AML patients with more than 70% blasts in the blood and PBMCs from six healthy donors. The cells were investigated for TNT formation by fluorescence microscopy. Both cell lines and primary AML patient cells were treated with cytarabine (AraC) alone (6 and 24h) or in combination with the two anthracyclines idarubicin and daunorubicin (4 and 24h). Results: We found that all investigated cell types expressed TNT connections. The cell lines have small variation in percentage TNTs (0.33-7.8) as well as the PBMCs derived from healthy donors (3.6-8.3) while the PBMCs derived from the AML patients showed greater variation (0-11.5). Treatment of cells with AraC resulted in a decrease in TNT numbers both in AML cell lines and in three investigated AML patients. Interestingly, idarubicin seems to have an antagonizing effect on AraC with more effect compared to daunorubicin (24h). The level of TNFαIP2 seemed to correlate with TNT number in the cell lines investigated. Discussion: We demonstrated the existence of TNTs in both AML cell lines and primary AML cells. We observed a variance in TNT numbers between the different cell types and greatest deviation was observed in the different patient samples. The conventional chemotherapeutics daunorubicin and idarubicin caused different TNT responses, strikingly, AraC quenched TNT formation.

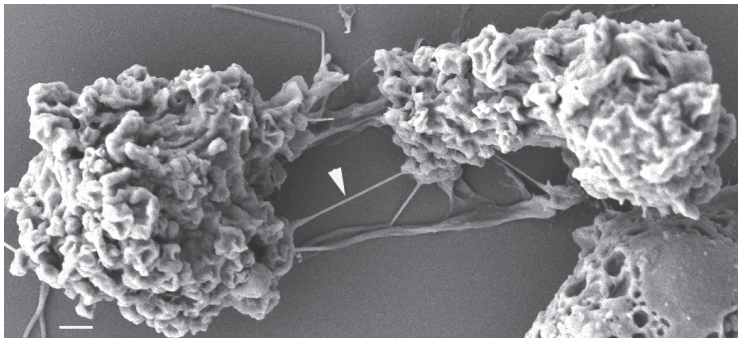

OCI-AML3 cells connected by a tunneling nanotube (TNT) (arrow). Scale bar: 1µm. (Maria Omsland, unpublished)

Participant category: PhD Candiate/Research Program Student

Stretch-Induced modulation of cardiomyocyte Ca2+ homeostasis, signaling and structure

Marianne Ruud [1,2], Michael Frisk [1], Åsmund T. Røe [1,2], Ole M. Sejersted [1,2], Geir A. Christensen [1,2], William E. Louch [1,2]

marianne.ruud@medisin.uio.no

1. Institute for Experimental Medical Research, Oslo University Hospital and University of Oslo, Oslo, Norway
2. KG Jebsen Cardiac Research Center and Center for Heart Failure Research, University of Oslo, Oslo, Norway

T-tubules (TTs), essential for propagating action potentials into the cardiomyocyte, maintain a close proximity between L-type Ca2+ channels (LCCs) and ryanodine receptors (RyRs) on the sarcoplasmic reticulum (SR). This proximity between LCCs and RYRs ensures efficient Ca2+-induced Ca2+ release (CICR), essential for normal contractility. TTs are disorganized during heart failure (HF), disrupting this proximity leading to de-synchronization of CICR and weakened contraction (Figure 1; Louch et al., J Biomed Biotechnol, 2010), characteristic of HF in several species including humans (Quinn et al., J Physiol, 2003; Heinzel et al., Circ Res, 2008; Lyon et al., Proc Natl Acad Sci USA, 2009). Mechanisms leading to TT disruption remain unclear. We hypothesize that increased mechanical loading of the heart during hypertrophy (HT) and HF development is an important trigger (Figure 1; Frisk et al., in preparation). Confocal imaging of regions of the post-infarcted rat heart which are proximal to the infarction exhibit markedly impaired TT structure and Ca2+ handling; distal regions are less affected. ECG and MRI show that the drag of the infarction in proximal zones prevents normal contraction; these regions are stretched outward. We will investigate the potentially causative link between the abnormal regional work load on the heart during HF and TT disruption. Isolated cardiac muscle strips will be subjected to different amounts of stretch (pre-load) and contractile resistance (after-load). Experiments will include in situ and in vitro examination of TT structure by confocal imaging, and in vivo imaging of cardiac structure and function by MRI and ECG. Additionally, the role of [Ca2+] handling in triggering TT disruption will be examined, as Ca2+ homeostasis is a key regulator of established pathological signaling pathways. Stretch of single cardiomyocytes causes sensitization of RyRs, triggering Ca2+ release from the SR (Prosser et al., Science, 2011). We will investigate if and how these Ca2+ signals are linked to TT disruption by applying stretch to single cardiomyocytes using the Cell Tester System. Altered expression and activity of the NFAT pathway, assumed to be a load-sensitive regulator of cardiomyocyte structure, will be linked to changes in [Ca2+] as assessed by confocal imaging and whole-cell photometry. Novel treatments targeting stretch-dependent signaling may circumvent cellular alterations and extracellular matrix leading to HT and HF development.

See image on next page.

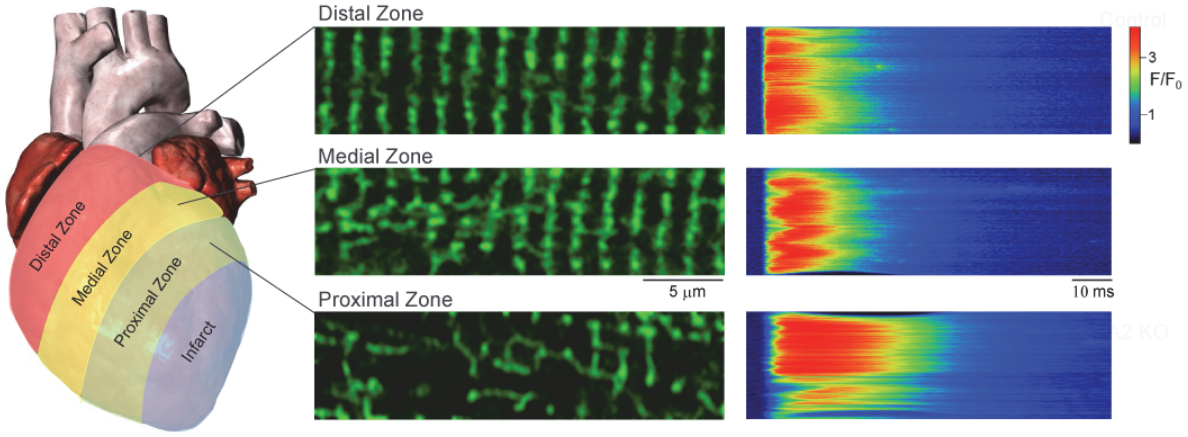

Preliminary data correlate regional stretch of post-infarction rat hearts (left panel) with cardiomyocyte disruption. Degree of TT disruption (middle panel) and dyssynchronous Ca2+ transients (right panel) correlate with proximity to infarct site; proxima

Participant category: PhD Candiate/Research Program Student

Optimization of NTR reporter genes for preclinical and GDEPT imaging

Endre Stigen [1], Maik Grohman [2], Kjetil Børve Lund [1], Elvira Gracia de Jalon [3], Bengt Erik Haug [3], David Micklem [4], Jim Lorens [5], Veronika Mamaeva [1], Mihaela Popa [6], Emmet McCormack [7]

endre.stigen@gmail.com

1. Hematology Section, Department of Clinical Science, UoB
2. Department of Human Molecular Genetics, Max Planck Institute for Molecular Genetics, Germany
3. Department of Chemistry, UoB
4. BerGenBio AS
5. Department of Biomedicine, UoB
6. KinN Therapeutics AS
7. Hematology Section, Department of Medicine, Haukeland University Hospital

In cancer research bioluminescence imaging of luciferase is one of the most applied techniques, and currently the most sensitive optical reporter system of preclinical models. However, maximal emission spectra are only 615 nm which limits deep tissue imaging due to light scatter by bioluminescent photons and light absorption by blood and water. With a shift away from subcutaneous tumor models towards more representative metastatic and orthotopic cancer models, a great emphasis has been put on the development of fluorescent probes that emit light in the near-infrared (NIR) spectrum where light absorption by haemoglobin and deoxyhaemoglobin is minimal. One such reporter system is nitroreductase (NTR) NIR reporter platform. Nitroreductase (NTR) is a bacterial flavoprotein that reduces aromatic nitrogroups to the corresponding hydroxylamines and has been used in gene directed enzyme prodrug therapy (GDEPT) together with prodrug 5-(azaridin-1-yl)-2,4-dinitrobenzamide (CB1954) which has entered clinical phase 1 trials. The ability of NTR to reduce compounds with nitrogroups has also been utilized within optical imaging. For the first time this was shown in orthotopic and metastatic models where NTR both activated metronidazole and the fluorescently quenched NIR substrate probe CytoCy5S (McCormack et al., 2013, Cancer Research) In this study we used a codon optimized NTR called NTRo where site-directed mutagenesis was performed in order to change the codons to a mammalian preference (Grohman et al, 2009, BMC Cancer). The NTRo gene was used to evaluate the efficacy as a reporter enzyme together with the NIR substrate probe CytoCy5S. The gene was stably transduced into lung and breast cancer cell lines, H460 and MDA-MB-231 respectively. In vitro validation and quantification of NTRo was performed by flow cytometry and fluorescence microscopy including live cell confocal imaging. In vivo validation was performed by optical imaging of sub-cutaneous xenograft mice models. It is suggested that translation of NTR is to some extent impaired due to divergent codon usage between eukaryotes and prokaryotes. We propose that development of GDEPT models of NTRo expressing cancer cell lines and subsequent in vivo xenografts imaging will lead to increased signal-to noise ratio due to more efficient translational process by the optimized codon usage. Subsequently this will allow for deep tissue imaging of clinically relevant orthotopic and metastatic models.

See image on next page.

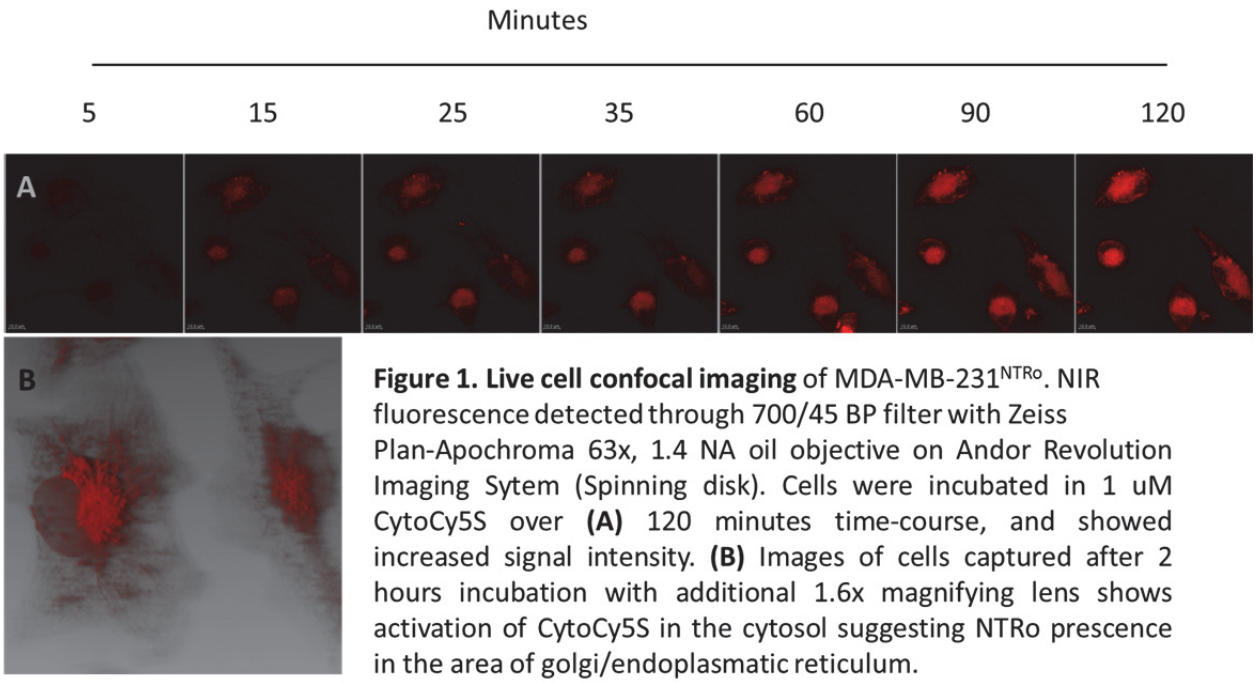

Figure 1. Live cell confocal imaging of MDA-MB-231^{NTRo}. NIR fluorescence detected through 700/45 BP filter with Zeiss Plan-Apochroma 63x, 1.4 NA oil objective on Andor Revolution Imaging Sytem (Spinning disk). Cells were incubated in 1 uM CytoCy5S over **(A)** 120 minutes time-course, and showed increased signal intensity. **(B)** Images of cells captured after 2 hours incubation with additional 1.6x magnifying lens shows activation of CytoCy5S in the cytosol suggesting NTRo prescence in the area of golgi/endoplasmatic reticulum.

Participant category: Invited speaker

Ultrasound-mediated delivery of nanoparticles to tumour tissue

Catharina Davies [(1)], Siv Eggen [(1)], Rune Hansen [(2)], Yrr Mørch [(3)]

catharina.davies@ntnu.no

1. Dept of physics, NTNU
2. Dept of Technology and Society, SINTEF
3. Dept of Materials and Chemistry, SINTEF

Nanotechnology has started a new era in engineering multifunctional nanoparticles (NPs) for improved cancer diagnostics and therapy, incorporating both contrast agents for imaging and therapeutics into so called theranostic NPs. Encapsulating the drugs into NPs improves the pharmacokinetics and reduces the systemic exposure due to the leaky capillaries in tumours. A prerequisite for successful cancer therapy is that the therapeutic agents reach their targets and limit the exposure to normal tissue. The delivery depends on the vasculature, the transport across the capillary wall, through the extracellular matrix, and across the cell membrane. Although the NPs may pass the tumour capillaries rather easily, the uptake of NPs and the released drugs is low and they are heterogeneously distributed in the tumour tissue. In order to improve the tumour uptake and distribution of NPs, the administration of NPs should be combined with a treatment facilitating the delivery. Ultrasound has been reported to be able to improve drug delivery by different mechanisms. In an acoustic field, cavitation is the oscillation and possible collapse of gas microbubbles. Such microbubbles are not common in the human body but can be introduced by intravenous injection. Cavitation can then generate shear stresses and jet streams on endothelial cells thereby improving the extravasation of NPs. Radiation force is the other non-thermal mechanism that can be utilized for improved extravasation and distribution of NPs in tumours. We have developed a novel multimodal, multifunctional drug delivery system consisting of microbubbles stabilized by polymeric NPs to be used in ultrasound-mediated delivery of NPs. Miniemulsion polymerization was used to prepare NPs of the biocompatible and biodegradable polymer poly(butyl cyanoacrylate) (PBCA). The NPs were coated with polyethylene glycol (PEG) to improve the circulation time and biodistribution. Combining these NP-microbubbles with focused ultrasound resulted in a higher uptake and improved distribution of the NPs in prostate tumors growing subcutaneously in mice. Thus our new NP-microbubble platform demonstrates promising clinical potential.

Abstracts for session
Clinical imaging

Abstracts are organized in the order of presentations

Participant category: Invited speaker

CEUS quantification in clinical practice

Christoph F. Dietrich [(1)]

christoph.dietrich@ckbm.de

1. Caritas Krankenhaus Bad Mergentheim, Med Klinik 2, Germany

Dynamic contrast-enhanced ultrasound (DCE-US), an imaging technique that utilizes microbubble contrast agents in diagnostic ultrasound, has recently been technically summarized and reviewed by the European Federation of Societies for Ultrasound in Medicine and Biology (EFSUMB) position paper. However, the practical applications of this imaging technique were not included. This current presentation reviews and discusses the published literature on the clinical use of DCE-US. DCE-US is the most sensitive cross-sectional real-time method for measuring non-invasively the perfusion of parenchymatous organs. DCE-US can measure parenchyma-perfusion and so can differentiate between benign and malignant tumors. The most important routine clinical role of DCE-US is the prediction of tumor response to chemotherapy treatment within a very short time, shorter than using Response Evaluation Criteria in Solid Tumours (RECIST) criteria. Other applications found for DCE-US are for quantifying hepatic transit time, diabetic kidneys, transplant grafts and Crohn´s disease. In addition, the problems involved in using DCE-US are discussed. 1. Dietrich CF, Averkiou MA, Correas JM, Lassau N, Leen E, Piscaglia F. An EFSUMB Introduction into Dynamic Contrast-Enhanced Ultrasound (DCE-US) for Quantification of Tumour Perfusion. Ultraschall Med 2012; 33(4):344-351. 2. Claudon M, Dietrich CF, Choi BI, Cosgrove DO, Kudo M, Nolsøe CP, Piscaglia F, Wilson SR, Barr RG, Chammas MC, Chaubal NG, Chen MH, Clevert DA, Correas JM, Ding H, Forsberg F, Fowlkes JB, Gibson RN, Goldberg BB, Lassau N, Leen EL, Mattrey RF, Moriyasu F, Solbiati L, Weskott HP, Xu HX. Guidelines and Good Clinical Practice Recommendations for Contrast Enhanced Ultrasound (CEUS) in the Liver - Update 2012. Ultraschall Med 2013; 34(1):11-29. 3. Fröhlich E, Muller R, Cui XW, Schreiber-Dietrich D, Dietrich CF. Dynamic contrast-enhanced ultrasound (DCE-US) for quantification of tissue perfusion: A review of the current literature. JUM 2014, in press. 4. Ignee A, Jedrejczyk M, Schuessler G, Jakubowski W, Dietrich CF. Quantitative contrast enhanced ultrasound of the liver for time intensity curves-Reliability and potential sources of errors. Eur J Radiol 2010;73: 153-158

Participant category: PhD Candiate/Research Program Student

CONTRAST ENHANCED ULTRASOUND OF THE PANCREAS SHOW IMPAIRED PERFUSION IN PANCREAS INSUFFICIENT CYSTIC FIBROSIS PATIENTS

Trond Engjom [1, 3], Kim Nylund [1,6], Friedemann Erchinger [1,2], Georg Dimcevski [1,3], Radovan Jirik [4,5], Odd Helge Gilja [1,3,6]

trond.engjom@helse-bergen.no

1. Department of Medicine , Haukeland University Hospital, Bergen, Norway
2. Voss Hospital, Voss, Norway
3. Department of Clinical Medicine, University of Bergen, Bergen, Norway
4. Institute of Scientific Instruments, Academy of Sciences of the Czech Republic, Brno, Czech Republic
5. International Clinical Research Center - Center of Biomedical Engineering, St. Anne's University Hospital Brno, Czech Republic
6. National Centre for Ultrasound in Gastroenterology, Haukeland University Hospital, Bergen, Norway.

Introduction: Pancreatic insufficiency is a prevalent feature of cystic fibrosis (CF). The affected CF pancreas is dominated by fatty infiltration, atrophy and necrosis. Little is known about pancreatic perfusion in CF. We aimed to evaluate pancreatic perfusion assessed by contrast-enhanced ultrasound (CEUS) in CF patients with known exocrine pancreatic function. Methods: CEUS was performed in CF patients (n=39) and healthy controls (n=32). Exocrine pancreatic function was assessed by secretin-stimulated endoscopic short test and/ or faecal elastase. The CF patients were defined as pancreas sufficient through fecal elastase >200µg/g or duodenal bicarbonate >80mmol/L. Perfusion data was analyzed on stored DICOM-files using DCE-US software (http://www.isibrno.cz/perfusion/) and a dedicated perfusion model. Mean transit-time (MTT), blood flow (BF) and blood-volume (BV) was calculated. Exclusions due to image quality and image analysis in the CF group were made without knowledge of pancreatic function. Results: 26 CF patients and 20 controls were included. 13 CF patients and 12 controls were excluded due to poor image quality. Subjects were divided as follows: CF, pancreatic insufficient (CFI, n=13), CF pancreatic sufficient (CFS, n=13) and healthy controls (HC, n=20). Results are displayed in the table (mean±SD). Discussion: The pancreatic insufficient CF patients had significantly longer MTT ($p<0.001$), lower BF ($p<0.001$) and lower BV ($p<0.05$) compared to healthy controls and pancreatic sufficient CF patients. CEUS can non-invasively differentiate between healthy pancreatic tissue and exocrine insufficient pancreatic tissue due to cystic fibrosis.

	CFI (n=13)	*CFS (n=13)*	*HC (n=20)*	*P (CFI vs all)*
MTT (s)	8.0±3.2	4.0±1.9	2.9±1.4	P<0.001
BF (ml/min/100ml)	18.4±10.5	76.8.0±54	117.4±70	P<0.001
BV (ml/100mL):	2.3±1.3	4.1±2.5	4.8±2.5	P<0.05

s=seconds, ml=millilitre

Participant category: PhD Candiate/Research Program Student

Longitudinal changes in visual working memory performance and frontoparietal intrinsic connectivity network synchronization after non-cortical stroke

Judit Haasz [(1)], Astri J. Lundervold [(2,3,4)], Thomas Espeseth [(5,6)], Lars Thomasssen [(1)], Karsten Specht [(2,7)]

judithaasz@gmail.com

1. Department of Clinical Medicine, University of Bergen, 5020 Bergen, Norway
2. Department of Biological and Medical Psychology, University of Bergen, 5009 Bergen, Norway
3. Kavli Research Centre for Aging and Dementia, Haraldsplass Deaconess Hospital, 5009 Bergen, Norway
4. K. G. Jebsen Center for Research on Neuropsychiatric Disorders, University of Bergen, 5009 Bergen
5. Department of Psychology, University of Oslo, Oslo, Norway
6. Norwegian Centre for Mental Disorders Research (NORMENT), and KG Jebsen Centre for Psychosis Research, Division of Mental Health and Addiction, Oslo University Hospital, Oslo, Norway
7. Department of Clinical Engineering, Haukeland University Hospital Bergen, Norway

Introduction Working memory deficit is a major symptom after stroke and can adversely impact cognitive and occupational performance and success of rehabilitation in more general. However, the effect and dynamics of small non-cortical structural lesions on working memory performance and intrinsic functional connectivity are not known. Therefore, we combined computer-based assessment of visual short-term memory (vSTM) capacity (K) and resting state functional connectivity magnetic resonance imaging (rs-fcMRI) and repeatedly tested a group of patients with initial mild stroke severity. Method We recruited 11 consecutive stroke patients with subcortical and cerebellar lesions and 15 age- and sex-matched healthy controls. Subjects performed the whole report version of Theory of Visual Attention based assessment that yielded vSTM K. Also, participants underwent rs-fcMRI examinations. Examinations were performed on average 4, 30, 82 days from symptom onset. We used mixed design ANOVA to investigate main effect of group, time and group × time on vSTM K. After preprocessing the rs-fcMRI data by FSL, we performed a high model order group independent component analysis in GIFT. Finally, we explored longitudinal between group differences in functional synchronization of left- and right-lateralized frontoparietal intrinsic connectivity networks (ICNs) using voxel-wise statistical inference in FSL's Randomize. Group differences in synchronization were related to vSTM K by partial correlation analyses. Results Patients had reduced vSTM K in the early phase after stroke and at about 3 months. Additionally, both groups improved significantly over time. We found a significant group difference in longitudinal right lateralized fronto-parietal ICN organization, in favor of the control group. The change in within network synchronization positively correlated with improvement in vSTM K in the control group but not in the patient group. Discussion The present study indicates that non-cortical structural lesions are associated with vSTM capacity deficit and altered longitudinal fronto-parietal ICN organization. Findings imply that patients will have difficulties with complex cognitive operations and acquiring new skills in the acute and sub-acute phase after stroke.

Participant category: PhD Candiate/Research Program Student

Multimodal MRI analysis of brain structure and connectivity in young adults born preterm with very low birth weight: Visual-motor function in early adulthood

Kam Sripada [(1)], Gro C. Løhaugen [(1,2)], Live Eikenes [(3)], Knut Jørgen Bjuland [(1)], Asta Håberg [(3)], Ann-Mari Brubakk [(1,4)], Jon Skranes [(1,2)], Lars M. Rimol [(1)]

kam.sripada@ntnu.no

1. Norwegian University of Science and Technology, Department of Laboratory Medicine, Children's and Women's Health
2. Sørlandet Hospital, Department of Pediatrics
3. Norwegian University of Science and Technology, Department of Circulation and Medical Imaging
4. St Olavs University Hospital

Background: Individuals born preterm and at very low birth weight (VLBW: birth weight ≤1500 grams) are at an increased risk of perinatal brain injury and neurodevelopmental deficits over the long term. Previous studies of visual function in VLBW children and adolescents have revealed an increased prevalence of visual-motor problems including with eye-hand coordination, fine motor skills and speed, visual-motor integration, and reduced visual acuity. Our aim was to assess whether those born with VLBW have problems persisting into early adulthood with visual-motor integration, motor coordination, and visual perception compared to controls, using the Beery-Buktenica Developmental Test of Visual-Motor Integration-IV, and to relate these findings to cortical and connectivity changes seen on structural magnetic resonance imaging (MRI) and diffusion tensor imaging (DTI). Methods: We examined young adults (47 VLBW and 56 term-born controls) at approximately 19-20 years of age with a combined clinical, MRI, and DTI evaluation. Maternal age and socioeconomic status were statistically equivalent between the two groups. 3D-T1 weighted MPRAGE images and DTI were done at 1.5 Tesla, and neuroimaging data were processed using FreeSurfer and Tract-Based Spatial Statistics. Results: VLBW subjects achieved significantly lower scores on all 3 visual-perceptual tests compared to controls. There were significant relationships between test scores on all 3 VMI subtests and cortical surface area but not cortical thickness. Scores on the copying task was related to cortical surface area in several regions in the occipital, temporal, frontal, and parietal lobes, with highest effect sizes bilaterally in the ventral occipital and temporal lobes. The motor coordination test scores had a significant relationship to cortical surface area primarily in the occipital and ventral temporal lobes bilaterally, and visual matching test scores related to cortical surface area in several smaller regions. DTI analysis indicated lower fractional anisotropy correlated with all 3 VMI test scores in several regions bilaterally and in the corpus callosum. Conclusion: Our multimodal analysis indicated that, when compared with controls nearly two decades after birth, the VLBW young adults in our study had reduced visual-motor integration, motor coordination, and visual perceptual skills, which may be due to perinatal brain injury or aberrant cortical development secondary to injury.

Participant category: PhD Candiate/Research Program Student

High Order Diffusion Tensor Imaging for Breast Cancer Differentiation

Jose R. Teruel [1,2], Hans E. Fjøsne [3,4], Agnes Østlie [5], Pål E. Goa [5,6], Tone F. Bathen [1]

jose.teruel@ntnu.no

1. Department of Circulation and Medical Imaging, NTNU
2. St. Olavs University Hospital
3. Department of Surgery, St. Olavs University Hospital
4. Institute of Cancer Research and Molecular Medicine, NTNU
5. Clinic of Radiology and Nuclear Medicine, St. Olavs University Hospital
6. Department of Physics, NTNU

Diffusion Tensor Imaging (DTI) for breast lesion differentiation has been explored previously reporting high sensitivity and specificity by means of diffusivity parameters. However, limited potential have been shown by anisotropy parameters derived from DTI. In this study, the potential benefit of using a high order tensor model (4th order) in comparison of standard 2nd order DTI for differentiation of malignant and benign lesions, and healthy fibroglandular tissue (FGT) in breast are evaluated. Thirty-eight patients with biopsy proven breast lesions were examined using a Siemens 3T Skyra scanner and a 16-channel breast coil. The imaging protocol collected fat-suppressed unilateral sagittal images using a twice-refocused spin echo sequence with an EPI readout (TR/TE: 9300/85 ms, matrix: 90x90, in-plane resolution: 2x2 mm, s.thick: 2.5 mm) and 30 directions for two b-values (0 and 700 s/mm2). Regions of interest (ROI) were obtained segmenting the full extent of each lesion, and 20 healthy FGT ROIs were included for comparison. DTI analysis by means of 2nd and 4th order tensors was carried out using Matlab. The tensor fields, as well as derived parametric maps of mean diffusivity (MD), fractional anisotropy (FA), and largest diffusion eigenvalue ($\lambda 1$), were obtained for both models. 17 malignant lesions and 26 benign lesions were found. No variation in MD was observed between the models for any of the tissues under study. Increased $\lambda 1$ for malignant, benign and FGT, was observed when the 4th order model was applied, the differences being highly statistically significant ($p<0.001$) for all of them. Significant increased ($p<0.001$) values of FA for malignant lesions and healthy tissue were observed, while for benign lesions, FA did not show significant change between the two models ($p=1.0$). Classification between benign and malignant lesion using binary logistic regression yielded the highest accuracy when combining $\lambda 1$ and FA from the 4th-order DTI model (95.3 %). The results of our ongoing study suggest that for proper depiction of anisotropy in breast, higher order DTI models have to be applied (Fig.1). Significant differences in anisotropy between benign and malignant lesions when using a 4th-order DTI model allowed for higher classification accuracy in combination with $\lambda 1$. Our results present the potential of high order tensor derived FA to play a role in the improvement of automated detection of malignant lesions when combined with a diffusivity measure.

See image on next page.

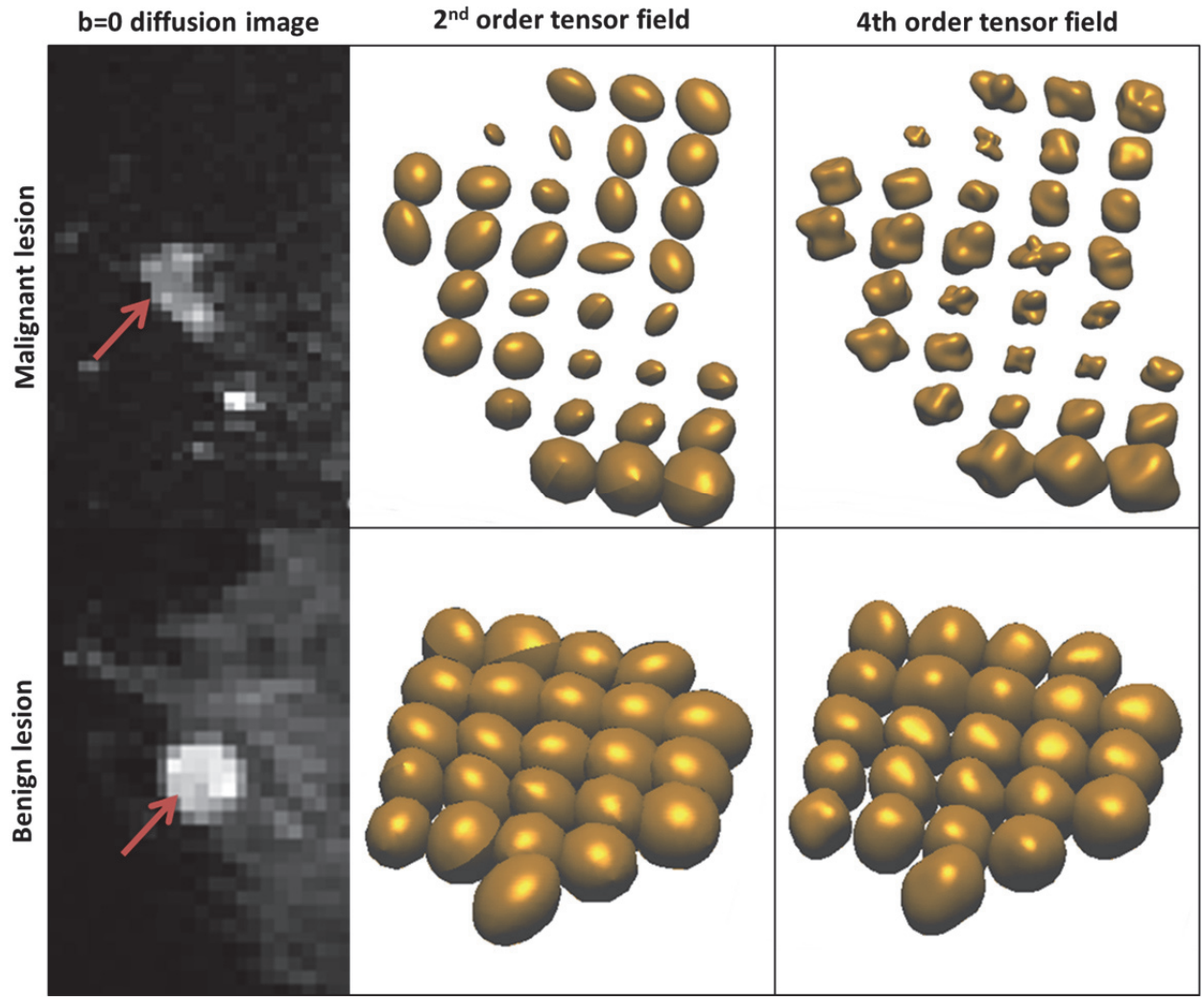

Figure 1. Comparison of tensor fields obtained applying a 2nd and a 4th order DTI model for a malignant (top row), and a benign lesion (bottom row), pointed by the red arrows.

Functional imaging for individualized cancer treatment

Ingfrid Haldorsen MD PhD,
Bergen Abdominal Imaging Research Group and Bergen Gynaecologic Cancer Research Group, Haukeland University Hospital/University of Bergen, Norway.
E-mail: ingfrid.haldorsen@helse-bergen.no

Introduction

Gynecologic cancers originating from the uterus and ovaries have significant overlap for histological subtypes reflected in clinical phenotypes, supported by recent data from molecular profiling of primary tumors.[1] Ovarian cancer is the most lethal while endometrial carcinoma is the most common pelvic gynaecologic malignancy.[2] In the metastatic setting, all types of pelvic gynecologic cancers have very poor survival, with minimal improvement over the last decades. No targeted therapeutics is yet available for routine clinical use. This has been linked to lack of molecular stratification in clinical trials, irrelevant preclinical models and little knowledge regarding relevant targets for treatment and tools for early detection of response in the metastatic setting.[3] This project is building on an existing network of preclinical, paraclinical and clinical scientists with the overall aim to promote **improved preoperative identification of high-risk patients** in order to facilitate **individualized treatment, reduced morbidity and implementation of targeted therapy** amongst patients with gynaecologic cancer.

Specific background

Endometrial cancer arises in the inner layer of the uterine cavity i.e. the endometrium (Fig 1), and the incidence is increasing. Since 2009 patients with endometrial cancer have been preoperatively subjected to functional imaging by MRI and PET-CT at Dep. of Radiology, Haukeland University Hospital (n=300) (Fig. 2).[2, 4]

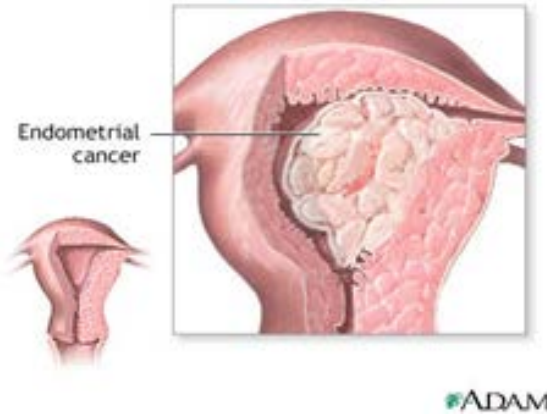

Fig 1. Endometrial cancer arises in the inner layer of the uterine cavity.

The research laboratory at the Dep. of Gyneacology, Haukeland University Hospital has since 2001 collected specimen from more than 2000 clinically annotated patients. Fresh frozen and paraffin embedded tissue are analyzed with a panel of established markers: tissue microarray, immunohistochemical staining, mRNA microarray and mutation analysis.

In parallel two orthotopic mouse endometrial cancer models have been developed by the research group (Fig. 2), and this provides a unique opportunity for experimentation and drug testing that would be impossible in human patients.

[1] Ojesina AI Nature 2014;506:371-375.
[2] Salvesen HB, Haldorsen IS, Trovik J. Lancet Oncol 2012;13:e353-e361.
[3] Salvesen HB et al, Proc Natl Acad Sci U S A 2009;106:4834-4839.
[4] Haldorsen IS et al,Eur Radiol 2012; 22:1601-1611 and Clinical Radiology 2012;67:2-12.

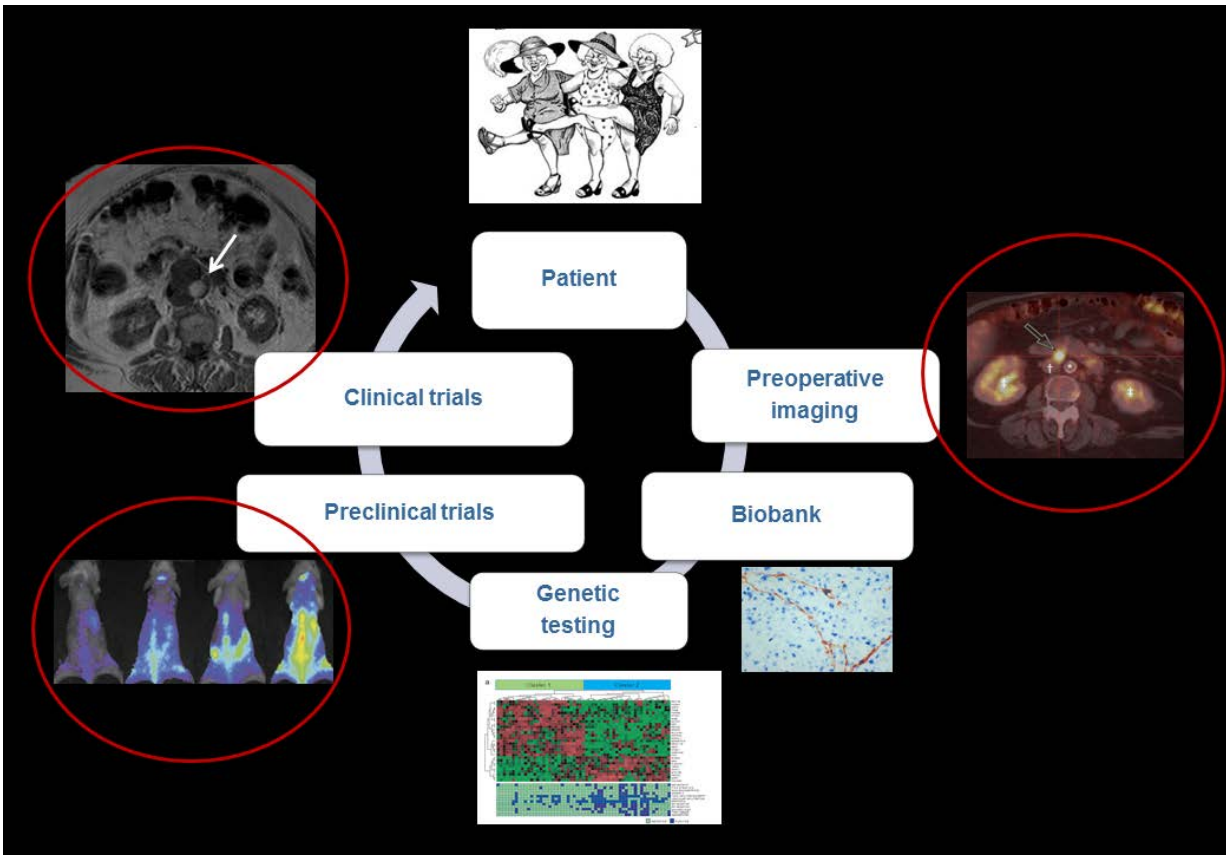

Fig 2. The diverse activity of the research group includes preoperative imaging, tissue collection in biobank, genetic testing, preclinical trials in orthotopic mouse models and clinical trials.

Recently, we have documented that a method for assessment of blood flow in tumour by dynamic contrast-enhanced (DCE)-MRI represent a clinically valid imaging biomarker for preoperative risk stratification in endometrial carcinoma patients (Fig 3). Furthermore, we have found that these imaging markers overlap with markers reflecting angiogenesis in the same tumour tissue. Interestingly, these immunohistochemical angiogenesis markers are also associated with outcome, and as new drugs target angiogenesis as biologically relevant processes in the tumours, we infer that this may open the avenue of further exploring these biologic processes through advanced imaging during antiangiogenic therapy in clinical trials for detection of early response (Fig 3).[5]

The primary research questions studied in this imaging project are as follows:

WP 1. Does preoperative imaging by MRI and FDG-PET provide functional tumour characteristics relevant for prognosis and therapy?
WP 2. Are functional imaging parameters of tumours in patients and mice related to clinically relevant biomarkers?
WP 3. Are the functional imaging characteristics based on preoperative MRI/FDG-PET in patients similar to that of MRI/FDG-PET imaging in orthotopic mouse models?
WP 4. Do the functional tumour characteristics observed in the orthotopic mouse models change during disease progression and during administration of targeted therapy?

[5] Haldorsen IS et al, Eur Radiol 2013; 23:2916-2925 and Br J Cancer 2014; 110:107-114.

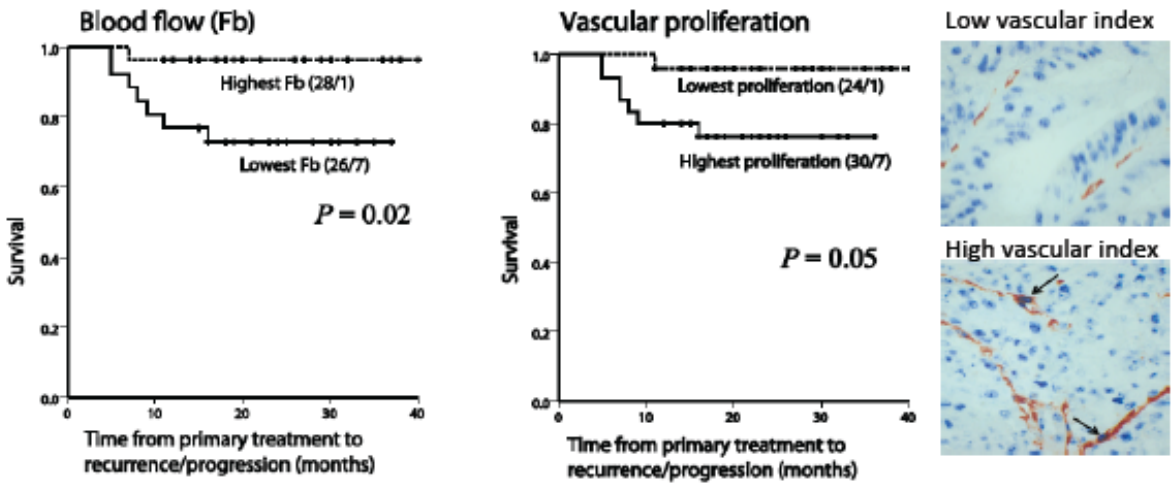

Fig 3. Survival according to estimated tumour blood flow (left panel) and angiogenic phenotype (middle and right panel) in tumours investigated in parallel preoperatively by fMRI and postoperatively for angiogenic biomarkers (vascular proliferation). For each category: number of cases/cases with recurrence or progression. P-value refers to Log Rank test.

The research group consists of investigators with a wide range of expertise covering preclinical models, molecular profiling, advanced diagnostic imaging methods and clinical patient care. This multidisciplinary collaboration is absolutely crucial in order to succeed in the implementation and interpretation of the studied advanced imaging techniques and is essential for successfully bridging the gap between preclinical and clinical cancer models.

Abstracts for poster session

Abstracts are organized in alphabetical order, presenting author

Participant category: Post doctoral fellow

Interactive Visual Analysis of Heterogeneous Cohort-Study Data

Paolo Angelelli [(1)], Steffen Oeltze [(2)], Judit Haasz [(3)], Cagatay Turkay [(1)], Erlend Hodneland [(3)], Arvid Lundervold [(3)], Astri J. Lundervold [(4)], Bernhard Preim [(2)], Helwig Hauser [(1)]

paolo.angelelli@uib.no

1. Department of Informatics, University of Bergen
2. Department of Informatics, University of Magdeburg
3. Department of Biomedicine, University of Bergen
4. Department of Biological and Medical Psychology, University of Bergen

Medical cohort studies enable the study of medical hypotheses with many samples. Often, these studies acquire a large amount of heterogeneous data from many subjects, to also enable retrospective analyses at later points in time. Usually, for each of these analyses, researchers study a specific data subset to confirm or reject specific hypotheses. Our new approach enables the interactive visual exploration and analysis of such data as a whole, helping to generate and validate hypotheses. A data-cube-based model handles the partially overlapping data subsets from such studies during the interactive visualization. This model enables seamless integration of such heterogeneous data and the linking of spatial and nonspatial views of the data. We implemented this model in a prototype application and used it to analyze data acquired in a cohort study on cognitive aging. Case studies employed the prototype to study aspects of brain connectivity, demonstrating the potential and flexibility of the approach.

See image on next page.

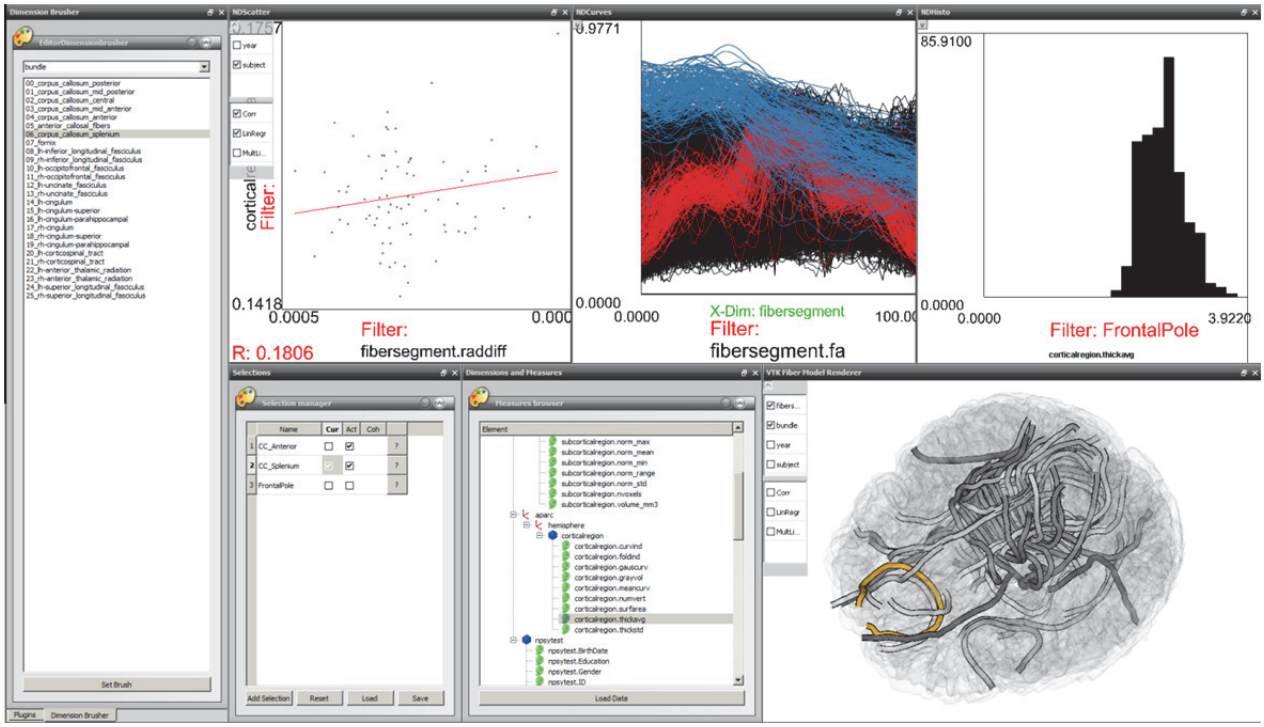

Prototype implementation of the proposed model. Spatial and non-spatial views of the data are linked together with coordinated multiple views.

Participant category: Post doctoral fellow

Delivery of multifunctional nanoparticles across the blood-brain barrier

Andreas Åslund [(1)], Sigrid Berg [(2)], Yrr Mørch [(3)], Wilhelm Glomm [(3,6)], Per Stenstad [(3)], Axel Sandvig [(4,5)], Sjoerd Hak [(5)], Rune Hansen [(2)], Catharina Davies [(1)]

andreas.aslund@ntnu.no

1. Department of Physics, NTNU
2. SINTEF Technology and Society, Trondheim
3. SINTEF Materials and Chemistry, Trondheim
4. Department of Neurosurgery, Umeå University Hospital, Umeå, Sweden
5. Department of Circulation and Medical Imaging, NTNU
6. Department of Chemical Engineering, NTNU

Today, there are few or no ways of treating most diseases associated to the brain, like cancer, Alzheimer's, ALS and many more. And many treatments that exist only treat the symptom, not the cause, e.g. Parkinson´s disease. The main reason for the lack of efficient drugs is the blood-brain barrier (BBB) which is much more restrictive compared to capillaries in other parts of the body. The BBB effectively hinders almost all large molecules and more than 98% of small molecular drugs from entering the brain. This is due to the tight packing of endothelial cells, that the capillaries are composed of, and they have an increased ability to pump out unwanted chemicals using so called efflux pumps. Focused ultrasound (FUS) in combination with gas filled microbubbles has been proven to permeate the BBB in several previous studies. When ultrasound comes in contact with the gas in the microbubble, the microbubble starts to oscillate and the oscillation can lead to a collapse of the microbubble. The oscillation, as well as the release of energy from the collapse, cause stress to the endothelial cells, which leads to local weakening of the BBB in the focus of the ultrasound. In Trondheim SINTEF Materials and Chemistry has developed a unique microbubble that is stabilized by nanoparticles made from organic polymers. The nanoparticle can be loaded with therapeutic and diagnostic agents and the effects created during the collapse of the microbubble will open the BBB and allow the nanoparticle into the interstitium of the brain. Since the last meeting, where the concept was described, we have now performed in vivo experiments to validate the concept. It will be shown how MBs can open the BBB transiently and safely, without causing bleeding, by MRI. Furthermore, ex vivo examination of the brain reveal that the nanoparticles are delivered into the brain.

See image on next page.

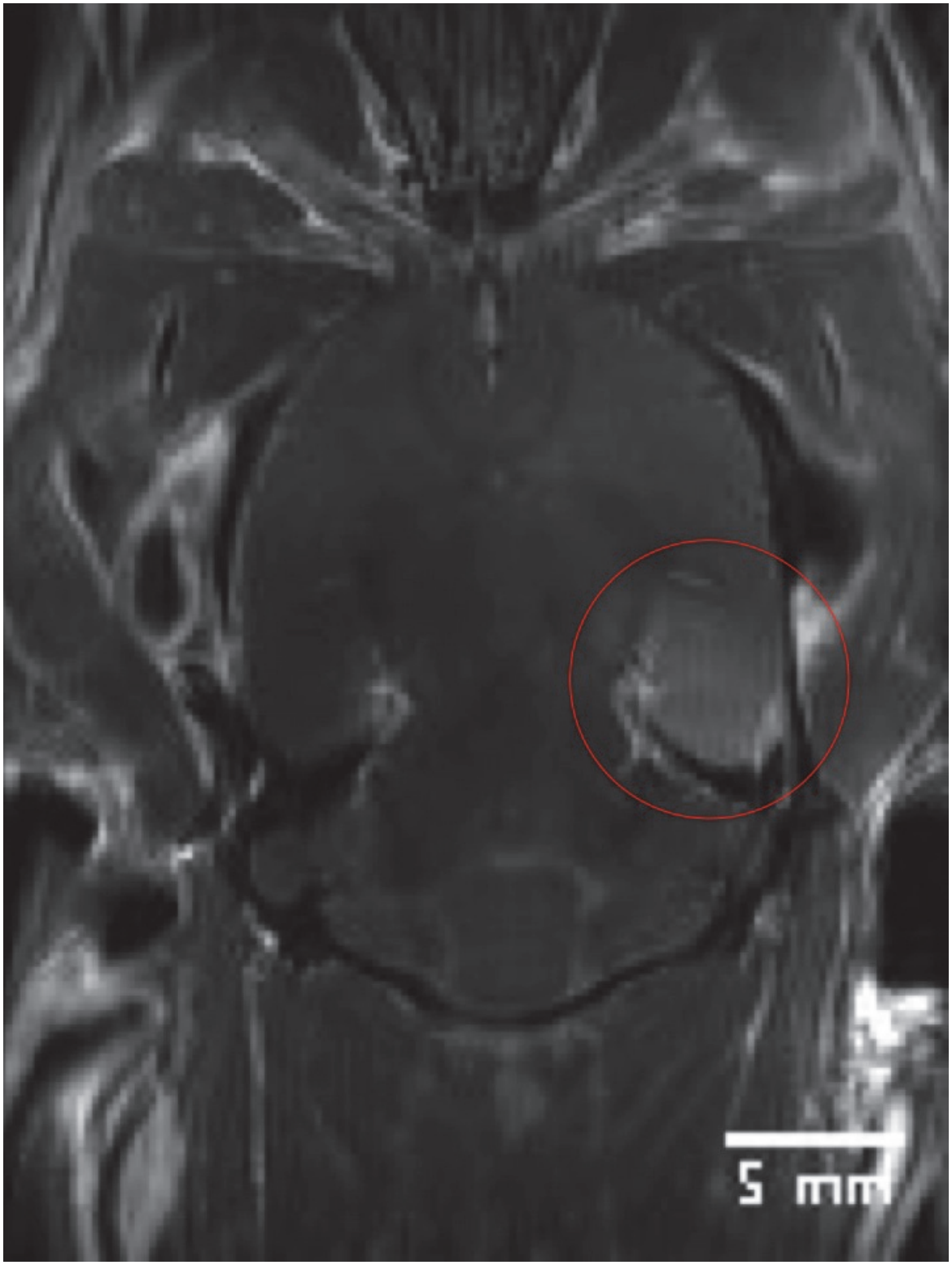

T1-weighted image the brain. The sonicated area (red circle) shows enhanced contrast compared to the other side of the brain, indicating selective opening of the BBB.

Participant category: PhD Candiate/Research Program Student

NMR Metabolomics predicts preeclampsia in first trimester blood and urine

Marie Austdal [1,2], Line Haugstad Tangerås [2,3], Ragnhild Bergene Skråstad [4,5], Kjell Åsmund Salvesen [5,6], Rigmor Austgulen [3], Ann-Charlotte Iversen [3], Tone Frost Bathen [1]

marie.austdal@ntnu.no

1. Department of Circulation and Medical Imaging, Faculty of Medicine, Norwegian University of Science and Technology (NTNU)
2. Liaison Committee between the Central Norway Regional Health Authority and Norwegian University of Science and Technology (NTNU)
3. Centre of Molecular Inflammation Research, and Department of Cancer Research and Molecular Medicine, Norwegian University of Science and Technology (NTNU)
4. Department of Laboratory Medicine Children's and Women's Health, Faculty of Medicine, Norwegian University of Science and Technology (NTNU)
5. National Center for Fetal Medicine, Department of Obstetrics and Gynecology, St. Olavs Hospital, Trondheim University Hospital
6. Department of Obstetrics and Gynecology, Clinical Sciences, Lund University, Lund, Sweden

Preeclampsia occurs in 3-4% of pregnancies and is defined by high blood pressure and protein in the urine after gestational week 20. The origins of the disease are thought to start with the development of the placenta. Improved prediction could direct care resources to high risk individuals, and provide better understanding of the origins of the disease and how it could be prevented. Nuclear Magnetic Resonance Spectroscopy metabolomics uses spectra of biofluids to create profiles of the current metabolism. The metabolome may change with disease even before symptoms present. These profiles can be input to predictive models to assess the risk of developing preeclampsia. Serum and urine were collected from 602 pregnant women with medium to high risk of preeclampsia, at gestational weeks 11+0 - 13+6. Standard 1H NOESY (urine) and CPMG (serum) NMR spectra were acquired on the samples using a Bruker Avance 600MHz spectrometer. The data were explored using principal component analysis, and a predictive model created using partial least squares discriminant analysis with double cross validation. Areas of the spectra that were important for discrimination were identified using HSQC, HMBC and TOCSY spectra of selected samples. Preeclampsia could be predicted with a sensitivity and specificity of 86% and 60% respectively, at 73% accuracy using urine spectra. Using serum spectra, the sensitivity and specificity were 67% and 55%. Metabolite differences included higher urinary creatinine and 2-hydroxyisobutyrate, and lower urinary hippurate, and 3-aminoisobutyrate in women who later developed preeclampsia. Serum spectra from the preeclampsia group contained higher levels of regions corresponding to triglycerides and lower levels of free cholines. Early urine changes may result from metabolic disturbances or low level kidney damage in the first trimester of pregnancies which later develop preeclampsia. Conventional “prior risk” methods can predict 30-40% of preeclampsia cases at a 10% false positive rate. It is possible that the metabolomics approach can improve this prediction. In our research, preeclampsia could be predicted from both urine and serum spectra, but with higher sensitivity from the urine spectra.

Participant category: PhD Candiate/Research Program Student

Imaging of the normal wrist in children with MRI, a study of normal development over time

Derk Avenarius [(1)], Lil-Sofie Ording Muller [(2)], Karen Rosendahl [(3)]

derk.avenarius@unn.no

1. UNN Tromsø and IKM UITØ Tromsø
2. Haukeland Sykehus
3. Oslo Universitets Sykehus

A healthy cohort of childen was imaged with MRI of the wrist in 2009, and again in 2013. The findings from the first examination changed our understanding of the normal maturation of the skeleton and the variations that should be considered normal. The overlapp with what was described as pathology in juvenile idiopathic artropathy was considerable and changed the way radiologist reported these studies. The follow up study was performed to follow these findings over time and increase our understanding of normal maturation that can mimic pathology. prelimenary results of this follow up wil be presented.

Participant category: PhD Candiate/Research Program Student

Nanoparticle uptake and nanoparticle-mediated silencing of efflux transporters in the blood-brain barrier

Habib Baghirov [(1)], Sulalit Bandyopadhyay [(2)], Ýrr Mørch [(3)], Wilhelm Glomm [(2,3)], Catharina Davies [(1)]

habib.baghirov@ntnu.no

1. Department of Physics, Norwegian University of Science and Technology
2. Department of Chemical Engineering, Norwegian University of Science and Technology
3. SINTEF Materials and Chemistry

A number of severe brain disorders remain intractable today, a major impediment to their treatment being the blood-brain barrier (BBB) - a dynamic interface that restricts the transport of potentially harmful substances into the brain, but also, unfortunately, filters out all large and the vast majority of small molecule drugs. Complementary to the BBB's mechanical barrier is the action of efflux transporters such as P–glycoprotein (P-gp) that intercept various small and/or lipophilic compounds that would otherwise be able to cross the BBB. Nanoparticles, owing to their ability to carry a large number of drug molecules and functionalization for specific targeting to or imaging inside the brain, are a promising solution to the issue of brain drug delivery. In our project, we address the drug delivery challenge posed by the BBB using two approaches. As part of one effort, we use a multifunctional platform consisting of poly (alkyl cyanoacrylate) nanoparticles and microbubbles enclosed by them to facilitate transport of nanoparticles and their payload into the brain with focused ultrasound exposure which has been shown to cause transient and reversible opening of the BBB. Our initial in vitro results show that polymeric nanoparticles are efficiently taken up by RBE4 rat brain endothelial cells serving as a BBB model. In addition, we use FeAu nanoparticles containing small interfering RNAs (siRNA) to silence efflux transporters in the BBB, ensuring unrestricted passage of their substrate drugs, and we have shown that our FeAu nanoparticles can deliver siRNA and silence P-gp inside RBE4 cells. In addition to their primary effect, both nanoparticle platforms can be used in theranostics as the polymeric nanoparticles contain a stably incorporated fluorescent dye and FeAu nanoparticles are natively visible using magnetic resonance imaging. Further experiments will be carried out to employ focused ultrasound exposure in the transport of nanoparticles both in vivo and in vitro and to improve the silencing effect of siRNA-containing FeAu nanoparticles.

See image on next page.

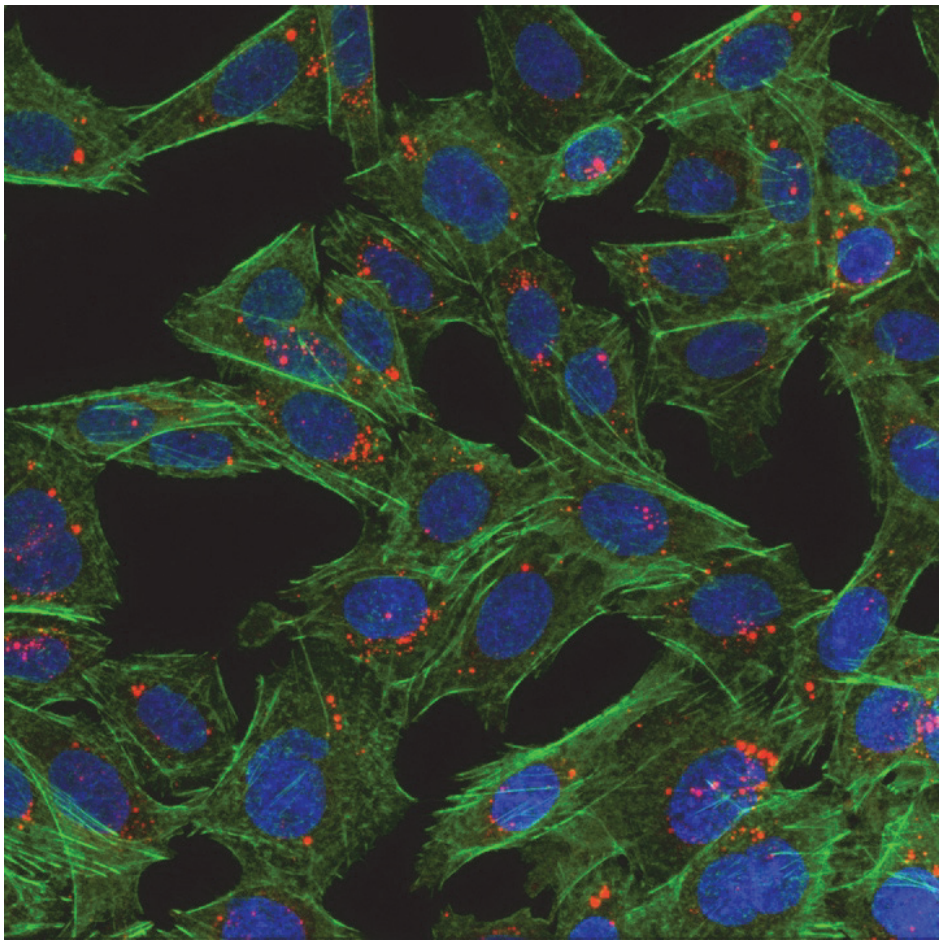

Fig.1. Poly (alkyl cyanoacrylate) nanoparticles taken up by RBE4 cells. Red: nanoparticles; blue – cell nuclei; green - actin filaments. Maximum intensity projection.

Participant category: PhD Candiate/Research Program Student

CEREBELLUM, THALAMUS AND CEREBRAL CORTEX IN VLBW ADOLESCENTS' MENTAL HEALTH

Violeta Botellero [(1)], Marit S Indredavik [(1)], Jon Skranes [(1)], Stian Lydersen [(2)], Ann-Mari Brubakk [(1)], Marit Martinussen [(3)]

violeta.lozano@ntnu.no

1. Laboratory Medicine Children's and Women's Health, Norwegian University of Science and Technology, Trondheim, Norway.
2. Department of Pediatrics. St. Olav's University Hospital, Trondheim, Norway
3. Department of Gynecology and Obstetrics. St. Olav's University Hospital, Trondheim, Norway

Background: Children born preterm with very low birth weight (VLBW; BW ≤1500g) are at risk of undergoing deviant brain development, sometimes accompanied by brain damage. The brain structures most commonly affected by preterm birth are the cerebral cortex, cerebellum and thalamus. These children also present a higher risk of psychiatric disorders during childhood and adolescence. However, the biological basis of this risk has not been established yet. Aim: To assess whether psychiatric symptoms are associated with changes in cortical thickness and volumes of thalamus and cerebellum in adolescents born preterm with VLBW. Design/Methods: Fifty VLBW and 57 term control adolescents were assessed at 14-15 years of age with: Schedule for Affective Disorders and Schizophrenia for School-Age Children, Strengths and Difficulties Questionnaire (SDQ Mother Report), Autism Spectrum Screening Questionnaire (ASSQ), and Children's Global Assessment Scale (CGAS). Cortical thickness (mm) and volumes of thalamus and cerebellum (ml) were obtained using an automated MRI segmentation technique (Freesurfer). Associations were analyzed by linear and ordinal logistic regression, adjusted for age, gender and total intracranial volume, and corrected for multiple comparisons (Benjamini-Hochberg). Results: VLBW adolescents had more psychiatric symptoms than controls. On MRI, they had several areas with thinner cortex and areas of thicker cortex compared to controls. Higher SDQ Emotional symptoms scores were associated with thicker insular cortex (Left: B=0.418 (0.192 to 0.644), p=0.001; Right: B=0.243 (0.061 to 0.426), p=0.010). Smaller cerebellar white matter (WM) volumes were associated with higher SDQ Hyperactivity scores (Left: B=-0.638 (-1.101 to -0.176), p=0.008; Right: B=-0.551 (-0.966 to -0.137), p=0.010) and lower CGAS scores (Left: B=4.653 (2.182 to 7.123), p<0.001; Right: B=4.255 (2.073 to 6.437), p<0.001). A trend of association in the same direction was observed with thalamic volumes (Left: B=4.995 (-0.576 to 10.566), p=0.078); Right: B=4.533 (-0.118 to 9.184), p=0.056). Conclusion: Our results indicate that psychiatric symptoms in VLBW adolescents may be related to structural brain anomalies in cerebellar WM and insular cortex, and probably the thalamus. We speculate that aberrant development of the cerebello-thalamo-cortical network may contribute to the higher risk of psychiatric symptoms. Further research is necessary to study this hypothesis.

Participant category: PhD Candiate/Research Program Student

GPU based Multi-Volume Rendering in FAST

Mohammadmehdi Bozorgi [(1)], Erik Smistad [(1,2)], Frank Lindseth [(1,2)]

mohammeb@idi.ntnu.no

1. Dept. of Computer and Information Science. Norwegian University of Science and Technology (NTNU)
2. SINTEF Medical Technology. Trondheim, Norway.

Medical imaging methods assist doctors in interpreting the available data and investigate the inner parts of the human body. CT, MRI and ultrasound scanners are a few examples of well-known modalities in the medical field that can generate 3D scalar data (volumes) of human anatomy and pathology. To directly extract a comprehensive 2D image from the produced 3D volumes several visualization techniques, commonly known as volume rendering have been proposed. Ray casting is the most widely used volume rendering technique for medical purposes today. Visualization of multiple volumes with overlapping regions can be very useful in the medical domain. Multi-volume rendering refers to a volume rendering technique that creates a 2D image by using several volumes that have overlapping regions. Using multiple volumes aids the analysis of the region of interest and decreases the chance of misinterpretation by medical doctors. High quality volume rendering at interactive frame rates are computationally demanding, multi-volume rendering even more so. In addition, a modern application in the medical imaging domain (e.g. surgical navigation system) requires concurrent visualization and image computing. In order to handle all the computationally expensive processes it is necessary to utilize and manage all the available computation resources (e.g. GPUs, CPUs and varies types of memory) in today's computers more efficiently. The authors are therefore developing FAST (FrAmework for heterogeneouS medical image compuTing), which is an open source cross-platform framework for medical image computing that has been designed to make this easier. In the current paper we propose a GPU-based multi-volume ray caster (MVRC) integrated into FAST to achieve high quality real-time 3D visualization. To integrate this kind of functionality in an existing toolkit is possible but this makes it challenging to measure the kind of performance that can be achieved, especially when real-time data are stream into the system and the data are being processed and displayed at the same time. In the proposed multi-volume ray caster, imaginary rays are sent through the volumes (one ray for each pixel in the view) and at equal and short intervals along the rays samples are collected from each volume. Samples from all the volumes are then composited using front to back α-blending. The performance of the MVRC in combination with different image computing loads can be benchmarked within the FAST framework.

See image on next page.

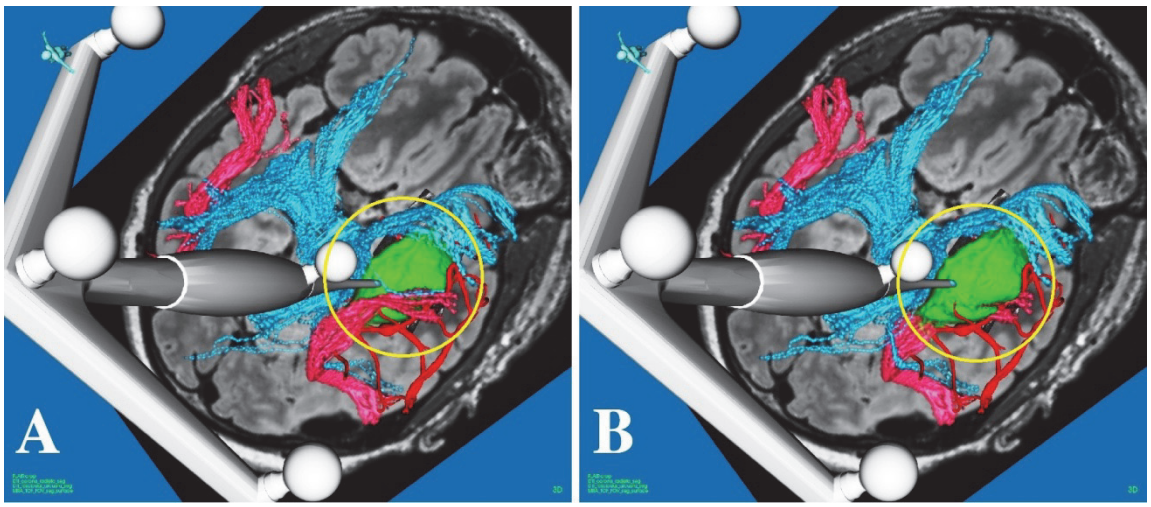

Multi-volume ray casting (A) vs. single volume rendering (B). In A, depth ordering of the structures is correct but in B, the apparent order of the structures is wrong. In a clinical setting loosing the depth information like this can of course have drama

Participant category: PhD Candiate/Research Program Student

MRgHIFU - experimental perivascular ablation in the liver

Ulrik Carling [(1)], Leonid Barkhatov [(2)], Frederic Courivaud [(2)], Tryggve Storås [(2)], Richard Doughty [(3)], Eric Dorenberg [(1)], Per Kristian Hol [(2)], Bjørn Edwin [(2)]

u.carling@gmail.com

1. Oslo University Hospital, Dep. of Radiology and Nuclear Medicine, Rikshospitalet
2. Oslo Univeristy Hospital, The Intervention Centre, Rikshospitalet
3. Oslo Univeristy Hospital, Dep. of Pathology, Rikshospitalet

Introduction: High intensity focused ultrasound (HIFU) is an ablation modality in which energy in ultrasound waves is used to produce heat in a desired focal spot. This non-invasive thermal ablation modality can be guided either by ultrasound (USgHIFU), or magnetic resonance imaging (MRgHIFU) with the HIFU transducer mounted in the MR table. MRgHIFU allows superior soft tissue contrast for planning and post-ablation imaging, as well as thermal control by the use of temperature sensitive sequences. Thermal ablation techniques using heat conduction (e.g. radiofrequency ablation) are sensitive to the cooling effect of blood flow, called the heat sink effect. MRgHIFU sonication is not dependent on heat conduction, and produces sharply delineated ablated volumes potentially less sensitive to heat sink. The aim of the study is to ablate around large hepatic and portal veins, and to study the heat sink effect on these ablation clusters. A secondary aim is to study vessel wall patency. Method: This is an acute animal study using Norwegian land swine. The pig is under total intravenous anaesthesia, including muscle relaxation for optimal breath control. Procedural MR compatible equipment includes tracheostomy, gastric tube, arterial and venous accesses, urine catheter, and an oesophageal temperature monitor. The pig is positioned in the prone position on the MR table. T1w planning sequences are performed, and hepatic and portal veins with diameter > 5 mm within the reach of the ultrasound waves are identified. Two clusters of 6-7 ablation cells of 8x8x20 mm are placed around separate vessels. Sonications are performed during one minute breath-hold in exhale. A proton frequency shift sequence is simultaneously performed for thermal control. Post-sonication imaging includes diffusion weighted imaging, and T1w contrast enhanced imaging. The liver is extracted and put in formalin for histo-pathological analysis. Results: Preliminary results indicate that liver parenchyma adjacent to vein walls can be ablated, while keeping the vessel wall patent. However there are cases of insufficient heat deployment, as well as vein wall rupture. Arterial walls close to the ablation clusters seem to be patent. Conclusion: The preliminary work indicates that efficient thermal ablation of liver parenchyma adjacent to large hepatic vessels using MRgHIFU is feasible.

See image on next page.

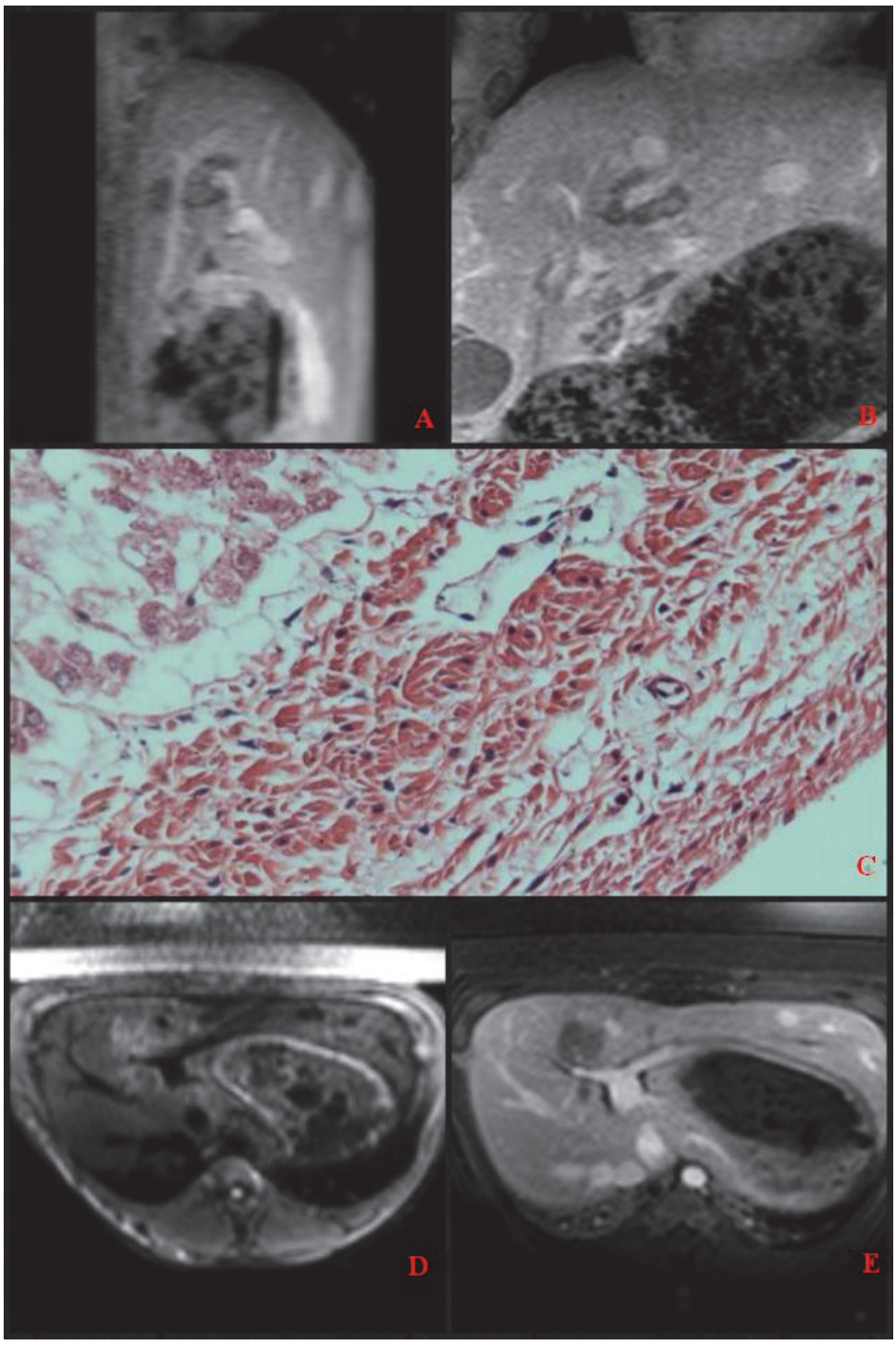

Post-sonication imaging, and histo-pathology at 400x enlargement A. Sagital T1w; cluster adjacent to liver vein, B. Coronal T1w; cluster around portal vein, C. Ablated hepatocytes upper left part, and intact vessel wall, D. DWI, and E. CE-T1w; cluster adj

Participant category: PhD Candiate/Research Program Student

Quality Assessment of multi-scanner MR images of the spine and the sacroiliac joints in patients with psoriatic arthritis

Ioanna Chronaiou [1, 3], Else-Marie Huuse-Røneid [2, 3], Tamara Hoffmann-Skjøstad [2], Ruth Thomsen [2], Beathe Sitter [1]

ioanna.chronaiou@hist.no

1. Radiation Therapy, Faculty of Technology, HiST, Trondheim, Norway
2. St. Olav's University Hospital, Trondheim, Norway
3. Department of Circulation and Medical Imaging, NTNU, Trondheim, Norway

The use of multiple scanners is common in the clinical practice and in multi-site studies. Different scanners and upgrades can introduce scanner-associated biases. When analyzing data from different scanners, it is important to assess the impact of multiple scanners in the image quality. Psoriatic Arthritis (PsA) is an inflammatory joint disease that develops in patients with psoriasis and manifests by highly heterogeneous clinical symptoms, including a broad spectrum of inflammatory changes in multiple locations of the body. Magnetic resonance imaging (MRI) allows direct visualization of inflammation and therefore can detect early inflammatory changes in PsA patients, due to intervention or progress of the disease. The main hypothesis for this study is that the changes due to intervention are large compared to scanner-induced changes and that there is no interaction of scanner with case and/or control groups. A patient cohort (N=40) diagnosed with PsA will undergo MRI examinations with two series of images (T1 and T2-weighted with fat suppression) of the spine and sacroiliac joints at three timepoints; before intervention, after 12 weeks intervention and 6 months after intervention. The cohort will be randomized into a control group (N=20) and an intervention group (N=20). MR scans will be performed at different scanners at the three time points. Multi-scanner data will be analyzed with regard to the interaction of scanner with effects of interest. Image quality will be assessed by measuring signal-to-noise ratio and contrast-to-noise ratio. Methods to be explored for image analyses will include automated segmentation of the spine (vertebrae and intervertebral disks) and voxel-by-voxel analyses. Images will be also judged using a standardized scoring system for (1) overall image quality (2) anatomical delineation and (3) ghosting/distortion artifacts and quality of the fat saturation. The inter- and intra-site variability will be assessed and correlated to the radiological evaluation and registration of changes. This project aims to assess objective measures of the quality of MR images of the spine and sacroiliac joints in PsA patients acquired with different scanners. These images will be further used for measuring the effect of intervention in these patients.

Participant category: PhD Candiate/Research Program Student

Quantification of glomerular filtration rate (GFR) using a model-based MR renography technique provides good agreement with IohexolGFR and eGFR in 20 healthy subjects.

Eli Eikefjord [(1)], Erling Andersen [(1)], Jan Ankar Monssen [(1)], Erlend Hodneland [(2)], Frank Zøllner [(3)], Arvid Lundervold [(2)], Einar Svarstad [(1)], Jarle Rørvik [(2,1)]

eli.eikefjord@helse-bergen.no

1. Haukeland University Hospital
2. University of Bergen
3. Heidelberg University

Purpose: To explore the intra-subject and repeated estimation of GFR with a model-based MR-renography technique (FLASHGFR) compared to Iohexol clearance (IohexolGFR) and creatinine clearance (eGFR). Materials and methods: Twenty healthy volunteers (mean 25±5 years, BMI: 22.6±2) with no history of renal disease and normal creatinine level (mean 70±5 µmol/L) underwent two 3D DCE-MRI examinations (MR1, MR2) and blood sampling for Iohexol clearance (gold standard) and creatinine clearance within a time span of 10 days. A whole-kidney 3D FLASH-sequence was applied with repeated breath-hold and a TR/TE/FA/matrix/slice thickness/no slices of 2.36 ms/0.8 ms/ 20°/192x192/3 mm/30, respectively. At each examination, dynamic measurements were acquired during contrast media bolus injection at 3 mL/s of 0.025 mmol/kg of GdDOTA. After automated motion correction using in-house software, the contrast-enhancement curves were analyzed with a two-compartment filtration model (the UMM Perfusion plugin to Osirix). Manually delineated renal parenchymal ROIs for left and right kidney (Fig. 1) applied to the tubular filtration (GFR) maps were used to estimate single kidney FLASHGFR. For assessing the agreement between GFR methods, Bland-Altman statistics were performed. For assessing reproducibility between MR1 and MR2 of single kidney GFR, we calculated intra class correlation coefficient (ICC). Results. Mean and standard deviations (SD) in total GFR-values across all subjects estimated from Iohexol clearance, creatinine clearance, MR1 and MR2 were 102.9 (SD9.8), 103.1 (SD16.4), 102.5 (SD15.1) and 99.4 (SD 21.5) ml/min/1.73m2, respectively. Bland-Altman statistics (Fig.2) showed a good agreement with IohexolGFR both for eGFR (bias=0.2, 2σ=28.3 ml/min/1.73m2) and FLASHGFR (n=40) (bias=-2.0, 2σ =39.1 ml/min/1.73m2). The ICC between single kidney GFR measured at time 1 versus time 2 was for left and right kidney 0.47 (P= 0.083) and 0.3 (P=0.218), respectively. ICC for total GFR was 0.290 (P=0.227). Conclusion. Estimation of total MRGFR with our 3D FLASH sequence showed a good agreement with both IohexolGFR and eGFR. However, the single kidney reproducibility results were only moderately according to the ICC values. To be clinically useful and robust, our MRI-based method needs to be improved regarding the model-based estimation, automation of parenchyma segmentation, and will also need to be tested on patients with kidney disease.

See image on next page.

Fig.1 Manually delineated ROI of right renal parenchyma used for GFR-estimation.

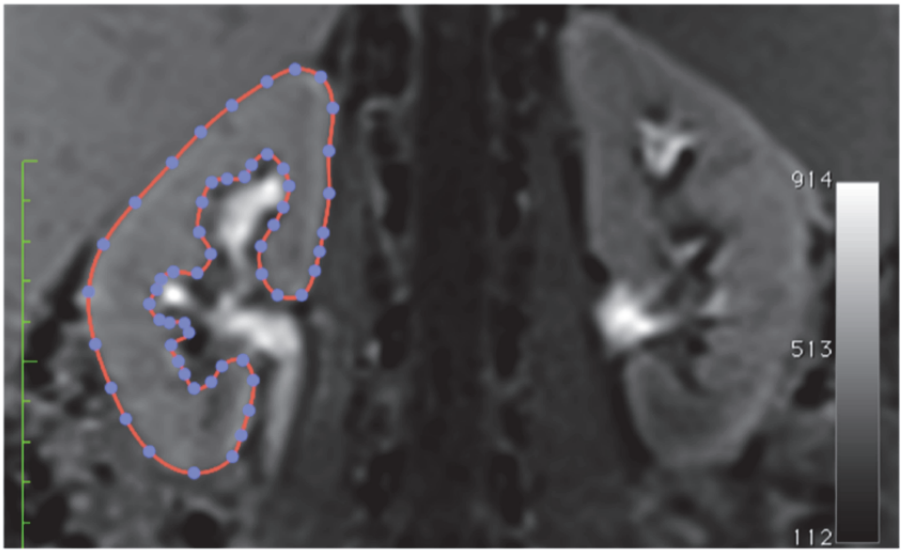

Fig. 2 Bland-Altman plots; agreement between $Iohexol_{GFR}$, eGFR and MR_{GFR}

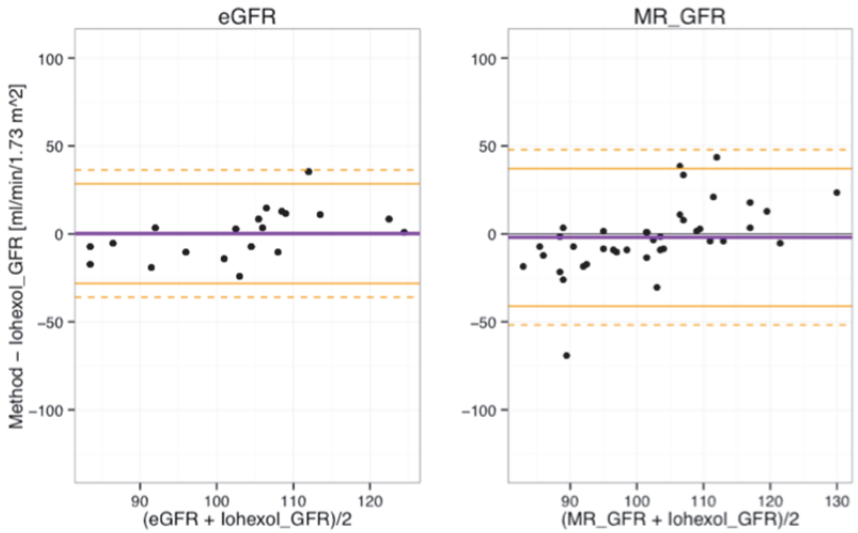

Participant category: Post doctoral fellow

Posterior parahippocampal cortex supports the representation of current location and anterior parahippocampal cortex and anterior hippocampus an abstract overview of the environment

Hallvard Røe Evensmoen [(1)], Asta Håberg [(1,2)]

hallvard.r.evensmoen@ntnu.no

1. Department of Neuroscience, Norwegian University of Science and Technology (NTNU), Trondheim, Norway
2. Department of Medical Imaging, St. Olav's Hospital, Trondheim, Norway

In rodents the hippocampus is given a more important role for the representation of current location than the parahippocampal cortex. In humans, however, this is still an open question. The participants (32 males) had to learn 36 small virtual environments and evaluate environmental images, during functional magnetic resonance imaging (fMRI) at 3T (Voxel size = 1.9x1.9x1.9mm, 32 channel head coil). The participants were given 40 seconds with free exploration to learn each environment. The environments either consisted of a unique outer wall (Outer wall), a unique inner and outer wall (Inner & outer wall), or three unique objects with specific locations and an outer wall (Objects & outer wall). The participants also evaluated the geometry in images from environments with an outer wall for 40 seconds (Environmental images). The participants completed four runs. Each run involved nine environments and three blocs with Environmental images. After each run, the participants' knowledge of the environments was tested, i.e. Inner wall test, Outer wall test, and Inner & outer wall test. Both the order of the runs and the order of the blocks were randomized. The activation in the posterior parahippocampal cortex increased for contrast Outer wall > Environmental images, Inner & outer wall > Outer wall, and Objects & outer wall > Outer wall. The activation in the anterior parahippocampal cortex and hippocampus decreased for contrast Outer wall > Environmental images and Inner & outer wall > Outer wall, and increased for contrast Objects & outer wall > Outer wall. Further, the activation in the posterior parahippocampal cortex contributed positively to the Inner wall test score while the activation in the anterior parahippocampal cortex contributed positively to both the Inner and Outer wall test score. The activation in the hippocampus contributed positively to both the Inner wall and the Inner & Outer wall test score. The posterior parahippocampal cortex supports a representation of current location from a local perspective while the anterior parahippocampal cortex and anterior hippocampus supports an abstract overview of the environment.

Participant category: PhD Candiate/Research Program Student

CT visualisation of the Eustachian Tube using focal contrast administration, a feasibility study.

Benedicte Falkenberg-Jensen [1], Juha Silvola [2], Helene Laurvik [3], Siri F. Svensson [5], Andreas Lervik [4], Greg E. Jablonski [2], Einar Hopp [1]

b-falkenberg@hotmail.com

1. Department of Radiology, Rikshospitalet, Oslo University Hospital, Oslo
2. Department of ENT, Rikshospitalet, Oslo University Hospital, Oslo
3. Department of Patholog, Oslo University Hospital, Oslo
4. Norwegian University of Life Sciences, NMBU, Oslo
5. Division of Diagnostics and Intervention, Oslo University Hospital, Oslo

Globally infectious-, inflammatory- or even destructive disease of the middle ear is common, and various medical and surgical treatments causes the patients pain, hearing loss and repetitive surgery. Dysfunction of the Eustachian tube (ET) is considered a main cause for these conditions. The ET consists of a bony part close to the tympanic cavity and a cartilaginous part to the epipharyngeal room. Recent years, balloon catheter dilatation of the cartilaginous part of the ET has emerged as a new treatment option with beneficial effect on ET dysfunction. Current radiological procedures are inadequate in characterizing the ET, and hence there is a demand for new thinking. Our main hypothesis is that contrast media application to the middle ear and subsequent CT examination of the temporal bone and epipharynx is feasible and provides clinically important information before ET balloon dilatation. Applying diluted contrast media to the middle ear on two human cadaver temporal bone specimens followed by CT examinations, we determined the ideal parameters regarding contrast dilution, CT algorithm and head positioning for visualisation of the middle ear anatomy and contrast passage through the ET. Ten rabbits are investigated with CT examination of the temporal bone after contrast media application to the middle ear. Contrast media application is performed surgically, with tympanic membrane perforation aided by otomicroscopy. The animals are followed one week to explore whether inflammation is induced after the procedure. Before euthanasia, repeat contrast media application and CT examination is performed for most of the individuals. Irradiation dose measurement is performed, and histopathological specimens are sampled. We regard this study necessary to prove feasibility and validate the method in order to enable clinical trials and possibly defining a new CT protocol for a large group of patients. Rabbit investigations will be performed this spring, and we plan the presentation of preliminary results in Bergen, focusing on contrast agent visualization.

See image on next page.

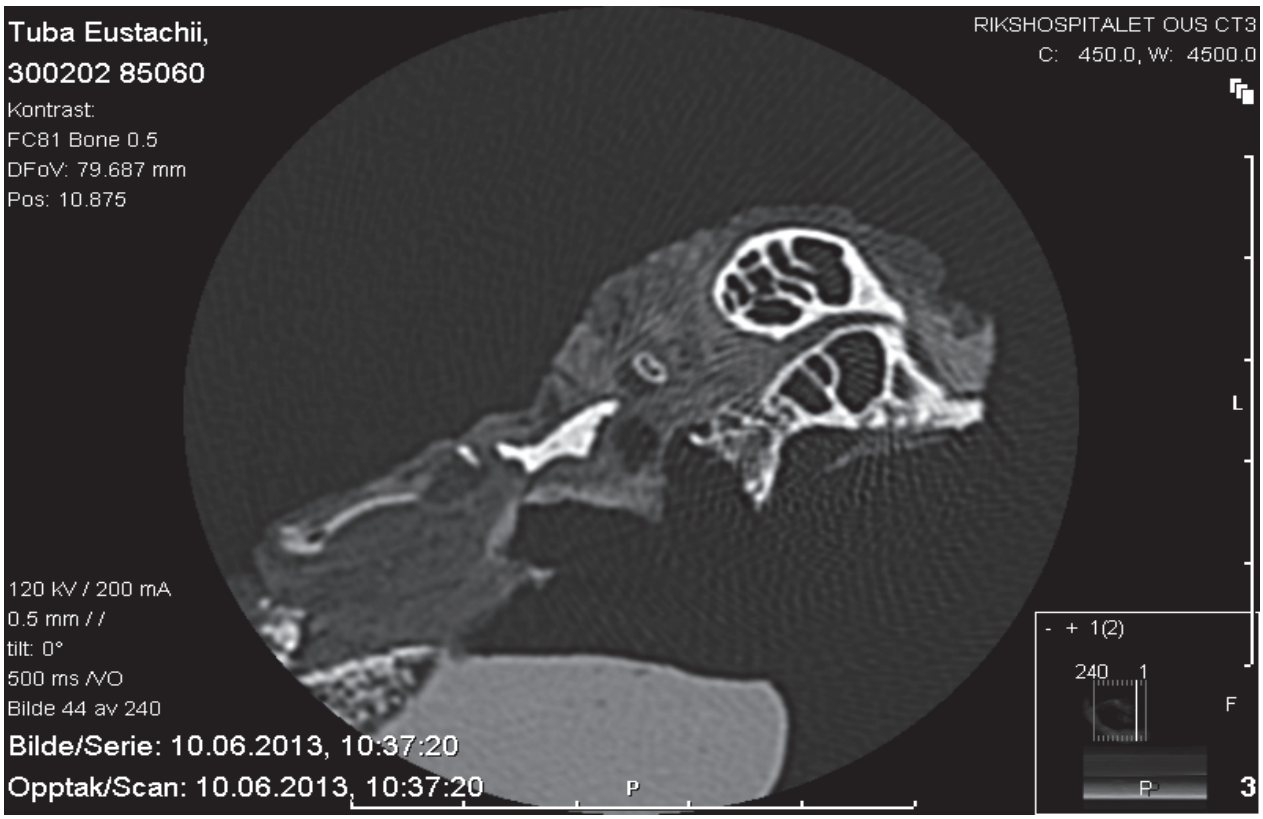

Contrast in ET on human cadaver

Participant category: PhD Candiate/Research Program Student

Characterization of growth cartilage in the femoral epiphyses of pigs by nonlinear optical microscopy

Andreas Finnøy [(1)], Magnus Lilledahl [(2)], Kristin Olstad [(3)]

andreas.finnoy@ntnu.no

1. Norwegian University of Science and Technology Department of Physics N-7491 Trondheim NORWAY
2. Norwegian University of Science and Technology Department of Physics N-7491 Trondheim NORWAY
3. Norwegian University of Life Sciences Faculty of Veterinary Medicine and Biosciences Department of Companion Animal Clinical Sciences P.O. Box 8146 Dep. N-0033 Oslo Norway

Second harmonic generation (SHG) microscopy is being established as a prevalent imaging modality for collagenous tissue due to its intrinsic confocality and being a non-invasive, label-free technique. This study has used SHG signals from collagen in combination with detection of endogenous two photon excitation fluorescence (TPEF) to characterize the cartilage in the developing epiphyses of the distal femur in pigs. Most long bones develop in a process where a cartilaginous template gradually is replaced by bone. There is evidence for a rich vascularization of the growth cartilage in the epiphyses prior to and during the ossification. The blood vessels are located in cartilage canals whose role has not yet been fully worked out. Focal necrosis of cartilage canals in developing epiphyses results in growth cartilage ischemic necrosis and focal disturbance of the ossification process, which is the hallmark of osteochondrosis, a condition associated with lameness in swine and horses. It is suggested that changes in fibril organization and type of collagen around and within cartilage canals may influence the susceptibility of cartilage canals undergoing necrosis because of lower tolerance to biomechanical stress. Studies have demonstrated alterations in the extracellular matrix of necrotic cartilage, which may cause weakening of the cartilage and be responsible for the progression from osteochondrosis to articular cartilage fissures and loose bodies. To address these issues, SHG and TPEF were used to image unstained 100 μm thick sections from the femoral condyles of nine 12-26 weeks old pigs. The youngest pigs revealed highest vascular density. The intensity of the SHG signal around cartilage canals was found to vary strongly between different canals and along the same canal, indicating that there is a heterogeneous organization of collagen fibrils around the cartilage canals. Cartilage regions with necrotic chondrocytes were identified but not consistently associated with alteration of SHG intensity from the cartilage matrix. Necrotic cartilage canals were always observed in association with necrotic chondrocytes. The variation in matrix around the cartilage canals and in the necrotic cartilage may reflect different physiological and pathological states. Further assessments will be done to clarify this and a possible correlation between necrotic chondrocytes and collagen fibril organization around adjacent cartilage canals.

Participant category: PhD Candiate/Research Program Student

Synthesis of CytoCy5S and its NHS ester for Optical Imaging

Elvira Garcia de Jalon [1,2], Kjetil Børve [2], Bengt Erik Haug [1], Emmet Mc Cormack [2]

elviragarciadejalonvi@gmail.com

1. Department of Chemistry and Centre for Pharmacy, University of Bergen
2. Hematology Section, Department of Clinical Science, University of Bergen, Bergen, Norway and Hematology Section, Department of Internal Medicine, Haukeland University Hospital, Bergen, Norway

Squaraines are 1,3-disubstituted compounds formed by an electron deficient four membered ring, derived from the squaric acid, and two electron donating methylene bases, that exhibit high absorption and emission wavelength in the near infrared region1,2. These NIR dyes, including CytoCy5S, are used as long-wavelenght probes in vitro and in vivo biomarker assay techniques thanks to their particular optical properties. We have synthesized an unsymmetrical compound introducing a dinitrobenzyl moiety to a Cy5 cyanine dye that quenches the CytoCy5S making it a suitable reduction substrate of nitroreductase. We have previously demonstrated that nitroreductase can be used as an alternative near infrared reporter gene platform to fluorescent proteins and bioluminescence, and is of particular use in the preclinical in vivo imaging of cancer metastasis and GDEPT strategies. Thus, synthesis of new optical probes as substrates and prodrugs of nitroreductase is highly desirable3. We have carried out two different reaction pathways based on the condensation of two distinct indolium-derived bases with squaric acid and squaric acid dibutyl ester. The two electrodonating moieties have been synthesized from simple and commercially available chemicals. Furthermore, CD33, which is over expressed in acute myeloid leukaemia, has been used as a biomarker of this disease. To couple the NTR substrate dye to CD33 targeting antibodies, an appropriate leaving group is required and N-hydrosuccynimide ester has been selected and obtained using TSTU as coupling reagent. Here we present the successfully synthesis of CytoCy5S and its NHS ester and conjugation to the leukaemia biomarker CD33. Preliminary results demonstrate the in vitro and in vivo imaging results from these novel optical probes and suggest further development of NTR imaging platforms as biomarker validation platform in vivo. 1. Sreejith S, Carol P, Chithra P, Ajayaghosh A. Squaraine dyes: a mine of molecular materials. J Mater Chem 2008, 18(3): 264-274. 2. Hassan M, Klaunberg BA. Biomedical applications of fluorescence imaging in vivo. Comparative Med 2004, 54(6): 635-644. 3. McCormack E, Silden E, West RM, Pavlin T, Micklem DR, Lorens JB, et al. Nitroreductase, a near-infrared reporter platform for in vivo time-domain optical imaging of metastatic cancer. Cancer research 2013, 73(4): 1276-1286.

See image on next page.

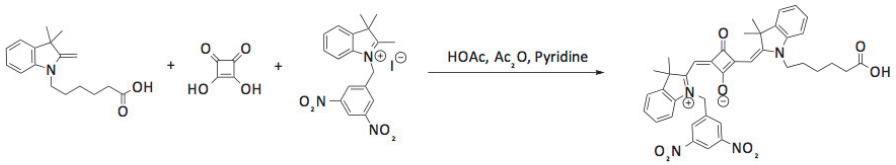

Scheme 2 Multistep condensation reaction of squaric acid

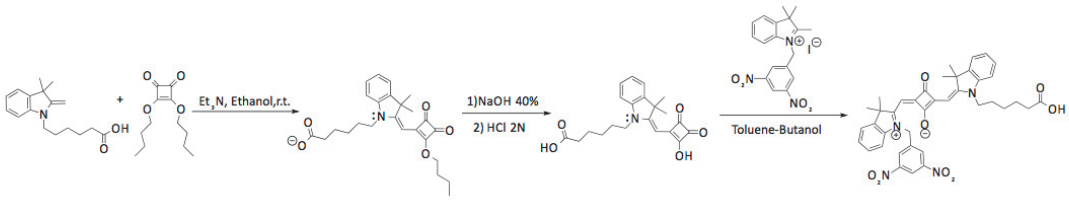

Scheme 2 Multistep procedure through the mono-substituted squaraine

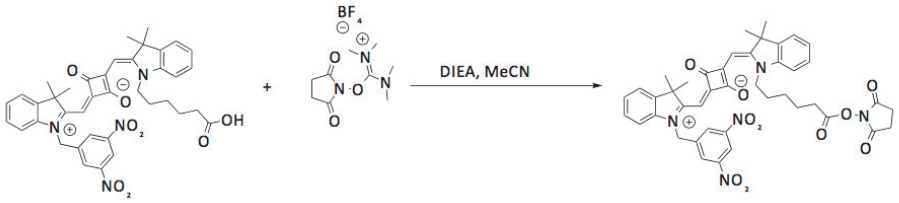

Scheme 3 One-step coupling to form the NHS ester

Participant category: PhD Candiate/Research Program Student

Metabolic and transcriptomic profiling of prostate cancer cells treated with O-linked N-acetylglucosamine transferase inhibitor (ST045849)

Saurabh S. Gorad [1,2], Harri M. Itkonen [3], Siver A. Moestue [1,2], Ian G. Mills [3,4,5], Tone F. Bathen [1,2]

saurabh.gorad@ntnu.no

1. Department of Circulation and Medical Imaging, NTNU, Trondheim, Norway
2. St. Olavs University Hospital, Trondheim, Norway
3. Prostate Research Group, Center for Molecular Medicine Norway, Nordic EMBL Partnership, University of Oslo and Oslo University Hospital
4. Department of Cancer Prevention, Oslo University Hospital, Oslo, Norway
5. Department of Urology, Oslo University Hospital, Oslo, Norway

Prostate cancer (PCa) is a frequently diagnosed cancer in males worldwide. A major challenge is the acquired resistance to androgen-deprivation therapy, with lack of curative treatments. We recently reported that O-linked N-acetylglucosamine transferase (OGT) functions as a metabolic integration point in PCa, and regulates the stability of an oncogene c-Myc. However, metabolic alterations triggered by targeting OGT are poorly described. Purpose of this study was to evaluate the effect of the OGT inhibitor ST045849 on metabolism and gene expression in prostate cancer cells. LNCaP cells were treated with 20mM ST045849 for 96h. Cell extracts and culture medium (3-biological replicates) was obtained. The 1H NMR data was acquired on 14.1T Bruker system and selected metabolites were quantified using the PULCON principle, with creatine as external calibration standard. mRNA was extracted from the cells and global gene expression profiles obtained. Treatment with ST045849 caused less than 20% decrease in cell viability compared to control. Gene expression profiles showed a significant downregulation of cell-cycle related genes and alterations in genes associated with glucose, amino acid and lipid metabolism. Expression changes correlated with changes in metabolite levels: increased expression of choline kinase β was concordant with increased phosphocholine concentration in cell extracts. Spectra obtained from both culture medium and cell extracts showed a significant decrease in lactate levels in cells treated with ST045849 (Figure 1). In addition, significant alterations in glycerophosphocholine and amino acid levels were observed ($p<0.05$). The alterations in phosphocholine and amino acid concentrations indicate that ST045849 cause a metabolic reprogramming in LNCaP cells. Altered expression of genes in glucose and choline metabolism could explain the observed metabolic changes. Reduced glycolytic activity may have caused the cells to utilize other substrates as a source for energy production and/or anaplerotic fueling of the citric acid cycle. This could provide opportunities to enhance cell death response by combining ST045849 with drugs inhibiting other metabolic pathways. Inhibition of OGT may be a novel approach for PCa treatment. ST045849 reduce glucose consumption and induce alterations in amino acid metabolism. Combination of metabolomic and transcriptomic data suggests potential for synergistic metabolic lethality, which we are currently validating.

See image on next page.

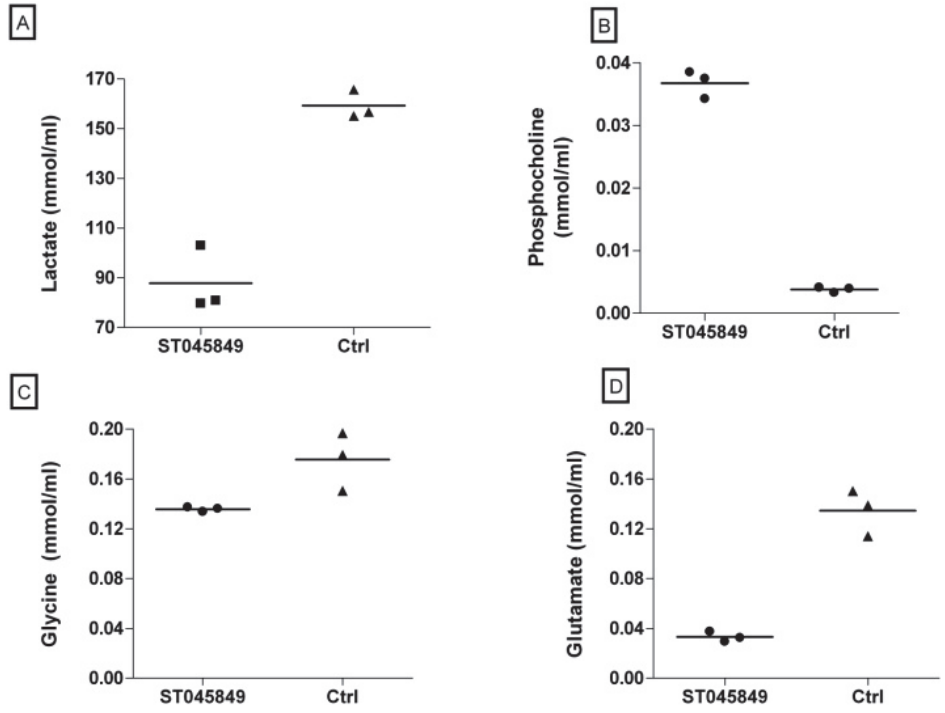

Figure 1. Concentrations of A) lactate in culture medium, B) phosphocholine, C) glycine and D) glutamate in cell extracts measured using 1H NMR.

Participant category: PhD Candiate/Research Program Student

US Image Registration for Intelligent Surgical Robotic System

Dilla Handini [(1)], Kim Mathiassen [(1,2)], Ho Quoc Phuong Nguyen [(1)], Ole Jakob Elle [(1,2)]

daffodilsky@gmail.com

1. The Intervention Center, Oslo University Hospital
2. Department of Informatics, University of Oslo

The project is a part of I-SUR (Intelligent Surgical Robotics), a project funded by the European Union within the 7th Framework Programme [1]. I-SUR aimed to develop a robotic system that could perform simple surgical actions automatically. One of the actions to be performed by the robot is automatic needle insertion procedure, with a scenario of cryoablation procedure to freeze a malignant tumor on the kidney. The system consists of two robots, one holding the needle and performing the insertion, and the other one holding the US probe to monitor the insertion procedure. The US probe being used is a 2D linear probe. The insertion was performed on a phantom made by one of the project partners. It had a gelatin skin layer, gelatin kidney organs and water filling up the spaces in between. The needle insertion was planned on the CAD model of the phantom, and to be executed in the phantom in physical space with the guidance of the US probe. Hence, a registration is performed to align the CAD model frame to the US image frame. Recently the project performed a preliminary test of a system inserting a needle automatically. The registration method that had been implemented in the robotics set up was a point based method. It used 4 spherical landmarks implanted in the phantom. By aligning the position of the landmarks both in the CAD model of the phantom and ones in the US image space, the transformation matrix between the CAD model and the US image can be obtained. Another method of registration is currently being explored. It is to perform the registration utilizing the organ itself instead of implanted landmarks. It could make the implementation more realistic. It involves the alignment of the kidney image of the CAD model and the one reconstructed from the US image slices. The method adopts ICP method, utilizing CloudCompare software [2].
Reference: 1. http://www.isur.eu/isur/ 2. http://en.wikipedia.org/wiki/CloudCompare

Participant category: Post doctoral fellow

Differentiation of metastatic and non-metastatic mesenterial lymph nodes by Real-time elastography evaluation

Roald Flesland Havre [1,2], Sabine Leh [2], Odd Helge Gilja [1,2], Svein Ødegaard [2], Jo Erling Riise Waage [4], Gunnar Baatrup [4], Lars Birger Nesje [1,2]

roald.flesland.havre@helse-bergen.no

1. Medical Department, Haukeland University Hospital
2. Dept. Of Pathology, Haukeland University Hospital
3. Institute of Clinical Medicine, University of Bergen, Norway
4. Department of Surgery, Haukeland University Hospital, Bergen, Norway

Purpose: To investigate if strain elastography could differentiate between metastatic and non-metastatic mesenteric lymph nodes ex vivo and to semi-quantify fibrosis in lymph nodes by histology. Material and Method: We investigated 90 mesenterial lymph nodes shortly after resection in 26 patients representing 17 cases with colorectal cancer and 8 cases with Crohn's disease. We used Real-Time elastography with a linear probe. Tissue hardness in lymph nodes was evaluated by three different methods: A continuous Visual Analogue Scale (VAS), by a four-point categorical visual scale and by measuring strain ratio (SR). B-mode characteristics such as long and short axis diameter, echogenecity, shape and lymph node architecture were also recorded. The pathological diagnosis was used as reference standard and a single pathologist performed a semi-quantitative fibrosis score was applied for each lymph node. Results: 20 lymph nodes were metastatic and 70 lymph nodes were non-metastatic (28 from Crohn specimens and 42 from cancer specimens). Metastatic and non-metastatic lymph nodes were significantly different for strain ratio (2.05 vs. 1.53, $p=0.041$) and fibrosis score (1.55 vs. 0.03, $p<0.001$). Semi-quantification of strain by VAS (64.0 vs. 55.1, $p=0.111$) and categorical classification (2.05 vs. 1.64, $p=0.154$) was not significantly different for metastatic and non-metastatic lymph nodes ($p>0.05$). The metastatic lymph nodes were more fibrotic than the non-metastatic lymph nodes. In a ROC analysis strain imaging was not superior to measurement of short axis diameter of lymph nodes in differentiating metastatic from non-metastatic lymph nodes. Conclusion: Semi-quantification by SR of mesenterial lymph nodes in resected tissue identifies a difference in strain value in metastatic and non-metastatic lymph nodes, but SR was not superior to B-mode ultrasound criteria for this differentiation.

See image on next page.

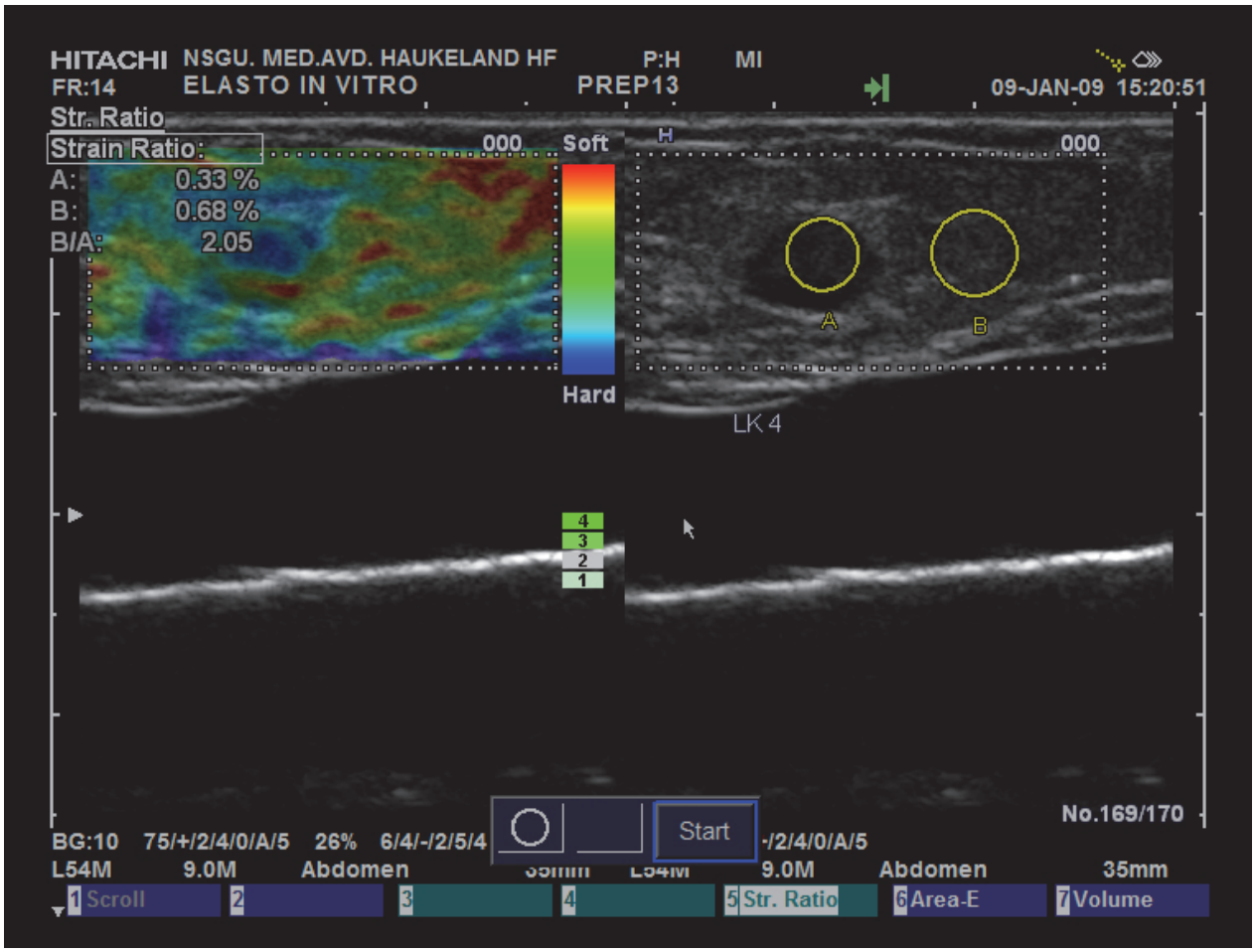

B-mode right and elastogram (left) of metastatic lymph node in colon cancer.

Participant category: Post doctoral fellow

Model driven segmentation of kidney DCE-MRI

Erlend Hodneland [(1)], Erik Hanson [(2)]

erlend.hodneland@uib.no

1. Department of Biomedicine, University of Bergen
2. Department of Mathematics, University of Bergen

Introduction Automatic and semi-automatic segmentation of tissue is an important processing step in quantitative medical imaging. The segmentation defines regions of interest (ROIs) for estimation of volume, shape, and for estimation of parameter values within the ROIs. For image time series the ROI definition typically corresponds to an orgen of interest for further analysis. Segmentation of image sequences is in general improved by utilizing temporal information in each voxel using clustering methods such as k-mean clustering, knn-clustering and principal component analysis (PCA). In this study we take advantage of the temporal information and present a novel segmentation strategy for medical image sequences. Our method is based on a combination of classical image processing, clustering methods and pharmacokinetic modeling. Methods The time series at each voxel was first fitted to a parameterized pharmacokinetic model by optimizing over n free parameters. This gave us n spatial parameter maps locally describing the tissue properties. We then apply the clustering methods to the lower dimensional space of 3D pharmacokinetic parameters instead of 4D image data. In order to obtain spatially coherent and sufficiently smooth segmentations, we can apply a spatial L1 or L2 regularizer either to the clustering method or directly to the parameterized pharmacokinetic model. Results We tested our method on data from a study using 4D DCE-MRI time series for the estimation of renal perfusion and glomerular filtration rate (GFR). Kidney and kidney-cortex ROIs were in this process segmented within 10 datasets. For the full-kidney ROIs, the results were compared to manual expert segmentation and to several sequential segmentation techniques for image sequences, utilizing first smoothening, then 4D clustering. The proposed method proved to be significantly more accurate then the classical approaches in terms of Dice coefficients. Discussion By combining the multi-channel information from the different parameter maps, the kidneys and kidney compartments are more easily detectable. The approach can be considered a guided clustering or a projection of the time sequence data to a lower dimensional space known to have favorable properties for segmentation. However, the current work will not address the question of which pharmacokinetic models (e.g. Patlak, Toft, Sourbron) are most suited to use for segmentation purposes.

Participant category: PhD Candiate/Research Program Student

Metabolic tumor volume on FDG-PET/CT predicts deep myometrial invasion, lymph node metastases and survival in patients with endometrial carcinoma

Jenny Husby [1,2], Bernt Christian Reitan [1], Jone Trovik [4,5], Øyvind Salvesen [3], Martin Biermann [1,2], Helga Salvesen [4,5], Ingfrid Haldorsen [1,2]

jenny.hild.aase@helse-bergen.no

1. Center of NM/PET, Dept. of Radiology, Haukeland University Hospital, Bergen
2. Section for Radiology, Center for Cancer Biomarkers, Dept. of Clinical medicine, University of bergen
3. Unit for applied Clinical Research, Department of Cancer Research and Molecular Medicine, Norwegian University of Science and Technology
4. Department of Obstetrics and Gynecology, Haukeland University Hospital
5. Centre for Cancer Biomarkers, Department of Clinical Science, University of Bergen

Purpose: Explore the value of metabolic tumor volume assessment on 18F-fluorodeoxyglucose Positron Emission Tomography / Computer Tomography (18-FDG-PET/CT) in the preoperative evaluation of endometrial carcinoma patients and explore the potential for prediction of outcome by this quantity. Materials and methods: In this prospective study, 104 consecutive patients with histologically confirmed endometrial carcinoma underwent preoperative FDG-PET/CT. The images were reviewed by a radiologist / nuclear medicine physician blinded to patient data, and metabolic tumor volume was calculated by placing a volume of interest (VOI) covering the portion of tumor with SUVmax > 2.5. Metabolic tumor volume was analyzed in relation to surgical staging parameters using logistic regression analysis and receiver operating characteristic (ROC) curves. The prognostic impact of metabolic tumor volume was explored using Kaplan-Meier method, log rank test and Cox regression analysis. Results: Large metabolic tumor volume was significantly related to presence of deep myometrial invasion (odds ratio (OR): 1.02, p=0.01) and presence of lymph node metastases (OR: 1.02, p=0.05). Metabolic tumor volume had a significant impact on recurrence-free survival with hazard ratio of 1.014 ($p<0.001$). ROC analysis identified the optimal cutoff for metabolic tumor volume to be 18.1 ml. Significantly better recurrence-free survival was observed in patients with metabolic tumor volume < 18.1 ml compared to patients with volume ≥ 18.1 ml (p=0.004). Conclusion: Preoperatively performed metabolic tumor volume measurements on FDG-PET/CT predict deep myometrial invasion, presence of lymph node metastases and prognosis in endometrial carcinoma patients, and may thus be a useful tool in risk stratification and decision-making prior to surgical and adjuvant treatment. Clinical relevance: Metabolic tumor volume measurements on FDG-PET/CT can aid in the prediction of deep myometrial invasion, presence of lymph node metastases and outcome in endometrial carcinoma patients, and thus be an important tool for preoperative risk stratification and choice of treatment.

See image on next page.

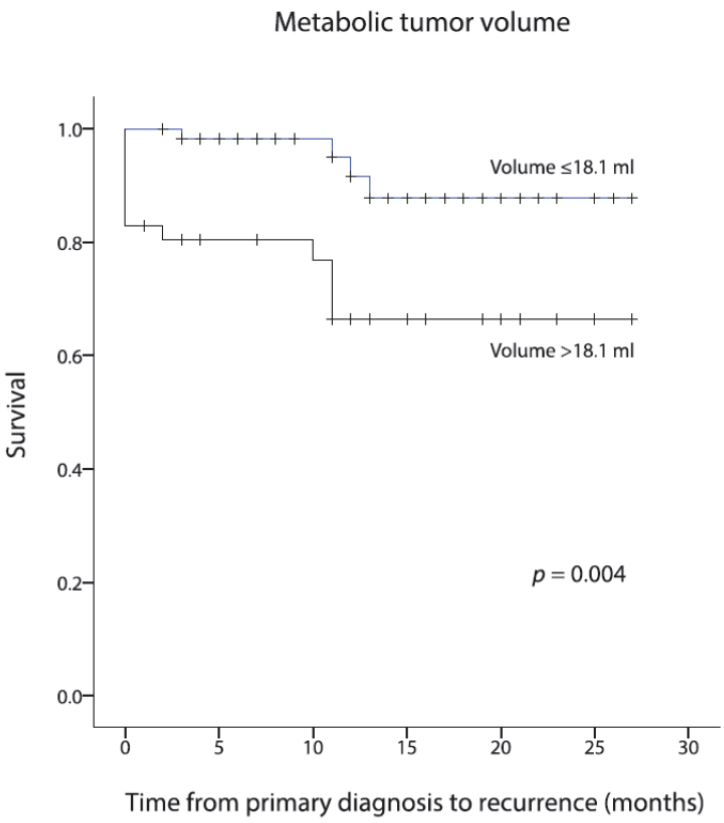

Kaplan-Meier survival curve depicting recurrence-free survival according to metabolic tumour volume (≤18.1 ml/>18.1ml). P-value refers to the Log Rank test.

Participant category: PhD Candiate/Research Program Student

Metabolic subgrouping of breast cancer using HR MAS MRS and hierarchical cluster analysis; correlation with molecular subtypes

Tonje Husby Haukaas [1,2], Leslie Euceda [1,2], Guro Giskeødegård [1], Marit Krohn [2,3], Ellen Schlichting [4], Rolf Kåresen [2,4], Sandra Nyberg [2,3], Kristine Kleivi Sahlberg [2,3], Anne-Lise Børresen-Dale [2,3], Tone Bathen [1,2]

tonje.h.haukaas@ntnu.no

1. Department of Circulation and Medical Imaging, Faculty of Medicine, NTNU, Trondheim, Norway
2. K.G. Jebsen Center for Breast Cancer Research, Institute of Clinical Medicine, Faculty of Medicine, University of Oslo, Oslo, Norway
3. Department of Genetics, Institute for Cancer Research Oslo University Hospital, The Norwegian Radium Hospital, Norway
4. Department of Surgery, Oslo University Hospital, Ullevål, Oslo, Norway

The heterogeneous biology of breast cancer (BCa) tumors has led to the need for detection of clinically relevant subgroups. Bridging information from several molecular levels in the same tumor and clinical metadata from the same patient may improve the understanding of BCa heterogeneity, and may lead to more patient specific treatment. Here we combine metabolic subgroups using unsupervised hierarchical cluster analysis (UHCA) of the MR metabolic profiles from tumor biopsies from BCa patients with data from gene expression and reverse phased protein arrays (RPPA) to search for relationships that can be related to clinical information. The metabolic profiles of a large cohort of primary tumors from BCa patients (n=280) were determined using ex vivo HR MAS MRS. UHCA using Ward's agglomerative method was carried out to separate four clusters. RPPA and UHCA were used for protein-based subtype classification. The samples were also classified into expression subtypes based on prediction analysis of microarray using the PAM50 method. The distribution of metabolic clusters classes within expression and RPPA subtypes was evaluated to establish metabolic characteristics that could be associated to each subtype. Four clusters classes based on metabolic differences were evaluated and correlated with expression and RPPA subtypes. Comparison of the mean spectra for each of these classes (Figure A) revealed the main differences to be the levels of Glc, Asc, Ala, Cr, Lac, Tau, Cho, PCho, GPC, Gly and lipids (Figure B). From the total cohort, 245 and 221 samples were classified using the RPPA and PAM50 methods respectively. The distribution of metabolic classes within RPPA subtypes revealed that 74% of Reactive I samples were grouped into class 3 (Figure C). As for expression subtypes, only in Luminal B were the majority of samples not grouped into this class (Figure D). Here we report four metabolic subgroups of breast carcinomas based on a large cohort of samples. The most prominent congruence between BCa subtypes and metabolic subgroups was the enrichment of Reactive I samples in class 3, which was characterized by higher Glc content (Figure B). However, this metabolic characteristic was found in a significant number of samples with different subtype; thus, there does not seem to be an association between metabolic profiles and BCa subtypes. This might make it possible for molecular subtypes to be further divided into subclasses based on metabolic differences.

See image on next page.

(A)

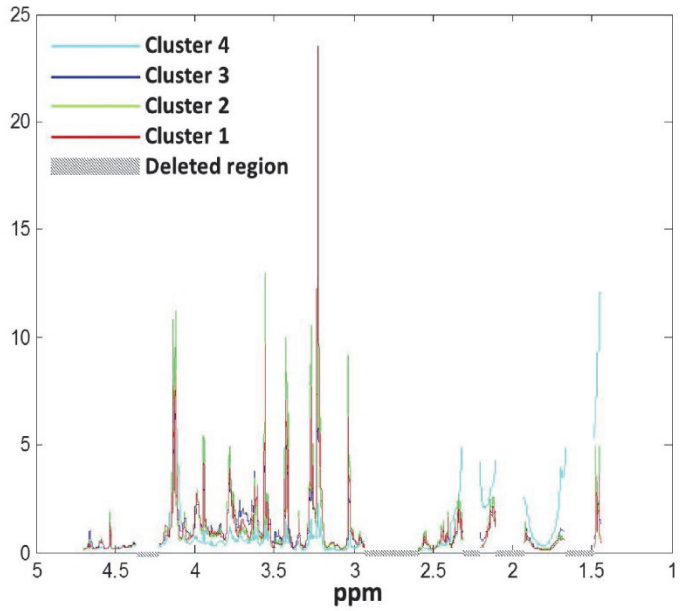

(B)

Metabolite	Cluster class			
	1 (n=64)	2 (n=62)	3 (n=138)	4 (n=16)
Al		↑	↓	
Cr		↑	↓	
Cho		↑	↓	
PCh, GPC	↑		↓	
Tau		↑	↓	
Gly		↑	↓	
Lac		↑	↓	
Asc		↑	↓	
Glc	↓	↓	↑	
Lipid content				↑

(C)

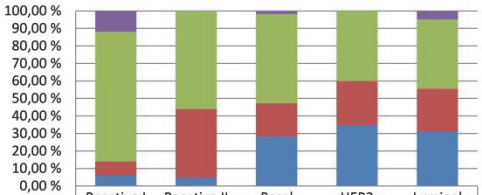

	Reactive I (n=50)	Reactive II (n=41)	Basal (n=53)	HER2 (n=20)	Luminal (n=81)
Class4(n=11)	12,00 %	0,00 %	1,89 %	0,00 %	4,94 %
Class3(n=127)	74,00 %	56,10 %	50,94 %	40,00 %	39,51 %
Class2(n=55)	8,00 %	39,02 %	18,87 %	25,00 %	24,69 %
Class1(n=52)	6,00 %	4,88 %	28,30 %	35,00 %	30,86 %

(D)

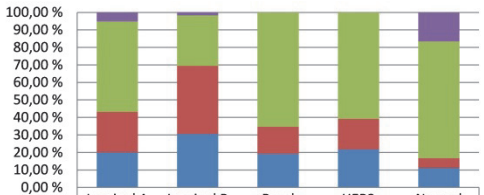

	Luminal A (n=95)	Luminal B (n=59)	Basal (n=26)	HER2 (n=23)	Normal (n=18)
Class4(n=9)	5,26 %	1,69 %	0,00 %	0,00 %	16,67 %
Class3(n=109)	51,58 %	28,81 %	65,38 %	60,87 %	66,67 %
Class2(n=54)	23,16 %	38,98 %	15,38 %	17,39 %	5,56 %
Class1(n=49)	20,00 %	30,51 %	19,23 %	21,74 %	11,11 %

(A) Comparison of mean spectra for the four metabolic classes. Five regions have been omitted as shown due to high lipid signals. (B) Table with main differences in metabolite levels between mean spectra from the four classes. Arrow pointing up represents

Participant category: PhD Candiate/Research Program Student

Possible molecular and functional correlation between the astrocyte water channel aquaporin-4 (AQP4) and the gap junction proteins connexin 43 and connexin 30

Shirin Katoozi [(1)]

shirin.katoozi@medisin.uio.no

1. Laboratory of Molecular Neuroscience, Department of Anatomy, University of Oslo

Possible molecular and functional correlation between the astrocyte water channel aquaporin-4 (AQP4) and the gap junction proteins connexin 43 and connexin 30. Shirin Katoozi(1) ,Laura Maria Azzurra Camassa(1) ,Henning Brunslow Boldt(1) ,Martine Cohen-Salmon(2) ,Mahmood Amiry-Moghaddam (1) 1 Laboratory of Molecular Neuroscience, Department of Anatomy, University of Oslo. 2 Centre for Interdisciplinary Research in Biology (CIRB), Collège de France, Institut National de la Santé et de la Recherché Médicale, 11 Place Marcelin Berthelot, Paris F-75005, France. Introduction: Astrocytes are believed to be involved in the energy supply of the neurons, controlling vascular tones and homeostasis of ions and water in the brain (Tsacopoulos and Magistretti, 1996; Simard et al, 2003; Gordon et al, 2007; Amiry-Moghaddam and Ottersen, 2003). They are enriched with the water channel protein AQP4 and two gap junction proteins, connexin 30 and 43. Through the gap junction proteins, astrocyte processes form a network where these membrane proteins allow astrocytes to exchange ions and small molecules (<1.5kDa). AQP4 water channels are mainly expressed at the perivascular astrocyte processes surrounding the microvessels and facing the pial surface where they are believed to be involved in water ion homeostasis (Amiry-Moghaddam and Ottersen, 2003). Different studies show possible correlation between AQP4 and connexin 43 and 30 expression in astrocytes. By Western blotting Enzan et al have shown that the level of AQP4 protein is decreased (by 30%) in mice lacking Cx 43 and Cx 30 (Enzan P. et al, 2012). In another study, Nicchia et al demonestrated a down-regulation of connexin 43 in primary cultured mouse astrocytes subjected to a knock-down of AQP4 using siRNA (Nicchia et al, 2005). Method: Based on these studies we analysed the perivascular AQP4 expression in neocortex and hippocampus of 3 months old connexin double knockout mice using quantitative immunogold electron microscopy. Results: Our results show that the perivascular AQP4 is significantly decreased in the connexin double knockout mouse brain. We are currently investigating possible functional and molecular correlation between AQP4 and the connexins.

Participant category: Post doctoral fellow

DCE-MRI reveals cPLA2 inhibition affects vascular function in a human breast cancer model

Eugene Kim [(1)], Jana Cebulla [(1)], Hanna Maja Tunset [(1)], Olav Engebråten [(2)], Gunhild Mari Mælandsmo [(2)], Astrid Jullumstrø Feuerherm [(3)], Berit Johansen [(3)], Tone Frost Bathen [(1)], Siver Andreas Moestue [(1)]

eugene.g.kim@gmail.com

1. MR Cancer Group, Dept. of Circulation and Medical Imaging, Norwegian University of Science and Technology
2. Dept. of Tumor Biology, Institute for Cancer Research, Oslo University Hospital Radiumhospitalet
3. Avexxin AS, Dept. of Biology, Norwegian University of Science and Technology

Basal-like triple-negative breast cancers (TNBC) are aggressive and unresponsive to current targeted therapies. They are more vascularized than other types of breast cancer, making the blood vessels a potential therapeutic target. Cytosolic phospholipase A2 (cPLA2) and its downstream effectors have been shown to play an important role in carcinogenesis and angiogenesis in various cancers, including breast cancer. We performed a pilot study to investigate the vascular effects of a novel cPLA2 inhibitor (AVX235, Avexxin AS) in a human basal-like TNBC model using dynamic contrast enhanced (DCE)-MRI. MAS98.12 human breast cancer xenografts were orthotopically implanted in eight athymic nude mice, which were randomized into treatment (n=5) or control (n=3) groups. Once the tumors grew to ~180 mm3, the mice received daily i.p. injections of AVX235 (45 mg/kg) or an equal volume of DMSO. The tumors were scanned on a Bruker 7T preclinical MRI system the day before the start of treatment (day 0) and again on day 4. For DCE-MRI, pre-contrast T1 maps were acquired, followed by a dynamic series of 200 spin echo images (temporal resolution=4.8 s). An intravenous bolus injection of gadodiamide (0.3 mmol/kg) was administered after the tenth baseline image. Ktrans (transfer constant between intravascular and extravascular-extracellular space [EES]), ve (EES volume fraction) and vp (plasma volume fraction) were estimated from the DCE data using the Tofts model and a population-based arterial input function. The changes in the tumor-wise median values of these parameters from day 0 to 4 were computed. Two-tailed Mann-Whitney U tests (α=0.05) were performed to test for differences in the changes in the DCE parameters and tumor volumes between treated and control tumors. AVX235-treated and control tumors were significantly different based on the change in median Ktrans – it decreased in all control tumors but increased in all but one treated tumor. There were no significant differences in the changes in ve, vp or tumor volume. Ktrans is a functional parameter related to blood flow, vessel permeability and surface area. Tumors have characteristically dysfunctional vasculature, often leading to high interstitial pressure and poor perfusion. The increase in Ktrans in treated tumors may have been caused by normalization of vascular function and increased blood flow. This suggests that AVX235 may have an early effect on vascular function before detectable structural changes occur.

Participant category: Post doctoral fellow

Tubular-Shaped Numerical Test Objects for Validation of 3D Blood-Vessel Image Segmentation Algorithms

Marek Kociński [(1)], Andrzej Materka [(1)], Michał Strzelecki [(1)]

marek.kocinski@p.lodz.pl

1. Institute of Electronics, Lodz University of Technology, Poland

Introduction: Segmentation of blood-vessel structures in 3D images is a fundamental step in medical image analysis e.g. for detection of vascular pathologies, or neurosurgery planning. The vascular system structure is unique for each patient, so there is no ground-truth model to assess the accuracy of blood-vessel image segmentation algorithms under development. It is neither easy nor cheap to construct physical phantom objects and use them to acquire MR or CT images. In such cases, computer simulated numerical test objects can serve as reference models. Methods: 3D isotropic images of tubular shaped objects are numerically generated (Fig. 1). The tubes, each of a fixed radius in the range <0.2, 10> and a length of 80 inter-voxel distances, take randomly chosen positions in space. For each tube radius and position, a simple 3D image simulator computes the intensity of image voxels, depending on the tube volume shared with each of them. Scanner artefacts and noise are modelled to account for brightness/contrast variation and Gaussian/Rician intensity disturbances. In our study, the level-set, mathematical-morphology and Hessian-based segmentation methods were evaluated and compared in terms of accuracy of the reconstruction of tube position, shape and geometric parameters. Conclusions: Numerical test objects constitute convenient means of evaluation of image segmentation methods accuracy. Their big advantage is in parameters flexibility. What is more, they are cheap and easy to "construct" in comparison with real-world phantoms. They allow simulation of real artefacts and distortions that appear during MRA acquisition. The presented approach is a basis and reference for more advanced projects carried on in our laboratory, which include numerical modeling of vascular tree images and MRA computer simulation software. Acknowledgments: This work is supported by the National Science Center, Poland (NCN 2013/08/M/ST7/00943).

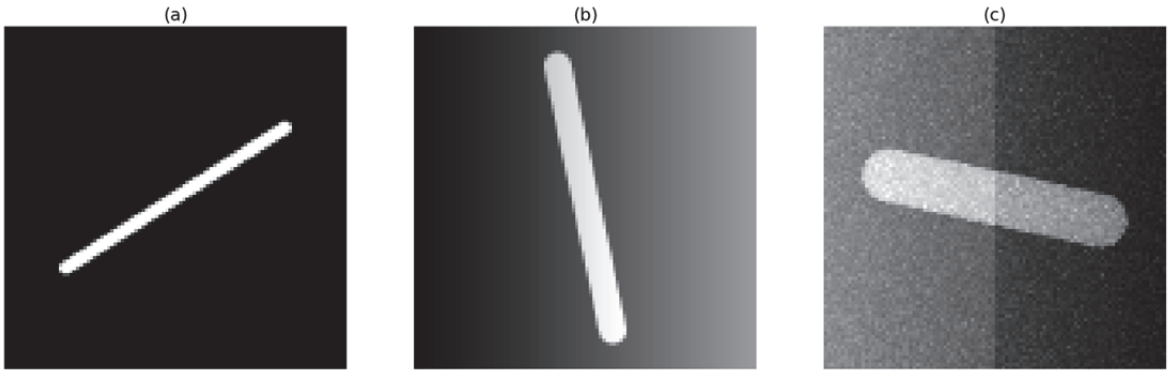

Numerical test objects, reference image R=2 (a), contrast changes R=4 (b), brightness modification with added Gaussian noise N(0,20) R=8 (c)

Participant category: PhD Candiate/Research Program Student

SERCA LOCALIZATION IN THE HEART

Terje Kolstad [(1)], William E Louch [(1)], Ole M Sejersted [(1)], Espen Stang [(2)], Sverre H Brorson [(2)], Clara Franzini-Armstrong [(3)]

t.r.s.kolstad@medisin.uio.no

1. Institute for Experimental Medical Research, Ullevål
2. Oslo University Hospital HF, Rikshospitalet
3. University of Pennsylvania School of Medicine Department of Cell and Developmental Biology, Philadelphia, USA

The sarcoplasmic reticulum (SR) Ca2+-ATPase (SERCA) is a key protein in the cycle of excitation-contraction-relaxation in the heart. SERCA pumps Ca back into the SR after the contraction and therefore not only controls how quickly Ca is removed from the cytosol, but also how much Ca that is available in the SR for the next contraction. Thus, the activity of SERCA controls both contraction and relaxation. For 20 years it has been known that this protein is downregulated in the failing human heart. This downregulation is thought to contribute substantially to disrupted Ca2+ handling and subsequent reduction in contractile performance. Our group recently showed that the negative consequences of SERCA loss appear to extend beyond Ca2+ handling and include dramatic changes to cellular morphology (Swift, Franzini-Armstrong et al. 2012). Surprisingly little is known concerning how SERCA is targeted and regulated. The exact location of SERCA in the membrane of the SR has not been established, and mechanisms regulating SERCA degradation are also unclear. Using the transmission electron microscope (TEM) on sections with immuno-gold labels (see attatched image), we have visualized the expression of SERCA in cardiac myocytes from normal mice and mice with conditional SERCA knockout. The results point towards a preferential SERCA-distribution near the Z-line in the healthy heart. Furthermore, our data indicate that SERCA ablation predominantly reduces SERCA levels near these Z-lines, suggesting that SERCA may be preferentially targeted to these sites. We aim to measure the effect of SERCA ablation on Ca2+ transients and its underlying event, the Ca2+ sparks. The in-vivo consequences of alterations to SERCA-localization, Ca2+ sparks and Ca2+ transients will be determined by including these measurements in an electro-mechanical model of the left ventricle (Collaboratian Steve Niederer, Kings College London)

See image on next page.

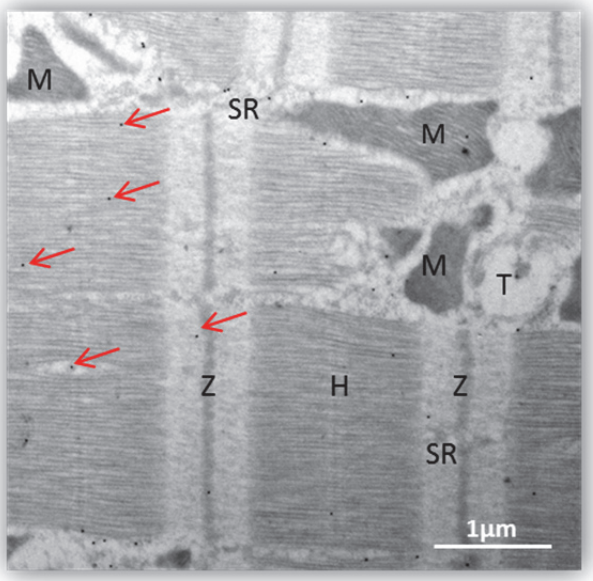

Electron micrograph of the mouse heart papillary muscle labelled with anti-SERCA and proteinA-5nm gold conjugate (PAG) (red arrows). Z–Z-line, H–H-Band, SR–Sarcoplasmatic Reticulum, T–T-Tubule, M-Mitochondrion

Participant category: Established MedViz researcher

Acoustically active antibubbles for ultrasound imagin and targeted drug delivery.

Spiros Kotopoulis [1,2], Kristoffer Johansen [2], Albert Poortinga [3], Odd Helge Gilja [4], Michiel Postema [2]

Spiros.Kotopoulis@uib.no

1. National Centre for Ultrasound in Gastroenterology, Haukeland University Hospital, Jonas Lies vei 65, 5021 Bergen, Norway
2. Department of Physics and Technology, University of Bergen, Allégaten 55, 5007 Bergen, Norway
3. FrieslandCampina Research, Harderwijkerstraat 6, 7418 BA Deventer, The Netherlands
4. Department of Clinical Medicine, University of Bergen, Jonas Lies vei 65, 5021 Bergen, Norway

In the current day and age, image guided and targeted drug delivery is becoming a necessity as it allowed a larger amount of therapeutic agent to be delivered to a precise location, allowing for tailored treatment to each and every patient, theoretically improving the treatment efficacy, whilst reducing systemic side effects. One of the most cost effective imaging modalities is ultrasound imaging. It is capable of deep tissue imaging in three dimensions in real time. In addition, it can be done bedside at any location, and has little to no known side effects. Sonoporation takes advantage of the behaviour of commercially available microbubbles, otherwise known as ultrasound contrast agents, under ultrasound sonication to form transient pores in cells, allowing for increased drug uptake. Pre-clinical and clinical trials have shown great promise. Nevertheless, in all instances, the therapeutic agent is delivered intravenously; hence there are still systemic side effects. Here we investigate the possibility of using drug-cored gas microbubbles (antibubbles) as an alternative to typical contrast agent. These antibubbles consist of a drug core, encapsulated air, encapsulated by a nano-particle stabilised shell. Our work here investigated the acoustic linear and non-linear behaviour of these antibubbles and compares them to commercial microbubbles. By adding the drug inside the bubble, we can theoretically force the drug into selected cells. Theoretical simulations were performed to evaluate the resonance frequency and radius time curves under sonication. Broadband acoustic attenuation measurements were performed to identify the resonant frequency and were compared to the size distribution. Ultra-high speed imaging was performed at high acoustic amplitudes to visualise the non-linear behaviour and to evaluate the gas content. The antibubbles were also imaged using a clinical scanner and several probes to evaluate the increase in contrast and non-linear acoustic backscatter. Our results showed that these antibubbles were acoustically active and highly non-linear, in a similar fashion to traditional contrast agents. These antibubbles may have potential as an ultrasound activated high-capacity drug carrier.

Participant category: PhD Candiate/Research Program Student

Novel, fast and user-friendly blood vessel segmentation method

Rahul Prasanna Kumar [1,2], Fritz Albregtsen [2], Martin Reimers [2], Bjørn Edwin [1], Thomas Langø [3], Ole Jakob Elle [1,2]

rahul.kumar@rr-research.no

1. The Intervention Centre, Oslo University Hospital, Norway
2. Department of Informatics, University of Oslo, Norway
3. Medical Technology, SINTEF, Norway

Many clinical practices of today perform angiography in multiple imaging modalities. This leads to an increasing need for visualization and segmentation of these blood vessels. Analysis of blood vessel morphology is very important in many clinical applications for diagnosis, planning and navigation. They are especially important in intraoperative procedures and, planning and navigation in interventional procedures. Procedures such as liver resection planning and catheter tracking require good knowledge of the blood vessels for good positioning of stents and value. Here we present a novel, semi-automatic method for blood vessel segmentation, centerline extraction and radius estimation, performed simultaneously. The method starts from a user initialized seed point, performing two-dimensional cross-section analysis of the connected blood vessel and tracking the blood vessel cross-sections to the end points. The cross-section analysis is done by our novel single-scale or multi-scale circleness filter, at the blood vessel trunk or bifurcation, respectively. The method was validated for both synthetic and medical images. Our validation has shown that the centerline error between our center and the geometric center of cross-section to be on average below 0.8 pixels and also that the Dice coefficient for the segmentation is found to be 80 ± 2.7. On combining our method with an optional active contour post-processing, the Dice coefficient for the resulting segmentation is found to be 94 ± 2.4. The post-processing step helps in filling gaps in the segmentation caused by sudden changes in the vessel cross-section angle and better fit the blood vessels. By restricting the image analysis to the interesting regions and converting most of the three-dimensional calculations to two-dimensional calculations, the processing in our method is more than 18 times faster than Frangi vesselness with thinning, 8 times faster than seed initiated active contour segmentation with thinning and 7 times faster than our own previous method.

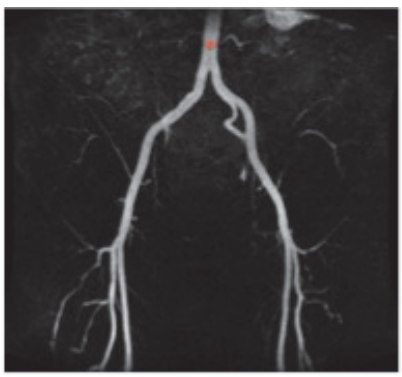

Maximum Intensity Projection image of input with red circle representing the user-initiated seed

Maximum Intensity Projection image of the centerline output from our proposed method

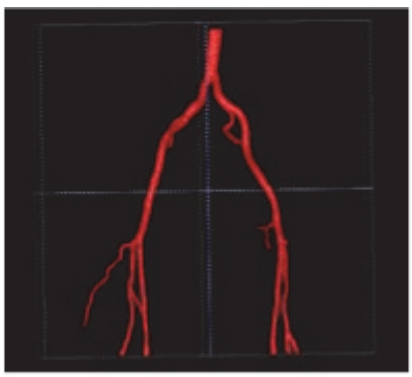

3D volume view of the blood vessel segmentation output from our proposed method

Participant category: PhD Candiate/Research Program Student

A Raman spectroscopic biochemical investigation of osteoarthritic human articular cartilge.

Rajesh Kumar [(1)], Kirsten Grønhaug [(2)], Vidar Isaksen [(3)], Catharina Davies [(1)], Jon Drogset [(4)], Magnus Lilledahl [(1)]

101rajesh@gmail.com

1. Department of Physics, Norwegian University of Science and Technology (NTNU), Norway
2. Levanger Hospital, Norway
3. UNN, Tromsø
4. St. Olavs Hospital, Norway

Objective: There are several biochemical changes at molecular level occur in human cartilage during the progression of osteoarthritis. Due to change in vibrational frequency at molecular level, Raman spectroscopy is capable to sense any pathological change in early stage of disease.The objective of the study is to find the suitability and potential of Raman spectroscopic technique for the analysis of cartilage disorder. Also we perform a quantitative analysis to show the degree of association between macroscopic and histologic assessment of different grades of osteoarthritis. Method: Experimental use of human tissue is approved by Regionale komiteer for medisinsk og helsefaglig Forskningsetikk (2013/265/REK midt). 12 human articular cartilage tissue sections were classified in different grade of osteoarthritis by using ICRS classification system. From the statistical point of view we performed our spectroscopic analysis to the sufficiently large number of sampling sites (n=108) with every ICRS grade of tissue sample. We also performed Safranin-O staining for histological analysis and assigning OARSI score to osteoarthritic tissue samples. Result: Multivariate data analysis performed on the data set obtained from three different ICRS grade of osteoarthritic samples. Three separate group of clusters appeared by unsupervised principal component analysis. Our analysis with doublet peak amide III ratio shows the increment in the content of random protein coil (defective collagen) while analysis with proteoglycan shows that there is overall decrement of content of proteoglycan, as degree of disorder increases. We also found a relationship between ICRS and OARSI grade score (R2=0.789). Conclusion: We were able to successfully classified different ICRS grade of osteoarthritis by applying Raman spectroscopic analysis. We have also shown how biocompositional changes can be assessed in cartilage matrix by using this technique. Furthermore, to validate this method more analysis have to be performed in statistically large number of population. Since Raman spectroscopy is highly evolving technique, we envision that our proof-of-concept study may be used as foundation and further may contribute towards the early stage diagnosis of cartilage disorder including osteoarthritis. In future the study may be extended with Raman probe such that it can be potentially implemented with arthroscope for in situ analysis by orthopedic surgeons.

See image on next page.

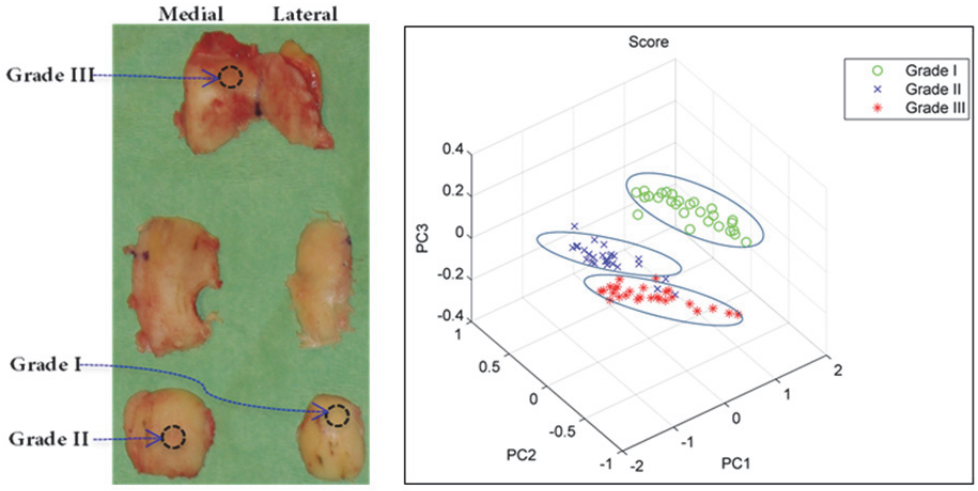

(a) (b)

Figure: (a) A picture of tissue sample obtained from osteoarthritic affected human knee articular cartilage. A representative image of ICRS Grade I, II and III. (b) Multivariate analysis based PCA algorithm distinguish different ICRS grade of osteoarthritis into separate clusters (Grade I: green o, Grade II: blue + and Grade III: red *).

Participant category: PhD Candiate/Research Program Student

Assessment of salivary gland pathology in a murine model of Sjögren's syndrome

Suzanne Ledahl [(1)], Petra Vogelsang [(1)], Nicolas Delaleu [(1)]

suzanne.ledahl@k2.uib.no

1. Broegelmann Research Laboratory, Department of Clinical Science, University of Bergen, Norway.

Sjögren's syndrome (SS) is a systemic autoimmune disease mainly affecting the exocrine glands, often resulting in severe functional impairment of affected organs, resulting in dry eyes and dry mouth. There exists several mouse models of SS, the choice of model depends on which trait of the disease one wishes to study. Common for all models, is that the current method for assessing the progression of inflammation or degree of disease in this model necessitates euthanasia of the animal and removal of its salivary glands (SGs). These then undergo further processing and analysis by means of histopathology, immunohistochemistry (IHC) or microarray. The lack of tools for quantitatively and repeatedly assessing the inflammation in the SGs in vivo is a major obstacle for obtaining valuable information about the pathogenesis as well as assessing any therapeutic effects in intervention studies. Importantly, the absence of such tools means that the number of animals needed in each study is quite large, as one cannot obtain data from one mouse at several time points. In a pilot study, we have used small animal magnetic resonance imaging (MRI) to assess glandular anatomical disturbance, and observed disease-specific alterations in target tissue structure. We aim to develop a method of assessing SS-like changes in the SGs of murine SS models, to learn more about the pathogenesis of this disease and to avoid the untimely euthanasia of animal during trials.

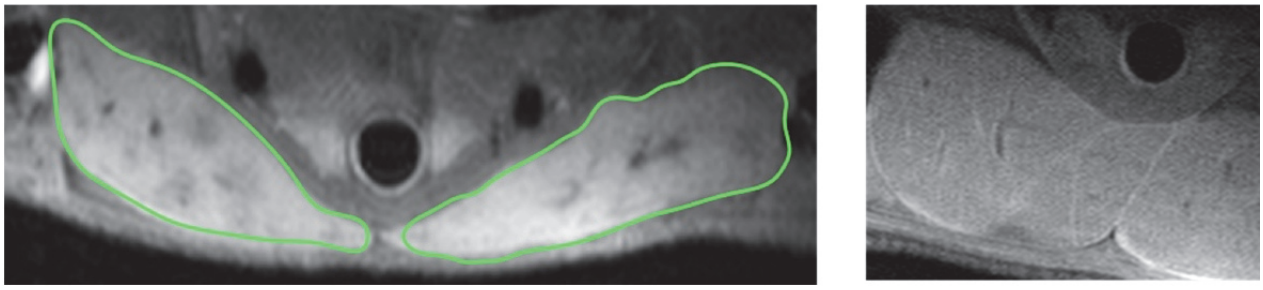

T1 weighted images of murine salivary glands showing sjögren's syndrome-like changes (left) and healthy tissue (right)

Participant category: PhD Candiate/Research Program Student

Integrated Visual Analysis of Spatial and Abstract Data

Andreas Johnsen Lind [(1)], Stefan Bruckner [(1)]

ali054@uib.no

1. University of Bergen

Considering the vast amounts of data involved in many scientific disciplines, it is essential to provide effective and efficient means for forming a mental model of data space and parameter space in order to gain a better understanding of their relationships. Visual knowledge discovery seeks to provide these means through interactive visualization and analysis tools for examining the available data, taking advantage of the extraordinary capability of the human brain to process visual information. However, this is particularly challenging when a single data point cannot be characterized by a few coordinates, but actually constitutes a sampled representation of a continuous spatial phenomenon. Furthermore, even though many successful tools have emerged that assist scientists in individual aspects of their work, there is no single solution which encapsulates the whole process. Within the scope of this project, I want to devise techniques to make sense of the vast amounts of information generated by current and future datadriven science. One example would be of a data set where the volumetric scans showing different developmental stages of in the brain coupled with gene expression information from each stage. Where said gene expression data is also local to specific brain regions. This kind of data has applications in the domains of neuroscience, connectomics, developmental biology and developmental psychology. Having this detailed information on the gene expression levels allows us to do visual analysis to identify how the different genes relate to brain development. The purpose of my project is to formulate and develop visualization techniques that can be used to explore and analyze the data in this and similar data sets which contain a multitude of abstract attributes linked by their relation to data of an inherently spatial nature. To accomplish this I intend to develop a framework for visualizing spatial data spaces. The project will combine techniques from scientific visualization with techniques from information and graph visualization to enable optimal extraction of information from the data. The framework will in particular focus combining visualizations of graph and volumetric data. A key challenge of this research is to provide interactive techniques to explore and analyze how multidimensional abstract attributes influence the spatial characteristics of the phenomenon under investigation.

Participant category: Post doctoral fellow

Registration of multiparametric MRI and whole-mount sections of the prostate

Are Losnegård [(1)], Arvid Lundervold [(2,1)], Erlend Hodneland [(2)], Lars A. Reisæter [(1)], Ludvig P. Muren [(3,4)], Markus Alber [(3)], Liv B. Hysing [(5)], Ole J. Halvorsen [(6)], Christian Beisland [(7)], Jarle T. Rørvik [(8,1)]

Are.Losnegard@k1.uib.no

1. Department of Radiology, Haukeland University Hospital, Bergen
2. Department of Biomedicine, University of Bergen
3. Department of Medical Physics, Aarhus University Hospital, Denmark
4. Department of Physics and Technology, University of Bergen
5. Department of Oncology and Medical Physics, Haukeland University Hospital, Bergen
6. Department of Pathology & Department of Clinical Medicine, The Gade Laboratory for Pathology, Haukeland University Hospital & University of Bergen
7. Department of Urology & Department of Clinical Medicine, Haukeland University Hospital and University of Bergen
8. Department of Surgical Sciences, University of Bergen

Introduction: Prostate cancer is the most common cancer among males in Norway and elsewhere, and computer-aided-detection (CAD) systems using multiparametric MRI (mpMRI) are promising as diagnostic tools. They have a large potential for automated voxel-wise localization and classification of tumours. However, the development of multi-modal CAD systems is challenging, due to non-overlapping images and movement artifacts. Methods: Proper alignment of the various mpMRI sequences (diffusion, perfusion, T1 and T2) was performed using affine registration as implemented in the elastix software. Further, whole-mount prostate sections were digitally scanned and aligned using rigid registration, as implemented in the FAIR Matlab toolbox, and then combined into a 3D model of the prostate. We built one low-resolution model with voxel size comparable to the mpMRI, which is expected to support the registration of the mpMRI to whole-mount sections. Also, we built a high-resolution model which could be used for cellular level analysis and quantification. Results: Visual inspection of the mpMRI affine registration for one patient showed reduced movement artifacts and improved organ and edge overlap, compared to the original data. Moreover, rigid registration of the whole-mount sections showed visually good slice-to-slice correspondence, and was used to build a 3D model of the prostate. Discussion: We conclude that image registration methods are promising for the alignment of mpMRI sequences, and useful for aligning whole-mount sections for constructing a 3D model. Future work includes mpMRI prostate segmentation and mpMRI to whole-mount sections registration, which will be used in the further development of the CAD system.

Participant category: PhD Candiate/Research Program Student

In vivo Noninvasive Multimodality Imaging of Nitroreductase in murine cancer models

Kjetil Børve Lund [1], Elvira García de Jalón [2], Endre Stigen [1], Mihaela Popa [3], Cecilie Brekke Rygh [4], Tom Christian Holm Adamsen [5], Anzhelika Vorobyeva [6], Ole Heine Kvernenes [5], Elena Dubikovskava [7], Bengt Erik Haug [2], Emmet McCormack [1,8]

klu005@student.uib.no

1. Hematology Section, Department of Clinical Science, University of Bergen
2. Center for Pharmacy, Institute of Medicine, University of Bergen
3. KinN Therapautics, Bergen
4. Translational Cancer Research, Department of Biomedicine, University of Bergen
5. Center for Nuclear Medicine/PET, Haukeland University Hospital
6. Laboratory of Bioorganic Chemistry and Molecular Imaging, École Polutechnique Fédérale de Lausanne, Lausanne, Switzerland
7. Institute of Chemical Sciences and Engineering, Swiss Federal Institute of Technology of Lausanne, Lausanne, Switzerland
8. Hematology Section, Department of Internal Medicine, Haukeland University Hospital

Bacterial nitroreductase, NTR has previously been reported as a GDEPT strategy for treatment with prodrugs (Christofferson et al 2009, Johansson et al 2003). NTR acts by 2-electron reduction of nitroaromatic groups in presence of NAD(P)H. The nitroaromatic group is known for its ability to act as an electron-sink and the conversion from a 4-nitro group to a hydroxylamine effectively can “switch” substrates into a more reactive form. We have previously shown that CytoCy5S, a quenched Near-Infrared fluorescent probe, can be used with NTR in an optical imaging strategy. In this project we aim to introduce novel NTR probes for preclinical imaging and study the use of the NTR enzyme as a multimodal imaging platform and developing suitable probes for fluorescence optical imaging, bioluminescence optical imaging and PET/CT.18F FMISO, a previously described positron emitting hypoxia tracer, was evaluated in vivo in a panel of mice with s.c. implanted NTR positive and negative tumours. CytoCy5S was conjugated to CD33 to develop a biomarker-directed and specific way of delivering the fluorescent payload, achieving a higher signal-to-noise ratio in cells that are both CD33 positive and NTR positive. The effectiveness of the conjugate was tested on a panel including CD33+/NTR+ cells and CD33-/NTR+ cells. A novel luciferin was evaluated both in vitro and in vivo. The novel luciferin is caged, which inhibits the luciferin from binding to the firefly luciferase. The luciferin cage can be removed through reduction of the nitroaromatic group. This caged luciferin was evaluated a panel of cell lines with different Luciferase and NTR status to establish the kinetics and luminescent signal, both in vitro and in vivo. This was compared to the kinetics and luminescent signal from equivalent doses of D-Luciferin. In vivo results show that 18F FMISO have a significantly higher signal in NTR+ compared to NTR- tumours (Fig A). In vitro and in vivo results show that the novel caged luciferin can produce a significantly higher signal in tumours that are Luciferase+/NTR+ compared to tumours that are Luc+/NTR- (Fig B). In vitro results show that CytoCy5S can be conjugated to biomarkers like CD33, and produce a significantly higher fluorescent signal in CD33+/NTR+ cells compared to CD33-/NTR+ cells. Our findings suggest that NTR can be used as a novel preclinical imaging strategy for the visualisation of metastatic cancer and biomarker validation with several imaging platforms.

See image on next page.

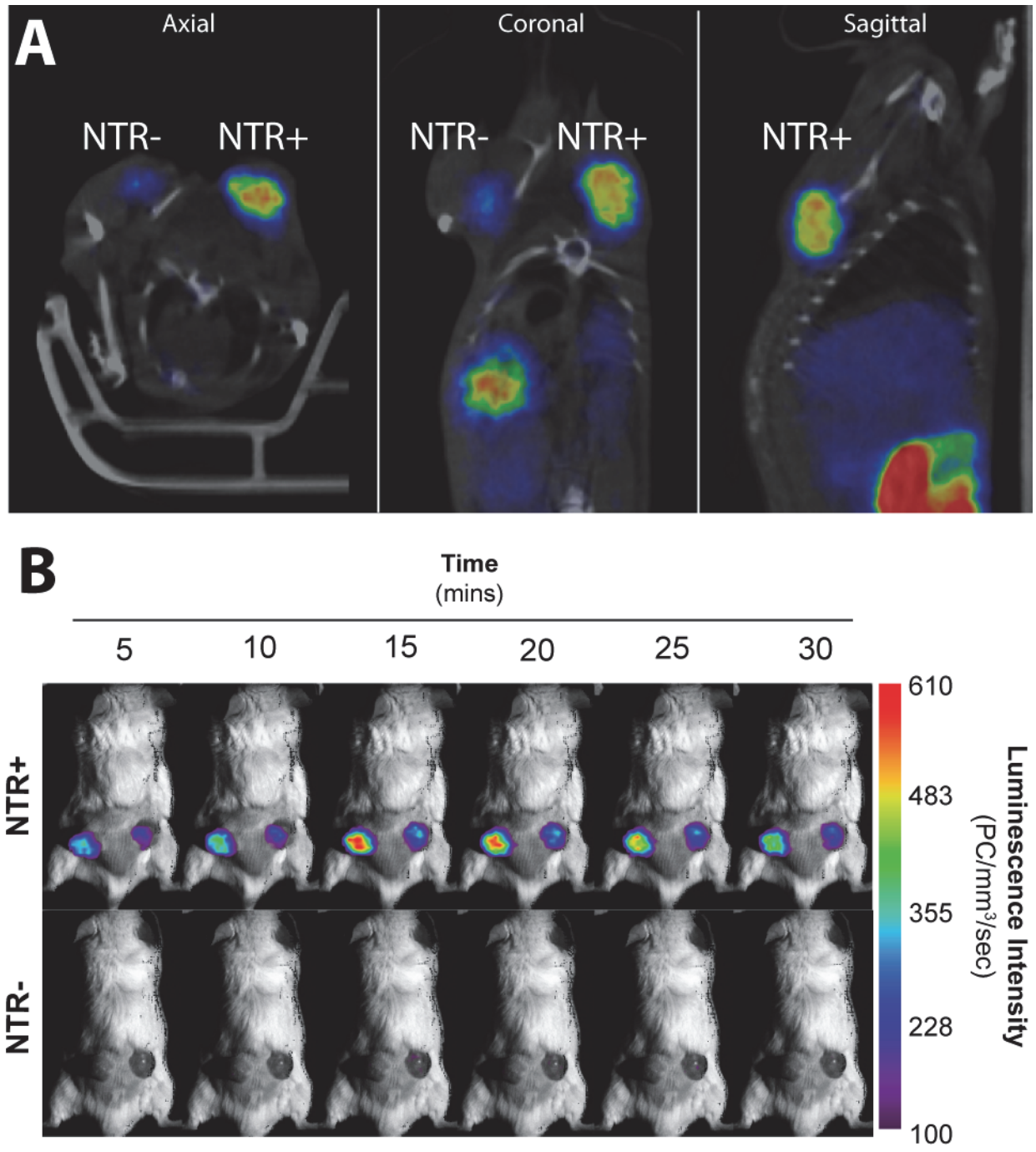

Fig A: Mice with non-small lung cancer (NCI-H460) sub cutaneous injected at the shoulders (n=8), one NTR- and one NTR+. Fig B: Mice (n=6) were scanned post injection to study the kinetics of a Caged Luciferin, injected i.p, 30 mg/kg, in both NTR+ and NTR

Participant category: PhD Candiate/Research Program Student

Biopsy Needle Tracking using Medical Ultrasound and a Surgical Robotic System

Kim Mathiassen [1,2], Dilla Handini [1], Phuong Nguyen Ho Quoc [1], Ole Jakob Elle [1,2]

kimmat@ifi.uio.no

1. The Intervention Center, Oslo University Hospital
2. Department of Informatics, University of Oslo

Ultrasound guided placement of a needle is frequently performed in clinical practice both for diagnostics and treatment. Examples include to take a biopsy sample from one of the patients organs to diagnose the patient or to use an ablation probe to freeze a malignant tumour in order to kill the tumour cells. As it is a very common procedure automating the task could save many resources in the health care system, either by reducing the number of staff required to perform the procedure or increasing the success rate of the treatment by having more accurate needle placement. The EU project Intelligent Surgical Robotics (ISUR) is exploring the feasibility of automating needle insertion procedures, using the insertion of a cryoablation probe to freeze a malignant tumour. Recently the project performed a preliminary test of a system inserting a needle automatically. It consist of two robots, one inserting the needle and one holding an ultrasound probe for monitoring the insertion. The insertion was performed on a phantom made by one of the project partners. It had a gelatin skin layer, gelatin organs and was filled with water. After the experiment, a modified version of the needle tracking method in [1] was tested. As the only position measurements of the needle related to the US probe was the robot joint angles, there was no ground truth needle position. The ground truth needle position was therefore found manually by inspecting the US images. In the original method the tracking algorithm was trained using an evolutionary algorithm. In this case it was not possible because it was not feasible to get sufficient samples for the training by manually inspecting all the images. Instead the parameters for the tracking algorithm was chosen heuristically. The tracking algorithm uses five image features. One of the features was chosen to be the dominating feature. This was the feature that is based on needle displacement. This gave a very accurate tracking while the needle was moving, but at the cost of poorer tracking when the needle was stationary. The tracking accuracy was evaluated using visual inspection. To conclude, a needle tracking algorithm was tested using surgical robotic system and the tracking accuracy was found acceptable. Future work should be to quantify the error. References [1] K. Mathiassen et. al., “Real-time biopsy needle tip estimation in 2d ultrasound images,” in Robotics and Automation (ICRA), 2012 IEEE International Conference on, 2013.

Participant category: PhD Candiate/Research Program Student

Fixed Point Motion Estimation for Frame Rate Up Conversion in Cardiac Ultrasound

Hani Nozari Mirarkolaei [(1)], Sten Roar Snare [(1)], Lars Hofsøy Breivik [(1)], Erik Normann Steen [(2)], Anne H Schistad Solberg [(1)]

haninm@ifi.uio.no

1. Department of Informatics, University of Oslo
2. GE Vingmed Ultrasound

Frame rate up conversion in a low frame rate cardiac ultrasound scan makes the images run smoother and potentially increases the diagnostic value of the scan. Linear interpolation is one way of increasing frame rate; however, ghosting and blurring are the main drawbacks of this type of interpolation. In low frame rate cardiac ultrasound imaging, motion estimation and motion compensation techniques commonly used in optical imaging are not suitable, because of speckle noise as well as large movement of the cardiac valves compared to other anatomical features. We proposed novel method termed Fixed Point Motion Estimation (FPME) to handle these problems. FPME is a bidirectional tracker which extracts search regions from the previous and next frames in a pyramidal manner. The bottom of the pyramids uses a large search area around the moving object. At the higher levels in the pyramid, the search region is narrowed down to capture the moving object. The motion vector at each level of the pyramid is used as an offset for the next level and the overall displacement will be the vector summation of motion vector at each level of the pyramid. This method works well if we don't have any out of plane movement. To have more reliable motion vectors at each level a vector median filter is applied on the vector field. The result is used as an initialization for an optical flow regularization to capture sub pixel movement. We demonstrate the performance of FPME on four standard cardiac ultrasound recordings. Our experiments show that, in ultrasound images, FPME works well compare to current motion estimation techniques in optical imaging. It removes ghosting and blurring artifacts. Fig. 1 shows a ground truth image as well as linear and FPME interpolated frames. FPME frame rate up conversion reduces the average sum of square error in the valve region by 5.6% relative to linear interpolation and increases the average peak signal-to-noise ratio by 2 dB.

Fig.1 (left) Ground truth image, (middle) Linear interpolation, (right) FPME interpolation

Participant category: PhD Candiate/Research Program Student

Multi-frequency ultrasonic transducer design: The acoustic stack

Ola Myhre [1,2]

ola.f.myhre@ntnu.no

1. NTNU
2. Samarbeidsorganet HMN-NTNU

Motive: Simultaneous ultrasound imaging and treatment of diseased tissue with minimal instrumentation requires transducers with good acoustic properties, and the ability to transmit large amounts of power. Methods: Vibrations and losses of a piezo-electric transducer are simulated using a Mason model. Key results: Introduction of a core layer can increase frequency separation of HF and LF response in a transducer, with improved or equal performance. Conclusions: The presented design seems to provide the transducer with the ability to image and treat patients simultaneously.

Participant category: PhD Candiate/Research Program Student

The Norwegian Sonothrombolysis in Acute Stroke Study (NOR-SASS): A randomised controlled trial of contrast enhanced ultrasound treatment in acute ischaemic stroke

Aliona Nacu [1, 2], Christopher Kvistad [1], Nicola Logallo [1], Halvor Naess [1, 3], Ulrike Waje-Andreassen [1, 2], Lars Thomassen [1, 2]

nacu_allionka@yahoo.com

1. Department of Neurology, Haukeland University Hospital, Bergen
2. Department of Clinical Medicine, University of Bergen, Bergen
3. Centre for age-related medicine, Stavanger University Hospital, Stavanger

Introduction: Ultrasound accelerates thrombolysis with tPA (sonothrombolysis). Ultrasound in the absence of tPA also accelerates clot break-up (sonolysis). Adding intravenous gaseous microspheres may potentiate the effect of ultrasound in both sonothrombolysis and sonolysis. The Norwegian Sonothrombolysis in Acute Stroke Study aims are to assess the effect and safety of contrast enhanced ultrasound treatment in acute ischaemic stroke patients eligible or not eligible for intravenous thrombolysis. Methods: Acute ischaemic stroke patients ≥18 years, with or without visible arterial occlusion on CT angiography and treatable ≤ 4½ hours after symptom onset, are included in NOR-SASS. The trial has two arms 1) the thrombolysis-arms (NOR-SASS A and B) includes patients given iv thrombolysis, and 2) the no-thrombolysis-arm (NOR-SASS C) includes patients with contraindications to thrombolysis. First step randomisation of NOR-SASS A is 1:1 to either tenecteplase or alteplase and second step randomisation is 1:1 to either contrast enhanced sonothrombolysis (CEST) or sham CEST. Randomisation of NOR-SASS B (alteplase group) is 1:1 to either CEST or sham CEST. Randomisation of NOR-SASS C is 1:1 to either contrast enhanced sonolysis (CES) or sham CES. Ultrasound is given for one hour using a 2-MHz pulsed-wave ultrasound probe. Microbubble contrast (SonoVue®) is given as a continuous infusion for ~30 minutes. Recanalisation is assessed at 60 minutes after start of CEST/CES. Magnetic resonance imaging and angiography is performed after 24 hours of stroke onset. Primary study endpoint is favourable functional outcome defined as mRS 0-1 at 90 days. Disscussion: Contrast enhanced ultrasound treatment is an emerging therapeutic option for patients with acute ischaemic stroke. NOR-SASS is the first randomised controlled trial designed to test the superiority of contrast-enhanced ultrasound treatment given ≤4½ hours after stroke onset in a general acute ischaemic stroke population eligible or not eligible for iv thrombolysis, and with or without a defined arterial occlusion on CTA. Also, NOR-SASS is the first sonothrombolysis study with tenecteplase. If a positive effect and safety can be proven, contrast enhanced ultrasound treatment will be an option for acute ischaemic stroke patients eligible or not eligible for intravenous thrombolysis, for patients with or without a defined arterial occlusion on CTA and for those who do not have access to intra-arterial treatment.

Participant category: PhD Candiate/Research Program Student

The impact of abdominoplasty on skin perfusion evaluated with Dynamic Infrared Therm

Solveig Nergård [(1)], James Mercer [(1)], Louis de Weerd [(1)]

solveig.nergard@unn.no

1. Department of Ortopedic and Plastic Surgery
2. The institute of medical biology, the faculty of healt sciences, University of Tromsø

Introduction: Abdominoplasty is one of the most frequently performed cosmetic procedures. Wound- healing problems and surgical site infections are one of the most frequently postoperative complications. We postulate that these wound-healing problems and infections are related to impaired skin perfusion. We evaluated the effect of this surgical procedure on abdominal skin perfusion with the use of dynamic infrared thermography. Method: 12 patients scheduled for abdominoplasty were included in the study. The study was approved by the regional ethical committee. Dynamic infrared thermography, (DIRT), was performed before and during the operation, and on the first and second postoperative day. DIRT included a 10 minute acclimatization period followed by a cold challenge using a desk top fan blowing over the abdominal skin. The rewarming of the skin after the cold challenge was registered over a period of three minutes. The same procedure was followed after the skin was washed using water at room temperature. Preliminary results: The pattern of hot spots changed dramatically after the surgical procedure compared to the preoperative findings. The first day postoperative showed a hyperthermic state on the whole abdominal skin expect in the lower mid-area. We noticed that this area became better perfused during the following day. Discussion: The surgical procedure for an abdominoplasty has a significant impact on the pattern of skin perfusion. Initially the lower mid-area is well-less perfused but this perfusion improves over time. It is this lower mid-area that is known to be the area for wound healing problems and infections.

Participant category: Post doctoral fellow

Transabdominal ultrasonography for treatment follow up of patients with Crohn's disease

Kim Nylund [(1)], Fredrik Sævik [(2)], Trygve Hausken [(2,1)], Odd Helge Gilja [(1,2)]

kim.nylund@helse-bergen.no

1. National Centre of Ultrasound in Gastroenterology, Haukeland University Hospital
2. Department of Clinical Medicine, University of Bergen

Introduction: Crohn's disease is a chronic inflammatory disease of the bowel frequently requiring long term medical treatment with potentially harmful and expensive drugs. Currently there are no optimal diagnostic tools for follow up of these patients. Abdominal ultrasound could potentially represent a one stop shop since contrary to other diagnostic modalities it can be used for examining the small and large bowel in less than 20 minutes and is cheap, well accepted by patients and radiation free. It is not clear when the optimal time to examine the patients is and which parameters should be used during follow up. Methods: In a prospective, longitudinal pilot study 17 patients scheduled for systemic medical treatment for an acute exacerbation of Crohn's disease were included. Ultrasound examination was performed and clinical and biochemical data collected before treatment start and after 1, 3 and 12 months. The outcome after 12 months was effective or ineffective treatment defined by a change in systemic medical treatment after 3 months which is when commonly the treatment is reevaluated. Results: Six of 17 patients had ineffective treatment and had a significantly thicker proper muscle ($p=0.003$) (Figure 1) as well as a higher colour Doppler score ($p=0.011$) one month into the treatment. After three months they also had more neutrophils in the blood ($p=0.022$) There were no differences between the groups for any of the other variables at any of the other time points. Discussion: Our results imply that patients with acute exacerbation of Crohn's disease could benefit from having their treatment reevaluated already 1 month into the treatment. A thickened proper muscle is related to fibrosis while an increased colour Doppler signal is related to increased perfusion and inflammation in these patients. As these processes to a certain extent run independently of each other it may be prudent to use both parameters in treatment follow up.

See image on next page.

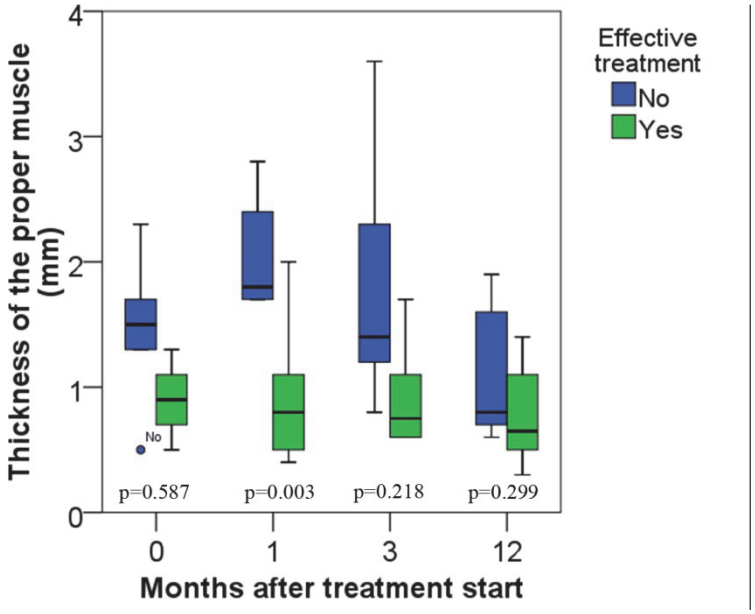

Boxplot of proper muscle thickness (mm) at each time point during the study. The proper muscle s significantly thicker in patients with ineffective treatment after one month.

Participant category: PhD Candiate/Research Program Student

Functionalization of Mesoporous Silica Nanoparticles for drug and contrast agents delivery (theranostics)

Melanie Ostermann [(1)], Emmet Mc Cormack [(1,2)], Veronika Mamaeva [(1)], Jessica Rosenholm [(3)], Didem Sen Karaman [(3)], Diti Desai [(3)]

melanie.ostermann@gmx.at

1. Hematology Section, Department of Clinical Science, University of Bergen
2. Hematology Section, Department of Internal Medicine, Haukeland University Hospital, Bergen
3. Laboratory of Physical Chemistry, Abo Akademi University, Turku, Finland

Mesoporous silica nanoparticles (MSNPs) are mainly spherical SiO2 particles with diameters in the range of 10–1000 nm. These particles are commonly synthesized using sol-gel process resulting in products with the ability to form homogenous products where the morphology can be controlled by simply varying the pH. Their popularity is due to their physiochemical properties, i.e., large surface area, tunable pore size, and high pore volume, suitable for carrying drug load up to 50% weight. MSNPs have been gaining attention for the use as drug delivery and targeting systems for cancer therapy in addition to their potential within imaging applications. For the effective usage of such nanomaterials in biomedicine a fundamental understanding and control of interactions between nanoparticles and biosystems is necessary. In this project surface modified MSNPs were developed and investigated in terms of stability of such colloidal systems in a physiological environment. Reduced interactions with serum proteins were obtained by coating the particles with an “inert” material, such as polyethylenglycol (PEG). PEGylation also enables the particles to remain longer in the bloodstream. Functionalization of MSNPs with polyethylenimine (PEI) led to a highly positive net surface charge, which increases cellular uptake. Drawback of PEI functionalization is the increased binding of serum proteins and cytotoxicity. Therefore PEG-PEI copolymers were carefully selected to improve safety and efficiency of the produced nanoparticles. Subsequently, cellular uptake can occur due to the enhanced permeability and retention (EPR) effect (passive targeting) or via active targeting e.g. with ligand-receptor interaction. Multifunctional MSNPs for targeting and diagnostic imagining will be obtained by adsorption of biomacromolecules, such as antibodies on the particle surface and accommodation of a near-infrared dye in the pores. We will further perform in vitro tests to establish biobehavior of nanoparticles within different cell cultures: uptake (internalization) of MSNPs, drug delivery efficiency vs free drug, toxicity studies. The size and fluorescence of the modified particles will be characterized using flow cytometry and UV-Vis-spectroscopy, and the zeta potential will be calculated using various electrophoretic mobility tests. Functionalized MSNPs are going to be used in ongoing projects in our lab: NTR gene delivery and novel MRI contrast agent development.

Participant category: PhD Candiate/Research Program Student

Virtual resections using tensor product surfaces

Rafael Palomar [1,2], Faouzi A. Cheikh [2], Azeddine Beghdadi [3], Bjørn Edwin [1], Ole J. Elle [1,4]

rafael.palomar@rr-research.no

1. The Intervention Centre, Oslo University Hospital
2. Gjøvik University College
3. University of Paris
4. Department of Informatics, University of Oslo

Introduction. Liver resection is the treatment of choice in selected patients with colorectal metastasis (even in recurrent cases). The procedure is performed under either open surgery or laparoscopic surgery. Either way, the challenges associated with this operations are: 1) guaranteeing a safety margin around the tumour; 2) guaranteeing enough functional remnant liver tissue and 3) reduction of bleeding avoiding the main vessels. Definition of virtual resections is a core functionality included in resection planning systems. This is often accomplished by means of deformable 3D surfaces and/or specification of the resection in several slices. In this work, we present a method for specifying virtual resections based on tensor product surfaces. Methods. Our method works analogously to 3D deformable surfaces. Initially, a resection plane is positioned arbitrarily in the liver according to the size and orientation of the parenchyma. This resection plane can be rotated, translated or scaled to roughly approximate the resection path (Figure 1a). Once the plane is placed correctly, a set of control points is computed by regularly sampling (in a grid) the resection plane. This set of points is employed to compute the tensor product surface, which initially matches exactly the resection plane. The control points can be moved to deform the resection surface defining the virtual resection (Figure 1b). Using tensor product surfaces we are able to generate smooth surfaces representing surgically correct resections. The number of control points indicates the degree of deformation. Increasing the number of control points increases the locality of deformation as well as the need of user interaction. The control points do not normally lie on the resection surface, which helps the visualization by avoiding occlusions. Results. A prototype of the method is currently under evaluation at The Intervention Centre, Oslo University Hospital. Preliminary results indicate that tensor product surfaces can be employed on planning liver resection procedures regardless of the type of resection. Initially we have employed surfaces generated by 4x4 control points in which deformations are driven by only 4 interior points. These surfaces seem to be sufficient to represent most resections.

See image on next page.

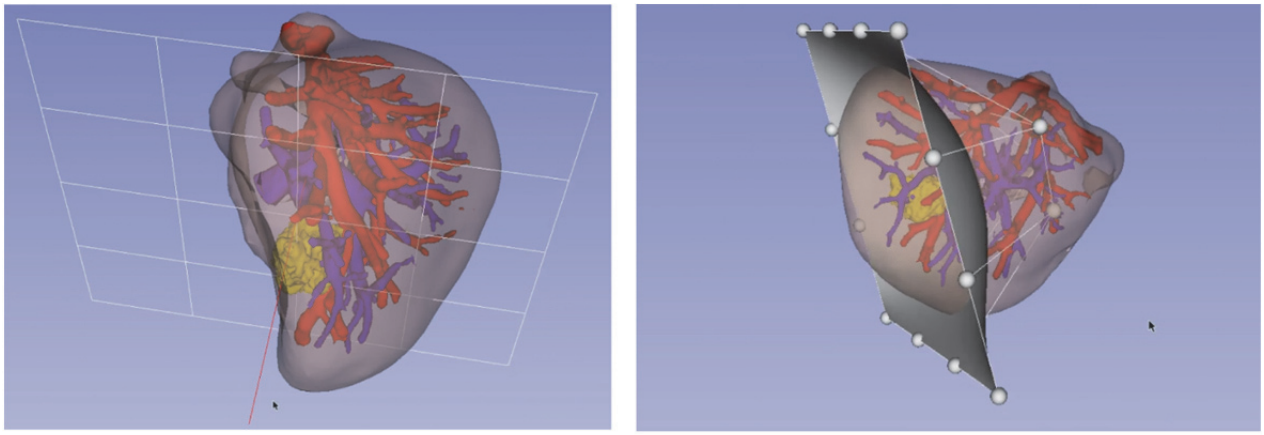

(a) (b)

Figure 1: *a) Initial resection plane placement. b) Deformation of the tensor product surface.*

Participant category: PhD Candiate/Research Program Student

Evaluation of Image Quality of CT vendors in Norwegian Market: low contrast detectability

Antonio Pelegrina Jiménez [(1)]

antonio.jimenez@hig.no

1. Gjovik University College, CIMET program

EVALUATION OF IMAGE QUALITY OF HIGH-END CT SCANNERS: LOW CONTRAST DETECTABILITY (A PHANTOM STUDY) Boundaries for medical and technical possibilities are constantly shifting and therefore, pose a continuous set of ethical challenges and dilemmas. The use of CT scan has increased dramatically over the last two decades in many countries. In difference with to other medical procedures, there is no binding regulation about CT dose management, but a collection of good practice recommendations by several institutions on the field. Manufacturers are looking onto image processing strategies in order to reduce the dose given to patient, while preserving the achieved image quality, here intended as the capacity to produce an equivalent diagnose. But lower dose, leads to more noise at image! where is the limit for an accurate diagnose? This study focus on the noise reduction filters possibilities (in example beam hardening reduction), and in the post-processing of images. Two examples of CT technology are compared, one of them being a Dual Energy CT scanner. We included size adjustment by rings onto the phantom, for its interest according to the current overweight trend in population. The initial hypothesis, is that noise magnitude and texture differs between the vendors of State-of-the-art CT scanners. We want to establish methods to quantify and compare low contrast detectability, and determine image quality. Two approachs are used: •numerical measurements (contrast to noise ratio) •and observers experiments. We are working with two groups: image procesing students and radiography students. We study how their answers could or not discern, through statistical tools as Mann-Wittney U test. We also study the distribution of their answers according to normality, to establish adequate confidence intervals. Counted circles at low contrast module of the phantom, will be translated to a minimum diameter discernible. Another possible approach, either if not used in Medical Imaging sector, could be a Forced Choice between 2 images, displayed simultaneously. The proposed áreas for further work are: ·Intra and inter-observer differences •Hystheresis of detectors ·Lighting configuration at observers experiment Graphics are kept confidential until Thesis evaluation concluded. Acknowledgements: Interventional Center Oslo University Hospital. Students at Hogskolen i Gjovik, Norway

See image on next page.

Image: Detail of modules of CAPTHAN Phantom 500

Participant category: Post doctoral fellow

A Robust Asynchronous SSVEP Brain-Computer Interface Based On Cluster Analysis of Canonical Correlation Coeffic

Pawel Poryzala [(1)], Andrzej Materka [(1)]

pawel.poryzala@p.lodz.pl

1. Institute of Electronics, Lodz University of Technology, Poland

Brain computer interface (BCI) systems allow a natural interaction with machines through a channel that does not involve the traditional motor pathways of the human nervous system. Thus they can be used by people with severe motor disabilities or those whose limbs are occupied with other tasks. Noninvasive interfaces, where electrical brain activity (EEG) is measured on the surface of the scalp recently showed greatest interest of researchers. Using the EEG measurements as the input to the BCI offers the advantages of low cost and high time resolution. However, due to small amplitude of the relevant signal components, poor spatial resolution, diversity within users' anatomy and EEG responses, achieving high speed and accuracy at large number of interface commands is a challenge. At present, the steady-state visual evoked potential (SSVEP) BCI paradigm is believed to provide the most promising way of optimizing the BCI performance in that sense. It is postulated that the SSVEP based BCI, combined with spatial filtering of the multichannel EEG data can provide the interface robustness to user diversity and electrode placement. A cluster analysis of the canonical correlation coefficients (computed for multi-channel EEG signals evoked by alternate visual half-field LED stimulation) can be used to achieve this goal. Experimental results combined with computer simulation are presented to objectively evaluate the performance of the proposed method. Additionally some of the concepts and methods may be implemented for time series analysis of fMRI data.

See image on next page.

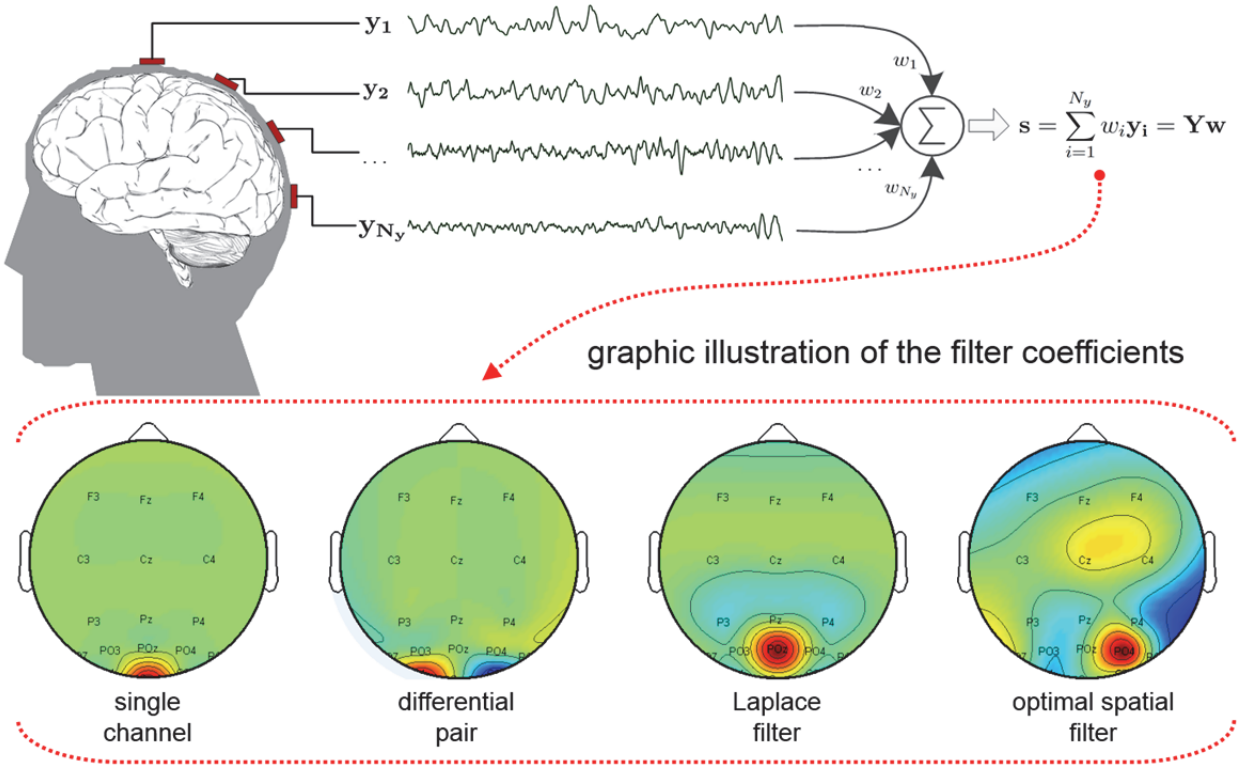
y_1
y_2
...
y_{N_y}
w_1
w_2
...
w_{N_y}
$s = \sum_{i=1}^{N_y} w_i y_i = Yw$
graphic illustration of the filter coefficients
single channel
differential pair
Laplace filter
optimal spatial filter

Participant category: PhD Candiate/Research Program Student

Comparison of the measured collagen structure in articular cartilage by diffusion tensor imaging and multi-photon microscopy

Elisabeth Inge Romijn [(1)], Øystein Risa [(2)], Pål Erik Goa [(1)], Marius Widerøe [(2)], Jose Ramon Teruel [(2,3)], Magnus Borstad Lilledahl [(1)]

elisabeth.romijn@ntnu.no

1. Department of Physics, Faculty of Natural Sciences and Technology, NTNU
2. Department of Circulation and Medical Imaging, Faculty of Medicine, NTNU
3. St. Olavs University Hospital

The purpose of this study is to compare the collagen structure of cartilage measured by multi-photon microscopy and diffusion tensor imaging. Diffusion tensor imaging measures the diffusion of water molecules. Since the water molecules are obstructed by tissue structures, diffusion tensor imaging can indirectly determine the tissue architecture. In cartilage, it is mainly collagen fibers that limit the movement of free water molecules. The collagen network determines to a high degree the function of cartilage, and is affected in diseases such as osteoarthritis. Using diffusion tensor imaging to examine the collagen structure in cartilage non-invasively and in-vivo is of great potential. This could be used for diagnostic purposes, but also for mechanical modelling where knowledge of the structural anisotropy of the collagen network is of high importance. By comparing diffusion tensor imaging to multi-photon microscopy the exact correlation between the collagen network and water diffusion is determined.

Participant category: PhD Candiate/Research Program Student

Correlating Quantitative MR spectroscopy with Gleason score and proliferative status in prostate cancer tissue

Elise Sandsmark [(1)], Ailin F. Hansen [(1)], Kirsten M. Sælnes [(1)], Anders Angelsen [(2)], Anna M. Bofin [(3)], Tone F. Bathen [(1)], May-Britt Tessem [(1)]

elises@stud.ntnu.no

1. Department of Circulation and Medical Imaging, Norwegian University of Science and Technology (NTNU), Trondheim, Norway
2. Department of Cancer Research and Molecular Medicine, Norwegian University of Science and Technology (NTNU), Trondheim, Norway
3. Department of Laboratory Medicine, Children's and Women's Health, Norwegian University of Science and Technology, Trondheim, Norway

Introduction: Prostate cancer is the most common visceral malignancy in Norwegian men, and the incidence is increasing. The selection of patients who will benefit from curative treatment is challenging. A better characterisation and understanding of mechanisms determining cancer aggressiveness may allow more accurate answers to important clinical problems. In this study HR MAS magnetic resonance spectroscopy (MRS) is used to investigate the relationship of metabolite concentrations with cancer/non-cancer, Gleason score and cell proliferation in prostatectomy tissue samples. Methods: Metabolic spectra of prostatectomy tissue samples (n=91) were acquired using HR MAS MRS. LCModel [1] was used to quantify 27 key metabolites of each spectrum. Subsequently the same tissue samples were histopathologically divided into non-cancer and cancer, and the latter were graded using Gleason score (GS) [2]. Proliferation index of the cancerous samples were obtained using immunohistochemistry with the proliferation marker Ki-67. Statistical analyses were performed in SPSS using Mann-Whitney U test and Spearman correlation. Results: Of the 91 samples, 50 were non-cancer, 22 were low grade prostate cancer (GS $\leq$ 3+4) and 19 were high grade prostate cancer (GS $\geq$ 4+3). Analysis of the data is not yet complete, but preliminary results suggest alterations in the energy and choline phospholipid metabolism in non-cancer vs. cancer, and in low vs. high grade cancers, and a weak negative correlation between proliferation and glucose concentration (Spearman's ρ=-0,385, p=0.16) (Figure 1). More throughout and accurate analysis will be preformed for future characterisation of the metabolism in the different groups. Discussion: The altered metabolic profile between non-cancer and cancer and between low and high grade cancer are in agreement with previous findings in the literature. The negative correlation between cell proliferation and glucose concentration might be due to increased glucose consumption by proliferating cell. Further analysis is required before any conclusions can be made. References: [1] Provencher, S.W. Magn Reson Med. 1993; 30(6):672-92. [2] Epstein, J.I., et al. Am J Surg Pathol. 2005; 29(9):1228-42.

See image on next page.

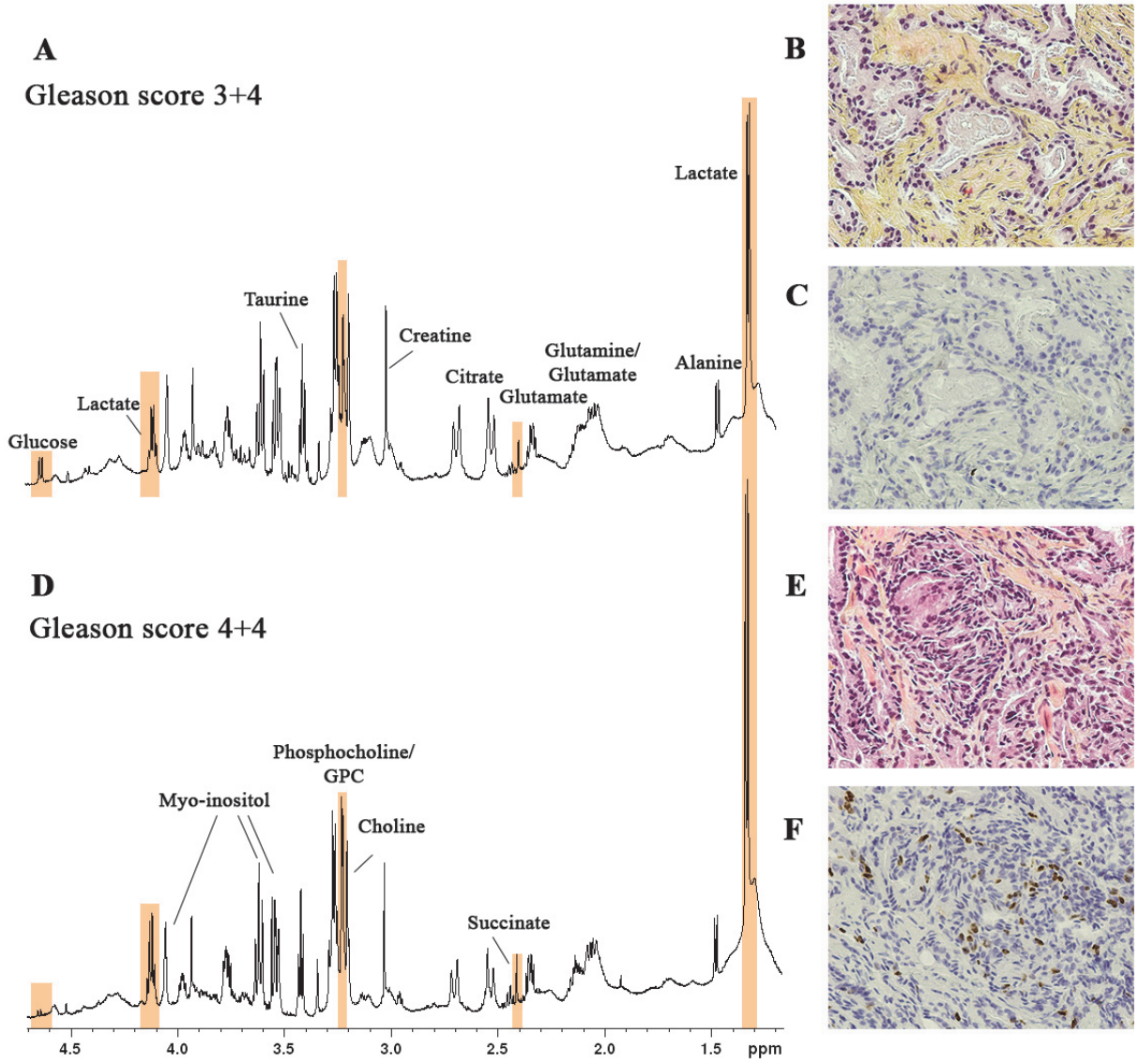

(A-C) Low grade cancer (GS 3+4) with low proliferation index (1.7%), (A) HRMAS spectrum (B) HES (C) IHC Ki-67. (D-F) High grade cancer (GS 4+4) with high proliferation index (10%), (D) HRMAS spectrum, low glucose and high lactate, succinate, PCho/GPC pea

Participant category: PhD Candiate/Research Program Student

Development in imagable xenograft models of the Myelodysplastic Syndromes (MDS)

Sahba Shafiee [(1)], Emmet McCormack [(1,2)], Astrid Olsnes Kittang [(1,2)], Biju Parekkadan [(3)], Mihaela Popa [(4)], Lars Helgeland [(5)], Jungwoo Lee [(6)], Bjørn Tore Gjertsen [(1,2)]

Shafieebio@gmail.com

1. Section of Hematology, Department of Clinical Science, University of Bergen
2. Department of Medicine, Haukeland University Hospital
3. Harvard Stem Cell Institute, Boston
4. KinN Therapeutics AS, Norway
5. Department of Pathology, Haukeland University Hospital
6. Center for Engineering in Medicine and Surgical Services, Massachusetts General Hospital, Harvard Medical School and Shriners Hospital for Children in Boston

Development in imageable xenograft models of the Myelodysplastic Syndromes (MDS) Introduction: MDS is a preleukemic disease with poor prognosis and few therapeutic options.In several studies, generating a preclinical model of MDS is found to be challenging due to difficulties in tracing the leukemic cells in vivo. Recently,by establish the most similar MDS like cell line (MDS-Lcells), researchers were able to identify the human myeloid cells in the bone marrow, however progression of the disease is not clearly understood. In our investigation, we transfect MDS-L cells with luciferase to increase the ability of tracking MDS-L in vivo. Methods: Main methods used in our investigations were fluorescent microscopy, bioluminescence and fluorescent imaging. Molecular imaging in our previous study revealed the ability of the MDS-L cells to proliferate in matrigel infused scaffolds as an artificial bone marrow structure in both in vitro and in vivo (first model). In further development, we have evaluated MDS modelling by employing the bone marrow stromal cells and use of two types of matrix (Matrigel and scaffold) in NSGS immunodeficinet mice (by expression of hIL-3,hGM-CSF, and hSF). Results: Bioluminescence imaging illustrate that matrigel matrix implanted only with stromal cells, support consistent and reproducible engraftment of MDS-L cells (second model), while only minimal engraftment was observed when using scaffold matrix implanted with stromal cells. Exvivo histological analysis of the scaffold matrix revealed dense vasculature in all the pores of the scaffold and presence of the MDS-L cells close to the vessels, which can illustrate minimal observed bioluminescence. Further on, to examined engraftment of the MDS primary patient materilas invivo, we utilize successful models system; Matrigel infused scaffold, Matrigel matrix and stromal cells. MDS patient cells invivo longitudinally imaged engrafted mice by time-domain optical imaging in vivo using multiplexed monoclonal antibodies (CD13, 33 and 45) as contrast reagent. Results from imaging suggests stromal cells mixed with matrigel, have even greater engraftment efficiency and consistency of patient cells. Conclusion: Using optical imaging in animal modeling of MDS disease, helped to explain the second xenograft model of the MDS. This highly supports the strategy of using stromal cells with matrigel matrix, better than using only scaffold matrix in engraftment of both MDS-L and patient materials.

Participant category: PhD Candiate/Research Program Student

FAST - Framework for Heterogeneous Medical Image Computing

Erik Smistad [1,2], Mohammadmehdi Bozorgi [1], Frank Lindseth [1,2]

smistad@idi.ntnu.no

1. Dept. of Computer and Information Science. Norwegian University of Science and Technology (NTNU)
2. SINTEF Medical Technology. Trondheim, Norway.

An increasing amount of medical image data is becoming available for any given patient today. Advanced image analysis techniques makes it possible to extract more and more information from the images, fuse more and more image modalities together and visualize the inner parts of the human body more and more detailed. The race for using the increasing amount of image data more and more efficiently is paramount for better diagnostics and therapy in the future. Still, concurrent medical image computing and visualization of both static and dynamic real-time data is computationally expensive and the consequence is that clinical personnel must wait to get the answers they need or alternatively get a less accurate answer. However, most image processing techniques can benefit from parallel processing on specialized hardware such as graphics processing units (GPUs) and multi-core CPUs. It's highly likely that the ultrasound scanner of the future or the next generation of therapeutic navigation systems will consist of software for concurrent computing and visualization running on top of such heterogeneous hardware architectures. The programming of this hardware is, however, difficult due to: * Software and hardware differences and errors. * A lot of low-level programming and explicit memory transfers between devices. * Challenges related to debugging of parallel applications and specialized hardware. To circumvent these problems we are developing an open source framework (FAST) that will make it easier to do processing and visualization of medical images on heterogeneous systems (CPU+GPU). The framework will accomplish this by: * Using familiar high-level programming paradigms such as a demand-driven execution pipeline inspired by popular toolkits such as VTK and ITK. * Hiding the details of memory management and transferring image data between heterogeneous processors. * Ensuring data coherency across different memory spaces and processors. * Streaming real-time data directly to different devices using the producer-consumer model. * Importing and exporting image data to and from VTK and ITK. * Having a testing and benchmarking framework that will enable the user to make sure that all the hardware and software is working properly and gives the performance required.

Participant category: PhD Candiate/Research Program Student

Multifunctional RGD targeted nanoparticles for drug delivery and diagnostic purposes

Sofie Snipstad [(1)], Yrr Mørch [(2)], Rune Hansen [(3,4)], Sigrid Berg [(3,4)], Siv Eggen [(1)], Einar Sulheim [(1)], Catharina de Lange Davies [(1)]

sofie.snipstad@ntnu.no

1. Department of physics, NTNU
2. Materials and Chemistry, SINTEF
3. Technology and Society, SINTEF
4. Department of Circulation and Medical Imaging, NTNU

The use of nanoparticles (NPs) opens new possibilities in cancer diagnostics and therapy. Leaky tumor vessels and nonfunctional lymphatics enable selective extravasation and accumulation of NPs in tumors, and improved pharmacokinetics compared to free drug, increased efficacy and reduced toxicity. The distribution of NPs in tumor tissue is however often heterogeneous and additional strategies are needed. Solid tumors can be targeted by the amino acid sequence Arg-Gly-Asp (RGD), which binds specifically to αvβ3-integrins on angiogenically activated endothelial cells. Further, focused ultrasound (US) can be applied to improve uptake and distribution of NPs in tumor tissue. A unique multimodal, multifunctional drug delivery system based on NPs and microbubbles (MBs) has been developed by SINTEF. The NPs are synthesized from biocompatible and biodegradable poly (alkyl cyanoacrylate) in a single step using miniemulsion polymerization. They contain drugs, magnetic resonance imaging contrast agents and fluorescent probes. They are coated with polyethylene glycol (PEG), and may be functionalized with RGD targeting ligands. The novelty of these NPs is that they can stabilize MBs, making them excellent carriers of drugs to be used in combination with US for improved drug delivery. The MBs are also promising agents for contrast-enhanced US imaging. First, we aim to characterize the RGD-NPs. Uptake and intracellular distribution will be studied in human umbilical vein endothelial cells using flow cytometry and confocal laser scanning microscopy (CLSM). Further, we aim to use MBs stabilized by RGD-NPs with US for enhanced uptake and distribution in tumors, in athymic mice with human prostate cancer growing subcutaneously or in dorsal window chambers (DWC). A whole animal imager will be used to study the biodistribution and circulation time of NPs, and mass spectroscopy to quantify accumulation in the organs after various US treatments. The microdistribution of NPs will be imaged on frozen tumor sections or intravitally in DWC using CLSM and multiphoton microscopy. The therapeutic effect of our new NP-MBs in combination with US will be studied by encapsulating the prostate anticancer cytotoxic drug docetaxel and measuring tumor volume. Finally, we aim to apply this platform for early detection of cancer, by selectively imaging blood vessels in tumors. Studies will be performed using the transgenic adenocarcinoma of the mouse prostate (TRAMP) model and US imaging.

Participant category: PhD Candiate/Research Program Student

A novel platform for electromagnetic navigated ultrasound bronchoscopy (EBUS)

Hanne Sorger [1,2,4], Erlend Hofstad [3], Tore Amundsen [1,2], Thomas Langø [3], Håkon Olav Leira [1,2]

hannesorger@msn.com

1. Department of Thoracic Medicine, St Olavs Hospital
2. Department of Circulation and Medical Imaging, Faculty of Medicine, Norwegian University of Science and Technology (NTNU)
3. SINTEF, Technology and Society, Dept. of Medical Technology
4. Department of Medicine, Levanger Hospital, Nord-Trøndelag Health Trust

Background: Endobronchial ultrasound fine needle aspiration (EBUS-FNA) of mediastinal lymph nodes is an essential part of lung cancer staging. Precision requirements are high, particularly in limited disease with a potential to cure, to avoid erroneous clinical decision-making. Navigation and multimodal imaging may improve the efficiency of EBUS-FNA. We wanted to demonstrate a prototype EBUS navigation system in a phantom, preceding approved human pilot studies. Methods: Using an EBUS bronchoscope with an integrated sensor for electromagnetic (EM) position tracking we performed navigated EBUS in a novel lung phantom containing silicone tumor models. Preoperative computer tomography (CT) and real-time ultrasound (US) images were integrated into an existing navigation platform for EM bronchoscopy. The coordinates of targets in CT and US volumes were determined in the navigation system, and the position deviation was calculated. Results: All tumor models were visualized, and their fused CT and US images were displayed in correct positions in the navigation system. The navigated EBUS bronchoscope had no noticeable limitations during endoscopy. EM navigation made sonographic target localization fast and easy, and fine needle puncture was successfully performed. Mean error observed between US and CT positions for 11 target lesions (37 measurements) was 2.8±1.0 mm, and maximum error was 5.9 mm. Conclusions: The feasibility of a new system for navigated EBUS was successfully demonstrated. The system may increase diagnostic accuracy and provide new opportunities for procedure documentation in EBUS-FNA.

See image on next page.

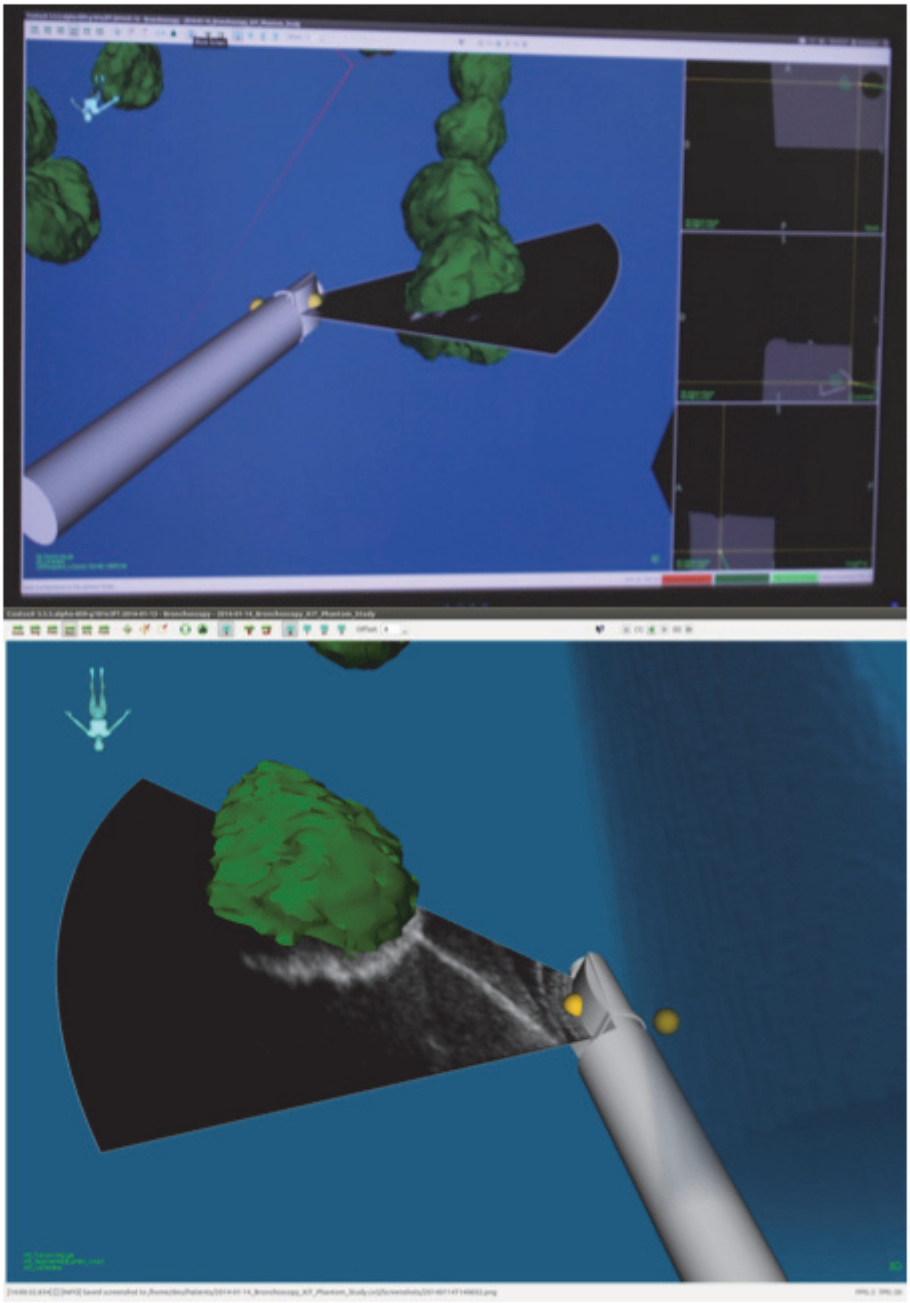

Top: Navigated endobronchial ultrasound (EBUS) graphical user interface. 2D ultrasound images are displayed in the navigation scene. The virtual tip of the bronchoscope performs a sweeping motion towards a target lesion (green). Bottom: Fine needle punct

Participant category: PhD Candiate/Research Program Student

Intra-observer variability in segmentation of glioblastomas

Anne Line Stensjøen [(1)], Ole Solheim [(2,3)], Asta Håberg [(4,5)], Erik Magnus Berntsen [(1,5)]

stensjoe@stud.ntnu.no

1. Department of Circulation and Medical Imaging, Faculty of Medicine, NTNU
2. Department of Neurosurgery, St. Olavs University Hospital
3. National Competence Centre for Ultrasound and Image guided Therapy
4. Department of Neuroscience, Faculty of Medicine, NTNU
5. Department of Radiology, St. Olavs University Hospital

Glioblastoma is the most common primary brain tumour. The overall prognosis for patients with glioblastoma is poor, with median survival less than one year. Tumour volume doubling time is a potential prognostic factor for survival time of these patients, although not extensively studied. Tumour doubling time may be studied non-invasively using repeated magnetic resonance imaging (MRI) scans before surgery. When studying the volumetric growth rate of glioblastomas, there is a need for highly accurate volumetric segmentation of the tumour. In clinical routine, high-resolution imaging is not always used at the first MRI scan where the tumour is discovered, introducing sub-accurate segmentations. In this study, we aimed to assess the intra-observer variability of volume estimates based on semi-automatic tumour segmentation on post-contrast T1-weighted images with high and low resolution. This retrospective study included preoperative MRI from 30 patients with histopathologically confirmed glioblastoma (WHO grade IV). The first group consisted of ten patients with image slice-thickness between 4 mm and 6.5 mm, and the second group of twenty patients with image slice-thickness below 1.5 mm. One experienced operator segmented the tumour volumes using the software BrainVoyager QX (Brain Innovation, Maastricht, the Netherlands). The tumour was defined as the contrast-enhancing rim of the tumour, as well as the non-enhancing parts within the contrast enhancing area. The segmentation was repeated after two weeks. For each group, any difference in estimated tumour volume between the two segmentations was investigated using the paired sample t-test. An intraclass correlation coefficient (ICC) was calculated to investigate the correlation between the estimated volumes. The mean tumour volume was 29.4 ml in group 1 (range 0.7 to 94.1) and 41.2 ml in group 2 (range 1.7 to 90.7). Neither group had significant differences in segmented volume between the two segmentations (p=0,438 and p=0,531). ICC values were 0.999 in both groups (excellent correlation). The mean relative difference in volume was -1.9% for group 1 and -0.6% for group 2. These findings indicate that when the same experienced operator is performing the segmentations, there is a high correlation between repeated measurements with no significant difference in estimated tumour volume between repeated segmentations. This is valid for MRI volumes with both thin and thick slices.

Participant category: PhD Candiate/Research Program Student

Brain Diffusion Tensor Magnetic Resonance Imaging on Irritable Bowel Patients

Kiniena Tekie [(1)], Eivind Valestrand [(2,3)], Trygve Hausken [(3)], Arvid Lundervold [(1,2,4)]

kiniena.tekie@gmail.com

1. Department of biomedicine, University of Bergen
2. Neuroinformatics and Image Analysis Laboratory, Department of Biomedicine, University of Bergen
3. Section of Gastroenterology, Department of Medicine, University of Bergen
4. Departement of Radiology, Haukeland University Hospital, Bergen

Background: Irritable bowel syndrome (IBS) is a symptom-based diagnosis. Chronic recurring abdominal pain with altered bowel habits are the classic symptoms that diagnose IBS by excluding other gastrointestinal disorders. Neurobilogical based classification is a future goal for evidence based IBS, since the symptoms are expected to have underlying neurobiological basis. The close interrelationship between the central nervous system and enteric nervous system, that is important in health and disease, can be studied to give insight into the underlying pathophysiology of IBS. Aims:The present study addresses the brain part of the brain-gut axis in patients with IBS. The brain-gut axis consists of a hierarchy of reflex loops that assure homeostatic control of GI function. The brain is at the top of the hierarchy by regulating visceral pain processing, gray matter density, regional white matter microstructure, and brain connectivity in this patient group. Materials and Methods: Brain diffusion tensor images of 15 IBS patients and 15 healthy control. DTI analysis can provide valuable information on the microstructural status of the brain white matter (WM). DTI is an MRI technique that is used to study microstructure of the brain white matter. Pathological alteration of the WM microstructure can be detected by comparing two populations, the health control with the IBS patients. Results:Using pooled FA values for each ROI and group, the most striking finding was slightly lower FA values (about 3-5% reduction in median FA) in caudal regions of the middle frontal lobes and bilaterally in subcortical white matter of the insula in IBS patients compared to healthy controls.

Participant category: PhD Candiate/Research Program Student

MYOCARDIAL PROTECTION: POLARIZING VS. DEPOLARIZING CARDIAC ARREST WITH REPEATED, COLD, OXYGENATED BLOOD CARDIOPLEGIA IN A TRANSLATIONAL PIG MODEL OF CARDIOPULMONARY BYPASS.

Aass Terje [(1)], Rune Haaverstad [(1)], Knut Matre [(2)], Ketil Grong [(2)]

terje.aass@me.com

1. Section of Cardiac and Thoracic Surgery, Department of Heart Disease, Haukeland University Hospital.
2. Department of Clinical Science, Faculty of Medicine and Dentistry, University of Bergen.

Objectives: Potassium-based depolarizing cardioplegia administered as cold, repeated, oxygenated blood is considered as the optimal mode of protection during cardiac surgery. Our hypothesis is that polarized arrest with esmolol/adenosine in cold, oxygenated blood will offer comparable myocardial protection in a clinically relevant animal model. Methods: Twenty anaesthetized young pigs, 42+2 kg (SD) on standardized tepid cardiopulmonary bypass were randomized, 10 in each group, to polarizing or depolarizing cardioplegic arrest for 60 min with esmolol/adenosine or potassium, administered in the aortic root every 20 min as freshly mixed cold, repeated, oxygenated blood. Together with haemodynamics, global left ventricular systolic and diastolic function was evaluated with pressure-volume conductance catheter before, and 1, 2 and 3 hours after declamping and weaning. Results: Preliminary results demonstrated no significant differences between groups when evaluating LV function and general haemodynamic variables before CPB. In both groups, cardiac asystole was obtained and maintained during the X-clamp period. Compared to data before CPB, heart rate was increased and LV end-systolic and end-diastolic pressures decreased in both groups. Three hours after declamping left ventricular systolic pressure and contractility, dP/dt, was increased in animals with esmolol/adenosine cardioplegia compared to potassium based cardioplegic arrest (P=0.023 and P=0.033). Neither Cardiac Index nor ESPVRslope, describing load independent contractility or EDPVRslope, describing ventricular compliance, differed between groups up to 3 hours after declamping. Conclusion: Our preliminary results suggest that polarizing oxygenated blood cardioplegia with esmolol/adenosine offers myocardial protection comparable to the standard potassium based blood cardioplegia.

		Before	1h declamp	2h declamp	3h declamp
HR (beats/min)	Esmo/Ado	88±2	118±8	130±6	140±7
	Potassium	86±2	119±6	128±11	138±8
$LVSP_{max}$ (mmHg)	Esmo/Ado	109±3	90±4	95±4	94±5 [x]
	Potassium	104±5	97±4	85±5	81±3
LVEDP (mmHg)	Esmo/Ado	11.1±0.6	8.3±0.8	8.9±1.3	7.4±1.0
	Potassium	11.2±1.3	7.8±0.6	7.0±0.8	8.2±1.3
$LV\text{-}dP/dt_{max}$ (mmHg/s)	Esmo/Ado	1574±95	1874±285	1651±124	1999±240 [x]
	Potassium	1572±72	1853±162	1464±80	1388±68
CI ($L/min\ per\ m^2$)	Esmo/Ado	3.9±0.3	4.5±0.3	4.3±0.2	4.5±0.3
	Potassium	4.0±0.1	4.6±0.3	4.0±0.2	4.1±0.3
$ESPVR_{slope}$ (mmHg/s)	Esmo/Ado	1.1±0.1	1.8±0.4	2.7±0.9	2.8±0.3
	Potassium	1.4±0.2	2.6±0.5	2.6±0.5	3.2±0.6
$EDPVR_{slope}$ (mmHg/s)	Esmo/Ado	0.20±0.02	0.17±0.02	0.22±0.03	0.22±0.03
	Potassium	0.26±0.03	0.16±0.03	0.18±0.03	0.21±0.04

Mean ± SEM, n= 10. [x]Denotes significant difference (P<0.05) from Potassium by two-sample t-test.

Participant category: Post doctoral fellow

A differentiated adaptive radiotherapy workflow using dose distributions from statistical motion modeling

Sara Thörnqvist [1,2], Liv Hysing [1], Andras Zolnay [3], Matthias Söhn [4], Mischa Hoogeman [3], Ludvig Muren [2], Ben Heijmen [3]

sarathoe@rm.dk

1. Department of Medical Physics, Haukeland University Hospital, Bergen, Norway
2. Department of Medical Physics, Aarhus University Hospital, Aarhus, Denmark
3. Department of Radiation Oncology, Erasmus MC-Daniel den Hoed Cancer Center, Rotterdam, the Netherlands
4. Department of Radiation Oncology, University Hospital Grosshadern, LMU München, München, Germany

Introduction: Image-guided radiotherapy could allow improved tumor control and reduced side-effects if taking into account temporal information of geometry changes in individual patients (pts) during a course of treatment. In this study we used feedback by daily CTs acquired at first week of treatment as input to an off-line adaptive planning process (Fig.1a). Treatment decisions regarding if and how to modify the pts's treatment after the first out of five weeks was based on estimated outcome distributions (Fig.1b) for the targets and organs at risk had the initial plan had been delivered for all five weeks. The patient-specific outcome distributions stemmed from MonteCarlo simulations of possible treatment courses. The motion model used in the simulations was PCA-based, generating realistic patient geometries by inter- and extrapolation of the five input geometries, deformed to the initial plan. Point correspondence between the sampled geometries enabled summation of dose to each tissue-element of the targets and organs at risk. Material& Method: The simulation study involved 16 locally advanced prostate cancer pts with treatment of the prostate (CTV-p), the seminal vesicles (CTV-sv) and the pelvic lymph nodes (CTV-ln). The initial plans used tight margins of 3mm for all targets to trigger adaptations. Two decisions were made from the estimated dose; the first based on the expected mean dose and its deviation from that intended and the second based on the variation around this mean. The action taken from the first decision aimed to correct for systematic deviations and the second to select those pts who had a large motion and might require a more resources intensive treatment. Result: Applying a criterion for a systematic error if the estimated mean dose to 99% of the target volume (D99) was less than 98% of the prescribed dose, all but three pts needed an adaptation for at least one of the three targets. Applying a criterion for the variability of D99 such that this should be within 2Gy for each target, plan libraries had been generated for CTV-p in two pts and for CTV-sv in 9 pts. An adaptation involving a single re-plan would have been initiated for one pts due to the motion of the CTV-p, two due to CTV-sv and one due to CTV-ln. Conclusion: Estimated dose was both pts and target dependent. The process triggered mostly plan selection strategies for CTV-sv, whereas the more rigid targets CTV-p and CTV-ln resulted in few but single re-plan adaptations.

See image on next page.

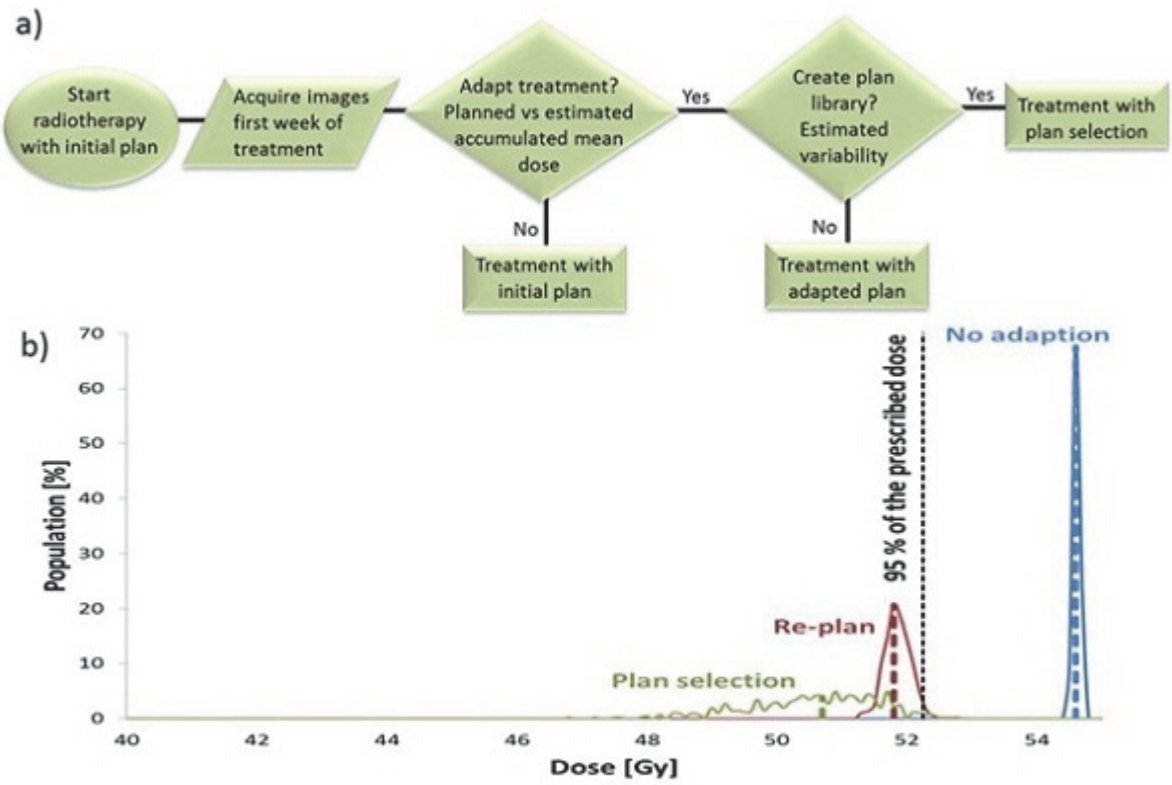

Figure 1. a) Flowchart of the adaptations triggered after treatment simulations with a statistical motion model. b) Example of the distribution of the dose to 95% of the target volume for the seminal vesicles. Estimated mean values marked with dashed colored lines.

Participant category: PhD Candiate/Research Program Student

Structural brain networks across psychotic disorders – a graph theoretical approach

Siren Tønnesen [1,2], Tobias Kaufmann [1,2], Ingrid Melle [1,2], Ingrid Agartz [1,3], Ole A. Andreassen [1,2], Lars T. Westlye [1,4]

siren.tonnesen@medisin.uio.no

1. NORMENT KG Jebsen Centre for Psychosis Research, Oslo University Hospital, Oslo, Norway
2. Institute of Clinical Medicine, University of Oslo, Norway
3. Diakonhjemmet Hospital, Oslo
4. Department of Psychology, University of Oslo, Norway

Psychosis is characterized by delusions, hallucinations, and cognitive impairment, in addition to negative symptoms including apathy and poverty of speech. The underlying brain pathology is largely unknown, but recent evidence suggests brain network abnormalities. Here we aim to characterize and compare structural network properties between healthy controls and across patients diagnosed with bipolar (BD) and schizophrenia (SCZ) spectrum disorders using diffusion tensor imaging (DTI) and graph theory. We utilise whole-brain probabilistic tractography to reconstruct white matter pathways and derive topological properties including connectivity strength and network efficiency. These network indices are sensitive to axonal density and myelin pathology, and may reveal novel network alterations underlying psychotic disorders. In order to localize pairs of brain regions in which structural connectivity might be altered in BD and SCZ we also employ a recently developed network-based statistic approach. The sample is drawn from the ongoing TOP-study and includes 47 and 49 patients diagnosed with BD (mean age: 31.33 (11.05)) and SCZ (mean age: 28.20 (7.48)), respectively, in addition to 222 healthy controls (mean age: 30.94 (7.51)). DTI data has been obtained on a 3T GE Signa scanner using 2D spin-echo whole-brain EPI DTI sequence with the following parameters: repetition time (TR) = 8000; echo time (TE) = 600msec; flip angle = 8°; slice thickness = 2.5 mm; field of view (FOV) = 240 x 240; acquisition matrix = 96x96; 30 gradients directions. Two images without gradient loading (b0 s/mm2) were acquired prior to the acquisition of 30 images (each containing 52 slices) with the uniform gradient loading (b=1000 s/mm2) and processing and analysis will be performed using a combination of FSL (http://fsl.fmrib.ox.ac.uk/fsl) and custom Matlab and R tools. Based on previous studies and theories of brain network disruption in psychosis, we hypothesize white matter (WM) microstructural alterations and disrupted topological organization of the WM networks across the disorders. We also hypothesize a significant reduction of betweenness centrality, reduced global efficiency of frontal, temporal and occipital brain regions and a loss of frontal hubs in SCZ and BD compared to healthy controls. Further, based on a dimensional approach to psychosis, we anticipate associations of WM alterations with symptom severity as assessed using the PANSS scale.

Participant category: PhD Candiate/Research Program Student

Tumour segmentation using pattern recognition techniques

Turid Torheim [(1)], Eirik Malinen [(2,4)], Ulf Indahl [(1)], Knut Kvaal [(1)], Heidi Lyng [(3)], Cecilia Futsæther [(1)]

turid.torheim@nmbu.no

1. Dept. of Mathematical Sciences and Technology, Norwegian University of Life Sciences
2. Dept. of Medical Physics, Oslo University Hospital
3. Dept. of Radiation Biology, Oslo University Hospital
4. Dept. of Physics, University of Oslo

The data considered in this study is a set of MR images for patients with locally advanced cervical cancer. For these patients, T2-weighted MRIs have been used for manual tumour segmentation. The aim of the study was to investigate the feasibility of automatic tumour segmentation for these patients, either by using only the T2-weighted images, or by combining T2- and T1-weighted images with dynamic contrast enhanced (DCE) MRI. Fisher's Linear Discriminant Analysis (LDA) is a supervised classification method for sorting samples into different classes. The multivariate data is projected onto the line that minimizes the within-class scatter and maximizes the between-class scatter. LDA is considered a robust classification method, and is computationally efficient. In this study we aim to classify image voxels as either healthy or belonging to the tumour. We combined the intensities from the different image types into a feature vector for each voxel. For the DCE MRIs, the intensities from each time step were included. The feature vectors were used as explanatory variables in the linear discriminant analysis, with the manually segmented tumour mask as response. To avoid over-optimistic classification results, a leave-one-out validation approach was used. Our study shows that combining the intensities from T2-weighted MRI, T1-weighted MRI and DCE-MRI into one feature vector for each voxel much improved voxel classification performance compared to classification based on only the T2-weighted images. ROC analysis of the LDA model based on all three image types gave AUC = 0.8567.

Participant category: PhD Candiate/Research Program Student

Radiofrequency ablation of the pancreas using endoscopic ultrasound in an experimental porcine model

Bogdan Ungureanu [(1)], Dan-Ionut Gheonea [(1)], Larisa Sandulescu [(1)], Adrian Saftoiu [(1)]

boboungureanu@gmail.com

1. Gastroenterology and Hepatology Research Center, Craiova, Romania

Treating pancreatic cancer represents a major objective in research, as it still remains the fourth leading cause of cancer deaths among men and women, with approximately 6% of all cancer-related deaths. Radiofrequency ablation uses electromagnetic energy deposition causing thermal lesions and overheating tissue which leads in a final stage to necrosis. We studied the assessment of an EUS-guided RFA probe through a 19-gauge needle, in order to achieve a desirable necrosis area in the pancreas. Radiofrequency ablation of the head of the pancreas was performed using a RITA Medical System device on 10 Yorkshire pigs with a weight between 25 to 35 kg. Using an EUS-guided RFA experimental probe we ablated an area of 2 to 3 cm wide at 5-10-15-20 watts for one minute a time. No major complications were noted. The ablation area was monitorised postprocedure and after 3 days with contrast (Sonovue). Necropsy pointed out a very well limited area with minimal invasion and inflammatory tissue at about 2 cm surrounding the lesion. No nearby fibrosis or adhesions were found and no major vessel injuries or adjacent organ damage was produced. The pathology examination revealed coagulative necrosis, a local acute inflamatory reaction with structured necrosis of the glandular parenchyma, steatonecrosis, and recent thrombosis of blood vessels.

Participant category: Post doctoral fellow

A phase-shift concept for ultrasound mediated local drug delivery

Annemieke van Wamel [(1)], Andrew Healey [(2)], Per Christian Sontum [(2)], Svein Kvåle [(2)], Catharina de Lange Davies [(1)]

Annemieke.wamel@ntnu.no

1. The Norwegian University of Science and Technology (NTNU), dept of Physics
2. Phoenix Solutions AS

Heterogeneity of disease affected vasculature makes it difficult to achieve a sufficient amount of drugs throughout pathologic tissue without reaching the maximal toxic dose for normal tissue. The current paper presents a novel approach to solve this problem. This new drug carrier system, developed by Phoenix Solutions AS, can be used to deliver drugs only where it is needed. It is based on a phase shift technology in which positively charged micron sized oil droplets (µd) and negatively charged microbubbles (µb) are mixed. After i.v. injection, the mix will circulate throughout the whole body, however, only upon local ultrasound exposure the µb transfer acoustic energy to the attached drug-loaded oil-droplets causing the oil to undergo a liquid-to-gas phase shift. This results in drug release and bubbles of ~30µm (fig.1) that are trapped in the microvasculature. These bubbles can be insonified with low frequency US resulting in bubble oscillations increasing extravasation of the released drug. Because of the local high drug concentrations, temporary slowing down of blood flow, and bubble oscillation, it is expected that this treatment will be very beneficially for drug efficacy through enhancing local concentration, exposure time, and treated area (fig.2). Here we show preliminary results confirming that US can be used to create phase shift bubbles from our µb-µd formulation. Microbubble-microdroplet mixture was subjected to diagnostics ultrasound (US). Microscopy/image analysis on the mixture before and after US expose was performed in order to detect and measure the amount of phase shift bubbles. In vivo activation was demonstrated using a mouse tumor model. The mixture was injected intravenously and tumor tissue was exposed for 75 seconds to US using a clinical ultrasound scanner. The phase shift bubbles were imaged with a small animal ultrasound imaging system. US can generate phase shift bubbles (fig.3). The size of bubbles in the mixture after exposed to US contains significant bigger bubbles than before US. Compared to controls, US treated tumors had 8 to 10 times higher echo intensity. Individual stationary phase shift bubbles could be detected after US treatment and were remained visible up to 5 minutes after treatment (fig.4). We have demonstrated the phase shift concept in-vitro and confirmed this an in-vivo model. As a general platform for local drug delivery the phase shift concept offers unique attributes for enhance drug efficacy.

See image on next page.

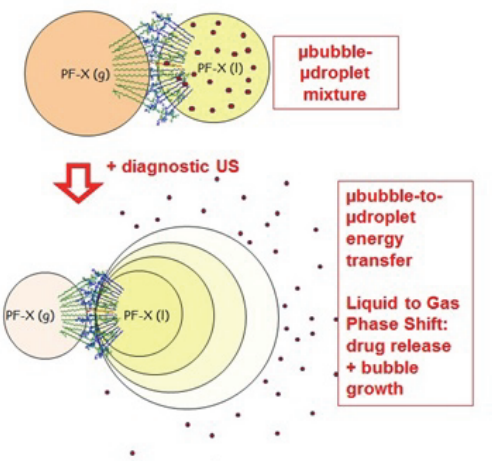

Figure 1. Diagnostic ultrasound controlled phase shift

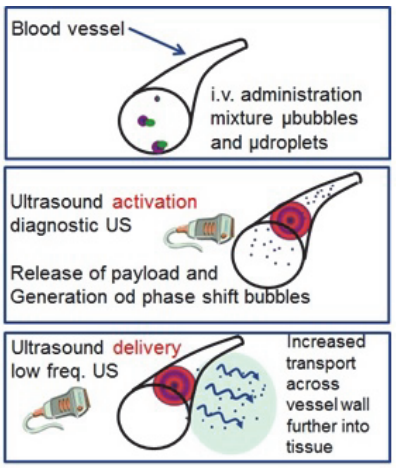

Figure 2. Ultrasound controlled local drug delivery

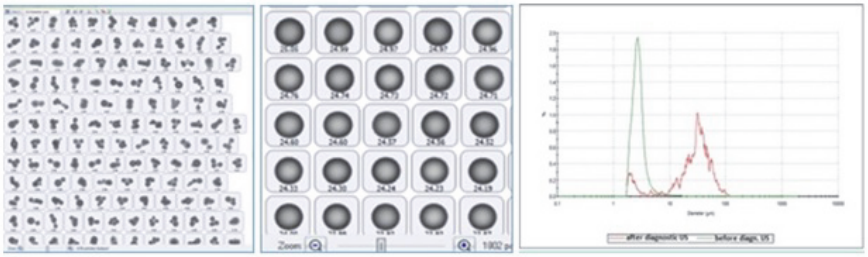

Figure 3 Mixture before (A), after (B) exposed to diagnostic ultrasound.
C) size of bubbles before and after US.

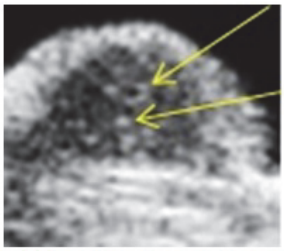

Figure 4. ultrasound image tumor after US treatment. Yellow arrows point at stationary phase shift bubbles

Participant category: PhD Candiate/Research Program Student

4D US motion tracking in the liver over abrupt changes in pattern and drift over time

Sinara Vijayan [(1)], Sebastien Muller [(2)], Ole Jakob Elle [(3)], Thomas Langø [(4)]

sinara.vijayan@ntnu.no

1. Norwegian University of Science and Technology
2. SINTEF Medical Technology, Trondheim
3. The Interventional Centre, Oslo
4. SINTEF Medical Technology, Trondheim

Purpose: Motion estimation is a key issue to be addressed in treatments such as radiotherapy and focused ultrasound, in order to optimize dosage delivery to the target and minimize damage to healthy tissues and critical structures near the target. In addition, drift of abdominal organs like the liver, due to gravity and peristalsis, influences the procedure. This study looks at determining drift using 4D ultrasound and a 4D registration method. We also evaluate qualitatively if motion can be recovered after involuntary organ motion from e.g. coughing. Methods: Seven 4D ultrasound sequences (three breathing cycles of 15seconds) were acquired from a healthy volunteer to isolate drift motion. These sequences were acquired every five minutes over a period of 30 minutes. The ultrasound probe was fixed to an arm to be able to scan the same window every time. In addition, two 4D ultrasound sequences were acquired when the volunteer was asked to cough. An offline analysis was performed on the data using a 4D non-rigid registration method designed specifically to track motion from dynamic images. Extracting the deformation from the registration results and looking at this information over time of 30 minutes determined the drift. Data including coughing was visually inspected to understand if the method was capable of compensating for the abrupt motion changes. Landmarks pinpointed by an engineer were used to evaluate the registration accuracy. Results: The registration method was capable of recovering deformations from data with normal breathing and involuntary patient motion. Initial results confirm a small drift when acquiring data over a longer period of time. Conclusion: We conclude that using 4D ultrasound, the method was able to track motion caused by breathing and sudden movements. We believe that motion tracking of organs/targets in the abdomen and accounting for drift using 4D ultrasound is a fast and accurate means to make patient specific motion models rather than relying on 4D MR acquisitions (MR guided focused ultrasound).

Participant category: PhD Candiate/Research Program Student

Preoperative tumor size measurements at MRI predict deep myometrial invasion, lymph node metastases and survival in patients with endometrial carcinomas.

Sigmund Ytre-Hauge [(1)], Jenny A. Husby [(1)], Helga B. Salvesen [(2)], Ingfrid S. Haldorsen [(1)]

sigmund.ytre-hauge@helse-bergen.no

1. Dept. of Radiology, Haukeland University Hospital, Bergen, Norway
2. Dept. of Obstetrics and Gynecology, Haukeland University Hospital, Bergen, Norway

Purpose: To explore the relation between preoperative tumor size measurements at MRI and the surgical pathologic staging parameters: deep myometrial invasion, cervical stroma invasion and metastatic lymph nodes, and to assess the prognostic impact of tumor size in endometrial carcinoma patients. Interobserver variability for tumor size measurements was also assessed. Materials and Methods: Preoperative conventional contrast enhanced pelvic MRI of 216 patients with histologically confirmed endometrial carcinomas were read independently by three radiologists, all blinded to patient data. Maximum tumor diameters were measured in three orthogonal planes: anterioposterior (AP) and transverse (TV) diameters on axial oblique images (perpendicular to the long axis of the uterus), and craniocaudal (CC) diameters on sagittal images, and tumor volumes were estimated. Tumor size was analyzed in relation to staging results and patient survival, and intraclass correlation coefficients (ICC) and receiver operating characteristics (ROC) curves for the different tumor measurements were calculated. Results: Large tumor diameters and volume were significantly related to presence of deep myometrial invasion (unadjusted odds ratios (OR): 1.06-1.13, $p<0.001$ for all, Figure), but AP diameter was the only size variable independently predicting deep myometrial invasion (adjusted OR: 1.14, $p<0.001$). All tumor measurements were related to lymph node metastases (unadjusted ORs: 1.02-1.05; $p< 0.005$ for all), however, only CC diameter independently predicted lymph node metastases (adjusted OR: 1.04, $p=0.05$). Large tumor size was associated with reduced recurrence-free survival (unadjusted hazard ratio (HR): 1.008-1.034, $p<0.001$ for all); only CC diameter independently predicted survival (adjusted HR: 1.028, $p=0.025$). Interobserver variability for the different size measurements was low (ICCs: 0.78-0.86). Conclusion: Tumor size assessed preoperatively by MRI predicts presence of deep myometrial invasion and lymph node metastases in endometrial carcinoma patients. Thus, tumor size may play a role in risk stratification for planning of surgical and adjuvant treatment. Clinical relevance statement: Tumor size assessment by MRI aids in the prediction of deep myometrial invasion and lymph node metastases and may improve the preoperative risk stratification in endometrial carcinoma patients.

See image on next page.

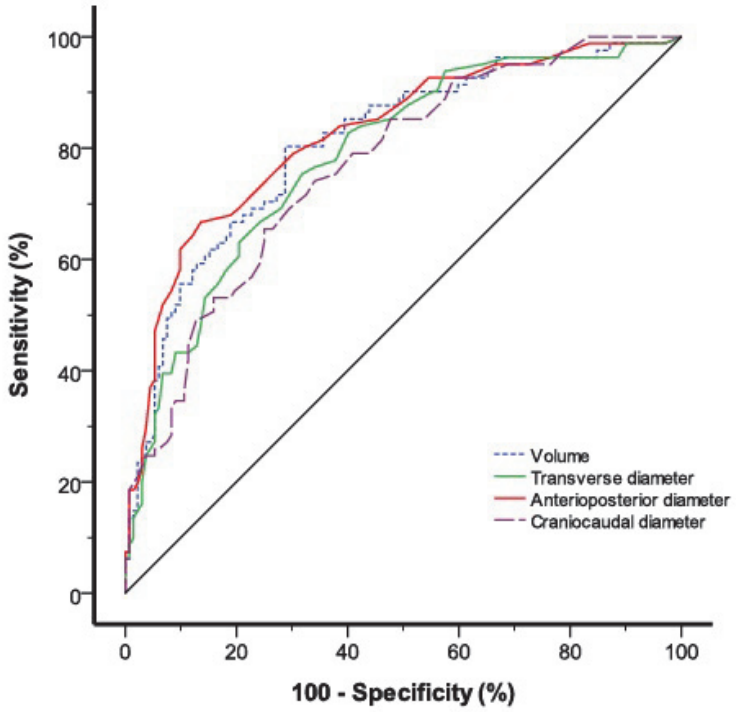

Receiver operating characteristic (ROC) curve for tumor size measurements for identification of deep myometrial invasion in endometrial carcinomas (n=213). Highest area under ROC curve is 0.824 for anterioposterior tumor diameter.

Errata

As a result of a technical problem, which was discovered immediately before the abstract book was sent to print, the last words of some of the image texts are missing. Any loss of information, crediting, or copyright information caused by this should not be regarded the responsibility of the abstract submitters. The organizer, MedIm, apologizes for any inconvenience or loss of information due to this problem.

NOTES